UNIVERSITY OF CALIFORNIA, SAN DIEGO

The MutS and MutL Protein Families and Their Role in the Initiation of DNA Mismatch Repair

A Dissertation submitted in partial satisfaction of the requirements for the degree

Doctor of Philosophy

in

Biomedical Sciences

by

Marc Laurence Mendillo

Committee in charge:

Professor Richard D. Kolodner, Chair
Professor John M. Carethers
Professor Scott D. Emr
Professor Alexandra C. Newton
Professor Matthew D. Weitzman

2007

The Dissertation of Marc Laurence Mendillo is approved, and it is acceptable in quality and form for publication on microfilm:

_____

_____

_____

_____

_____
Chair

University of California, San Diego

2007

Dedicated to

Barbara, Michael & Grandpa Pat

TABLE OF CONTENTS

LIST OF FIGURES

LIST OF TABLES

ACKNOWLEDGEMENTS

First and foremost, I thank Richard Kolodner for being a wonderful advisor and providing me every opportunity to flourish as a scientist. Thank you for allowing me to openly explore my ideas, for the infinite guidance you have provided and for believing in me. I thank Martin Hess, Dan Mazur and Chris Putnam for their contributions to the work in this dissertation as well as to their role in my training and development as a scientist. Dan and Chris have been amazing role models and mentors and I am truly grateful for their vast patience. I must say that it has also been a great deal of fun. I thank Ellen, Scarlet, Steph, Jill & Jason for their camaraderie and for being great friends as well as colleagues. I thank Sandra Martinez, for putting up with me and for being a great baymate and colleague. I thank Cecilia, Jorrit, Brian, Tiki, Team Hoffman, Hans, Eric, Katie & the rest of the Kolodner lab (past & present) for the good times and for making our lab a great place to work. I thank Ann Montgomery for all of her assistance & for the pounds of chocolate over the years. I must also thank Jim Gusella and Susan Slaugenhaupt for providing me my first true lab experience; I have fond memories of my time there and it was my first step on a path that has led me to the writing of this dissertation.

I thank the biomedical science graduate program and its coordinators for ensuring a seamless process and for the planning of all of the wonderful events. To my classmates and friends - I am very lucky to have met such an amazing group of people; I knew this was the place for me from day one.

I thank my west coast families, the Mayos and the Kodimers, for making sure this New Yorker had a place to go for the holidays when I could not go home. I thank Patricia & Babe Calvo as well as GP for always remembering me. I thank Theresa Operaña, my best friend and girlfriend, for everything you have been to me, for forcing me to see the world & for your unrelenting support and affection. Lastly and most importantly, I thank my parents, Michael and Barbara, and my sister, Melissa, for their unconditional love and support; this work is just as much a product of your efforts as it is of mine. I love you all & I could not have done this without you.

Chapter 2, in full, is a reprint of the material as it appears in Mendillo, M. L., Mazur, D. J. and Kolodner R. D. "Analysis of the interaction between the *Saccharomyces cerevisiae* Msh2-Msh6 and Mlh1-Pms1 complexes with DNA using a reversible DNA end-blocking system," *Journal of Biological Chemistry* (2005) Jun 10; 280(23): 22245-57. Chapter 3, in full, is a reprint of the material as it appears in Hess, M. T., Mendillo, M. L., Mazur, D. J. & Kolodner, R. D. "Biochemical basis for dominant mutations in the *Saccharomyces cerevisiae* Msh6 gene." *Proc Natl Acad Sci U S A* 2006 Jan 17; 103(3): 558-563. Chapter 4, in full, is a reprint of the material as it appears in Mazur, D. J., Mendillo, M. L., & Kolodner, R. D. "Inhibition of Msh6 ATPase activity by mispaired DNA induces a Msh2(ATP)-Msh6(ATP) state capable of hydrolysis-independent movement along DNA." *Molecular Cell* 2006 22: 39-49. Chapter 5, in full, is a reprint of the material as it appears in Mendillo, M. L., Putnam, C. D. and Kolodner R. D. "*Escherichia coli* MutS tetramerization domain structure

reveals that stable dimers but not tetramers are essential for mismatch repair *in vivo*," *Journal of Biological Chemistry* (2007) Jun 1; 282(22): 16354-54.

VITA

EDUCATION

2007 Ph.D., Biomedical Sciences, University of California, San Diego (La Jolla, CA).

1998 B.A. Biochemistry and Molecular Biology, Boston University (Boston, MA).

PROFESSIONAL EXPERIENCE

2000-2007 Graduate program in Biomedical Science, University of California, San Diego (La Jolla, CA).
Biochemical analysis of DNA mismatch repair initiation (in laboratory of Richard Kolodner)

2000 Consultant, Oscient Pharmaceuticals (Genome Therapeutics Corporation), (Waltham, MA)
Developed mammalian cytotoxicity assay for new drug discovery group

1998-2000 Assistant Scientist II, Anadys (Scriptgen) Pharmaceuticals, (Waltham, MA)
Antifungal Target validation; antimicrobial and mammalian cytotoxicity testing; MOA study development

1997-1998 Research Assistant, Harvard Institute of Human Genetics, Harvard Medical School (Boston, MA)
Involved in trying to find and clone gene for Familial Dysautonomia (in laboratory of Susan Slaugenhaupt)

TEACHING EXPERIENCE

2002 Graduate Teaching Assistant, Department of Biology, University of California, San Diego (La Jolla, CA)
Led discussion sections for undergraduate mammalian physiology (BIPN 100-Instructor: G. Fortes).

PUBLICATIONS

1. Kolodner, R. D., **Mendillo, M. L.**, Putnam, C. D. (2007). Coupling distant sites in DNA during DNA mismatch repair. *PNAS* **104**, 12953-54.

2. ***Mendillo, M. L.**, *Putnam, C. D. & Kolodner, R. D. (2007). *Escherichia Coli* MutS tetramer domain structure reveals that stable dimers but not tetramers are essential for mismatch repair *in vivo*. *J Biol Chem* **282**, 16345-54. ***Equal Contributions.**

3. Mazur, D. J., **Mendillo, M. L.**, & Kolodner, R. D. (2006). Inhibition of Msh6 ATPase activity by mispaired DNA induces a Msh2(ATP)-Msh6(ATP) state capable of hydrolysis-independent movement along DNA. *Mol Cell* **22**, 39-49.

4. *Hess, M. T., ***Mendillo, M. L**., Mazur, D. J. & Kolodner, R. D. (2006). Biochemical basis for dominant mutations in the Saccharomyces cerevisiae Msh6 gene. *PNAS* **103**, 558-563. ***Equal Contributions.**

5. **Mendillo, M. L.**, Mazur, D. J. & Kolodner, R. D. (2005). Analysis of the interaction between the Saccharomyces cerevisiae MSH2-MSH6 and MLH1-PMS1 complexes with DNA using a reversible DNA end-blocking system. *J Biol Chem* **280**, 22245-57.

6. Blumenfeld, A., Slaugenhaupt, S. A., Liebert, C. B., Temper, V., Maayan, C., Gill, S., Lucente, D. E., Idelson, M., MacCormack, K., Monahan, M. A., Mull, J., Leyne, M., **Mendillo, M**., Schiripo, T., Mishori, E., Breakefield, X., Axelrod, F. B. & Gusella, J. F. (1999). Precise genetic mapping and haplotype analysis of the familial dysautonomia gene on human chromosome 9q31. *Am J Hum Genet* **64**, 1110-8.

PATENTS

1. Moore, J., Buurman, E.T., Bradley, J., Desilva, T., Harris, S., Komarnitsky, S., **Mendillo, M**., Moore, D., McCoy, M., Sanderson, K., Haq, T., Zhu, S., Long, F., Davidov, E., Thompson, C.M. *Screening for Antifungal Compounds and Compositions Thereof.* US Patent Application #20030027243, Filed June 29, 2000

ABSTRACTS AND PRESENTATIONS

1. *Escherichia Coli* MutS tetramer and tetramerization domain structures reveal that stable dimers but not tetramers are essential for mismatch repair *in vivo*. *Fifth Annual SBDR Program Project Workshop*. Berkeley, California (11/2006). Poster.

2. Biochemical basis for dominant mutations in the Saccharomyces cerevisiae Msh6 gene. *American Society for Biochemistry and Molecular Biology at Experimental Biology*. San Francisco, California (4/2006). Poster.

3. Biochemical characterization of the Saccharomyces cerevisiae Msh2-Msh6 and Mlh1-Pms1 mismatch repair complexes. *UCSD Department of Cellular and Molecular Medicine Seminar*. La Jolla, California (11/1/04).

4. A biochemical characterization of the MSH2-MSH6 and MLH1-PMS1 complexes of S. cerevisiae. *Yeast Genetics and Molecular Biology Meeting*. Seattle, Washington (8/2004). Invited speaker.

ABSTRACT OF THE DISSERTATION

The MutS and MutL Protein Families and Their Role in the Initiation of DNA Mismatch Repair

by

Marc Laurence Mendillo

Doctor of Philosophy in Biomedical Sciences

University of California, San Diego, 2007

Professor Richard D. Kolodner, Chair

In *Escherichia coli*, MutS initiates mismatch repair (MMR) by binding mispaired DNA. MutL, an intermediary protein, recognizes mispair-activated MutS and activates downstream MMR proteins. In eukaryotes MMR is similarly initiated by a MutS Homologue (MSH) complex called Msh2-Msh6 that binds to a MutL Homologue (MLH) complex, called Mlh1-Pms1, which activates downstream proteins. While the *in vitro* reconstitution of a MMR reaction using purified *Escherichia coli* proteins was described nearly twenty years ago (and recently using human proteins), the molecular mechanism of this process is not well understood.

Accordingly, several models describe the coordination of MMR events. The studies described in this dissertation use various methods to explore the molecular mechanism of the initiation of MMR.

A system was developed for studying MMR protein movement along DNA. This system was characterized using MSH and MLH complexes from *Saccharomyces cerevisiae*. In addition, an assay was developed to monitor ATP binding in the MSH proteins. These studies revealed that Msh2-Msh6 hydrolyzes ATP to bind mispaired DNA in an ADP-bound form. Mispair binding enables the Msh2-Msh6 to bind ATP in its high-affinity ATP binding site, but inhibits ATP hydrolysis allowing Msh2 to bind an additional ATP, yielding a dual ATP bound form, which is competent for sliding along DNA. Mutant MSH complexes defective for binding ATP in Msh2 failed to slide. The MSH-MLH ternary complex also appeared to slide, but its affinity for DNA ends confounded dissociation analysis. Interestingly, a dominant mutant Msh2-Msh6 complex interacted with Mlh1-Pms1, but failed to slide, suggesting that sliding is important for MMR *in vivo*. Lastly, small angle x-ray scattering of *E. coli* MutS and the crystal structure of its C-terminal 34 amino acids containing the tetramer-forming domain provide a model for full length MutS; further analysis revealed that stable dimers, but not tetramers are essential for MMR *in vivo*.

Taken together, these results support a model of MMR initiation where a dimeric MSH complex recognizes the mispair, binds but does not hydrolyze ATP producing a conformational change that enables binding of the MLH complex and sliding along the DNA helix where downstream signaling can be initiated.

CHAPTER 1

Overview of DNA mismatch repair

1.1 INTRODUCTION

Cells have evolved an intricate network of DNA repair pathways in order to respond to various types of genotypic stress and maintain the stability of its genome. These stresses include errors that arise during DNA replication, endogenous damage, such as that which can result from free radicals generated during metabolism, as well as damage from exogenous insults, such as radiation or DNA alkylating agents. For most cells with a functional DNA repair network, the cellular mutation rate is reduced to extremely low levels (~1 x 10^{-9} to 1 x 10^{-10} per cell division) (Drake, 1991). The DNA mismatch repair system (MMR) is one such pathway in this network and its importance is reflected by its conservation from bacteria to humans (Iyer et al., 2006; Jiricny, 2006). The primary function of the MMR system is the removal of base-base mismatches and small insertion/deletion mismatches that arise during errors in DNA replication (Kolodner, 1996; Kolodner and Marsischky, 1999; Modrich, 1991; Modrich and Lahue, 1996) . MMR effectively reduces the error rate of DNA replication by 2-3 orders of magnitude (Marsischky et al., 1996; Reenan and Kolodner, 1992). MMR proteins and their homologues are also important for a number of other cellular processes, including meiotic recombination and the checkpoint response that leads to the induction of apoptosis in response to some DNA damaging agents (Harfe and Jinks-Robertson, 2000; Jiricny, 2006).

In humans, defects in MMR proteins cause Lynch Syndrome, which results in a predisposition to hereditary nonpolyposis colorectal cancer (HNPCC) as well as a

variety of other cancers, including endometrial, genitourinary, extracolonic GI cancers, ovarian, brain and sebaceous skin tumors (de la Chapelle, 2004; Lynch and de la Chapelle, 2003; Peltomaki, 2003). DNA from tumors marked with MMR defects display microsatellite instability (MSI), which is characterized by frameshifts in short DNA sequence repeats and is thus an excellent marker of MMR deficiency (de la Chapelle, 2004). In addition, since MMR defects in mammalian cells result in defects in response to certain DNA damaging agents, MMR defective tumors might not be responsive to certain chemotherapeutics (Jo and Carethers, 2006; Stojic et al., 2004).

1.2 MISMATCH REPAIR OVERVIEW

MutHLS System

The mechanism of MMR is best understood in *Escherichia coli*. The MutS protein initiates MMR by recognizing the mispaired base in DNA (Su et al., 1988). The MutL protein interacts with the MutS complex in the presence of a mispair and ATP, and stimulates the endonucleolytic activity of the MutH protein (Au et al., 1992; Grilley et al., 1989; Hall and Matson, 1999). MutH makes single strand breaks in the unmethylated DNA strand of transiently hemimethylated GATC sites and thus functions in distinguishing the unmethlyated daughter DNA strand from the methlyated parental DNA strand during and after DNA replication (Welsh et al., 1987). The GATC sites can be located 5' or 3' to the mispair, indicating that MMR is bidirectional (Cooper et al., 1993). The UvrD DNA helicase then unwinds the DNA while one of at least four redundant single-strand specific exonucleases (RecJ, ExoI, ExoVII or ExoX) degrades the error-containing strand (Burdett et al., 2001; Runyon et al., 1990). Lastly, the DNA Polymerase III holoenzyme resynthesizes the DNA, leaving a nick that is sealed by DNA ligase (Lahue et al., 1989). This reaction has been reconstituted *in vitro* with purified components (Lahue et al., 1989).

Eukaryotic MMR

In Eukaryotic cells, three different MutS homologues (MSH) form two different heterodimeric complexes, called Msh2-Msh6 (MutSα) and Msh2-Msh3

(MutSβ) that together recognize base-base mispairs and insertion-deletion loops (Kolodner, 1996; Kolodner and Marsischky, 1999; Marsischky et al., 1996). Similarly, three different MutL homologues (MLH) form two different heterdimeric complexes that function in MMR, called Mlh1-Pms1 (Pms1 in *Saccaromyces cerevisiae* is Pms2 in humans) and Mlh1-Mlh3 (Flores-Rozas and Kolodner, 1998; Prolla et al., 1994; Wang et al., 1999). Like their bacterial homologues, the MLH complexes bind to MSH complexes on DNA in an ATP-dependent manner, where they initiate downstream repair processes, such as excision by the 5'-3' exonuclease, Exo1 (Blackwell et al., 2001; Bowers et al., 2000; Genschel et al., 2002; Raschle et al., 2002; Tishkoff et al., 1997). Biochemical and genetic studies have also implicated additional factors in Eukaryotic MMR, such as the processivity clamp PCNA, its clamp loader RFC, and the single stranded DNA binding protein RPA (Constantin et al., 2005; Flores-Rozas et al., 2000; Lin et al., 1998; Umar et al., 1996; Zhang et al., 2005). The Eukaryotic mismatch repair reaction of a nick-containing mispaired plasmid has recently been reconstituted with purified proteins; however, the mechanism for strand discrimination is still not understood and eukaryotic MMR of nicked plasmids may represent partial MMR reactions (Constantin et al., 2005; Zhang et al., 2005).

1.3 MUTS HOMOLOGUES

Early Studies

Early studies documented mutator strains in a variety of organisms; most implicated defects in replication, recombination and repair genes (Drake et al., 1969; Green, 1970; Von Borstel et al., 1971). Soon after, genetic studies in *E. coli* demonstrated that mutations in MutS result in an increased frequency of transition mutations and later it was revealed that this occured because it is a factor in mismatch repair (Cox et al., 1972; Rydberg, 1978). An assay for repair of heteroduplex plasmids utilizing cell-free extracts of *E. coli* allowed the initial purification of MutS, and later on other proteins required for MMR were purified in this manner as well (Lu et al., 1983; Su and Modrich, 1986).

Seminal studies linked defects in human Msh2 with HNPCC (Fishel et al., 1993; Leach et al., 1993). Genetic and biochemical studies in *Saccaromyces cerevisiae* demonstrated that Msh2 forms two different heterodimeric MSH complexes function in MMR, Msh2-Msh6 and Msh2-Msh3 with partially redundant activities (Marsischky et al., 1996). Base-base mispairs are primarly repaired by Msh2-Msh6, while larger insertion/deletion mispairs are primarly repaired by Msh2-Msh3; however, both complexes are capable of repairing short insertion/deletion mispairs. Consistent with this, mutations in Msh6 are rare in HNPCC and mutations in Msh3 have not been reported (Lynch and de la Chapelle, 2003; Peltomaki, 2003). Several studies have further catalogued the affinity of MutS and the MSH complexes for a

variety of mispaired bases, providing additional insight on their function *in vivo* (Acharya et al., 1996; Alani, 1996; Marsischky and Kolodner, 1999; Su et al., 1988).

Sequence analysis of *salmonella typhimurium* MutS revealed a consensus nucleotide binding site (Haber et al., 1988) and it is now recognized that MutS and the MSH proteins belong to the Adenosine nucleotide Binding Cassette (ABC) superfamily. This family, which is possibly the largest family of proteins, contains more than 1000 members involved in a wide variety of processes, ranging from DNA repair to molecular transport (Gorbalenya and Koonin, 1990; Holland and Blight, 1999; Hopfner and Tainer, 2003). Subsequent experiments confirmed that MutS did indeed posses a weak ATPase activity, which was found to be essential for MMR (Haber and Walker, 1991). Additional studies demonstrated that this was the case for *E. coli* MutS as well as the *S. cerevisiae* and human MSH proteins as well (Alani, 1996; Gradia et al., 1997; Iaccarino et al., 1998; Worth et al., 1998). Furthermore, screens for dominant mutators using both *E. coli* MutS and *S. cerevisiae* Msh6 resulted in dominant mutator mutations yielding proteins with nucleotide binding defects, offering additional evidence of the importance of this activity (Das Gupta and Kolodner, 2000; Hess et al., 2002; Wu and Marinus, 1994).

Biochemical studies demonstrated that MutS and the MSH complexes have a reduced affinity for mispaired DNA in the presence of ATP (Blackwell et al., 1998; Gradia et al., 1997; Hess et al., 2002). Later studies indicated that the ATP-bound complexes could be trapped on a DNA substrate if the ends were blocked; thus the MSH proteins dissociate off of the mispair along the DNA helix (Acharya et al., 2003;

Blackwell et al., 1998; Gradia et al., 1999; Schofield et al., 2001). Additionally, it was noted that ATP was required for interaction with MutL and the MLH complexes. These observations, along with others, inspired a variety of mechanistic models of MMR, which will be discussed in more detail below.

MutS structure & ATP induced conformational changes

Mismatch recognition is central to the process of mismatch repair. C-terminal truncations were used to obtain structures of MutS and MutS complexed to a mispaired DNA substrate for both the *E. coli* and *Thermus aquaticus* (*Taq*) proteins (Lamers et al., 2000; Obmolova et al., 2000). The structures revealed a homodimeric complex bound to its mispaired DNA substrate in an asymmetric manner; thus the MutS homodimer acts as a functional heterodimer, similar to its Eukaryotic homologues.

MutS is a modular protein that can be divided into five domains, each one of which resembles another known structure (Figure 1-1A). The amino-terminal domain I contains residues critical for mismatch recognition. Domain II connects domain I with the ATPase domain (domain V). Domain III is a central scaffold, making contacts with all domains except for domain I. Domain IV is a long clamp, which at one end connects with domain III and the other end forms nonspecific DNA contacts and dimeric contacts.

The monomers assemble by making dimeric contacts at the top (domain V) and bottom (domain IV) of the structure. The top dimeric interface is the larger (2,922

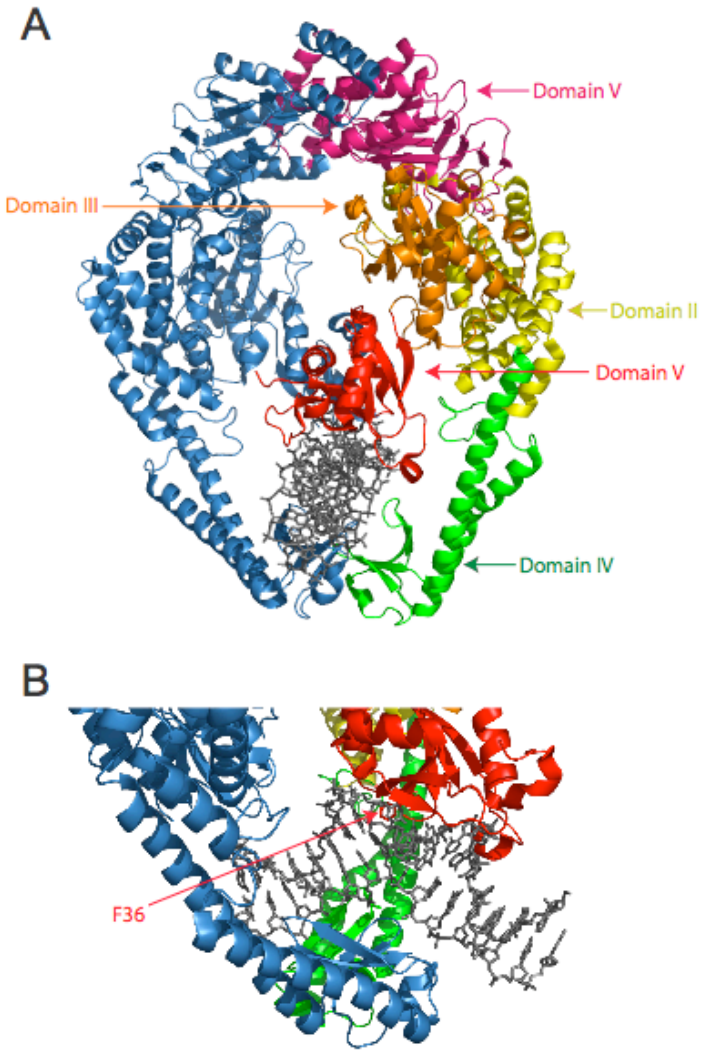

Figure 1-1. MutS bound to a GT mispair. A. The mismatch binding monomer is colored by domain, while the other monomer is colored in blue. The GT mispair DNA substrate is colored in grey. Domain I (2-115) is the mismatch recognition domain and is colored in red. Domain II (116-266) is the connector domain and is colored in yellow. Domain III (267-412 and 537-567) is the core domain and is colored in orange. Domain IV (413-536) is the clamp domain and is colored in green. Domain V (568-800) is the ATPase domain and is colored in magenta. B. F36 (shown in sticks) stacks with the mispaired thymidine base and is critical for mispair binding.

Å^2) and possesses both of the conserved ATPase domains. Both nucleotide binding sites are actually composite sites, each possessing critical residues from the reciprocal monomer. The bottom dimeric interface, which is formed by the clamp domains in the presence of a mispaired DNA substrate, is much smaller and adds ~600 Å^2. Basic residues in these domains coordinate nonspecific contacts with the negatively charged phosphates of the DNA backbone; however, in the absence of DNA, the domains are mobile and cannot be resolved. This mobility, most likely driven by an electrostatic repulsion generated by the same basic residues that contact the DNA, might allow the clamps to remain open and accessible for binding DNA.

A highly conserved phenylalanine stacks with the mispaired thymidine base (Figure 1-1B); previous studies in *E. coli* and *Taq* MutS and *S. cerevisiae* Msh6 demonstrated that this residue is critical for mispair specificity *in vitro* and MMR function *in vivo* (Bowers et al., 1999; Das Gupta and Kolodner, 2000; Malkov et al., 1997; Yamamoto et al., 2000). The long connector arms bridge the ATPase domains with the DNA binding domains and thus communicate the conformational change that results in altered DNA binding kinetics upon nucleotide binding. While numerous biochemical and biophysical studies of MutS and its orthologues imply that there are extensive ATP induced conformational changes in this region, structural studies have thus far provided only limited insight on what these changes are and how they are coordinated (Alani et al., 2003; Lamers et al., 2004). Comparison of MutS to other ABC ATPase family members, such as Rad50, have provided some clues, but there is still much left to learn (Hopfner et al., 2000).

The fact that there can be up to nine different states of nucleotide occupancy for the two ATP-binding sites (if each site can be empty, have an ADP, or an ATP) adds an additional level of complexity to the elucidation of the function of these sites. Several studies demonstrated that the two nucleotide binding sites in both MutS and the MSH complexes have different affinities and are somehow coupled to one another (Antony and Hingorani, 2004; Drotschmann et al., 2002; Lamers et al., 2003). Various effects of DNA on ATPase activity have been documented. Duplex DNA, and to an even greater extent, mispaired DNA, have been shown to stimulate steady-state levels of ATP hydrolysis (Gradia et al., 1997; Hess et al., 2002). In addition, a burst phase of ATP hydrolysis, which is inhibited by mispair binding, followed by a slower steady-state level has also been noted (Antony and Hingorani, 2003; Bjornson et al., 2000). How these nucleotide occupancy states are linked to conformational states and MMR mechanisms is not well understood.

MutS Oligomerization

While C-terminal truncations of the *Taq* and *E. coli* proteins were used to obtain dimeric crystal structures, the full-length proteins exist in an equilibrium mixture of dimers and tetramers (Biswas et al., 1999; Bjornson et al., 2003). The C-terminal region mediates tetramerization and includes the last 53 amino acids in *E. coli* MutS. This region is conserved in MutS proteins from the majority of bacteria; indeed, tetramerization has been observed in MutS from other prokaryotes as well (Takamatsu et al., 1996). Despite its crystallographic utility, the *E. coli* deletion

protein MutSΔ800 has severe biochemical defects, including defects in mispair recognition and MutH activation (Bjornson et al., 2003). Consistent with this, integration of MutSΔ800 onto the *E. coli* chromosome results in a substantial MMR defect (Calmann et al., 2005a), although the high level expression of MutSΔ800 from a plasmid can complement for a mutS deletion strain in mutation avoidance (Calmann et al., 2005b). These data have led to the suggestion that tetramerization is essential for MMR in *E. coli*, however, in addition to tetramerization defects, the MutSΔ800 protein has also been shown to have dimerization defects as well; this offers an alternative explanation for its *in vitro* and *in vivo* defects (Lamers et al., 2004). Moreover, no evidence exists for tetramerization of the Eukaryotic MSHs.

1.4 MUTL HOMOLOGUES

The MLH proteins function as intermediaries in MMR. *E. coli* MutL recognizes the mispair-activated MutS protein and binds to and stimulates the activity of downstream proteins, such as MutH and UvrD, which can then act at distances of ~ 1000 bp from the mispair (Au et al., 1992; Grilley et al., 1989; Hall and Matson, 1999; Yamaguchi et al., 1998). Similarly, the Eukaryotic MLH complexes bind to mispair-activated MSH complexes and stimulate the activity of Exo1. The mechanistic features of this coordination continue to be actively debated.

Analysis of a crystal structure of the monomeric 40 kilodalton N-terminal fragment of MutL (LN-40) corroborated earlier in-silico studies that suggested the MutL family is part of a larger group of ATPases, now known as the GHKL superfamily (Ban and Yang, 1998; Mushegian et al., 1997). This functionally diverse array of proteins gets its name from its collective members, which include the gyrase class of DNA topoismerases, the Hsp90 family of heat-shock protein chaperones, the DNA histidine kinases, as well as MutL and its homologues (Dutta and Inouye, 2000). The structural similarities of MutL with these ATPases prompted further experimentation and confirmed that MutL possesses a weak ATPase activity, which is required for MMR (Ban and Yang, 1998; Spampinato and Modrich, 2000).

Initial evidence from size-exclusion chromatography experiments and protein cross-linking assays of LN-40 bound to a non-hydrolyzable ATP analogue, showed that ATP binding, but not hydrolysis, induces dimerization of the LN-40 fragment,

while the full-length protein always remains intact as a dimer, independent of nucleotide occupancy (Ban and Yang, 1998). Truncation analysis of MLH proteins indicated that the dimerization of the full-length protein is mediated through the C-terminus; this was later confirmed by structural analysis (Guarne et al., 2004; Kondo et al., 2001; Kosinski et al., 2005; Pang et al., 1997). Taken together, this suggests that the N-terminal portion of the protein acts as clamp that can open and close depending on the nucleotide occupancy, while the protein remains dimeric at all times due to interactions of the c-terminal region. Additional evidence for this came with the solution of another structure of LN-40, this time, as a dimer bound with ADPnP (Ban et al., 1999). Biochemical and genetic studies indicate that the Eukaryotic MLH complexes undergo similar ATP-driven conformational changes, that are required for MMR *in vivo* (Tran and Liskay, 2000). While the N-terminal structural rearrangement that ATP binding confers is well documented, its function, at least in *E. coli,* is only beginning to be understood.

1.5 TERNARY COMPLEX & MMR INITIATION MODELS

Numerous biochemical studies have shown that MutL forms a ternary complex with MutS on DNA, in a reaction that is dependent on ATP (Acharya et al., 2003; Baitinger et al., 2003; Galio et al., 1999; Grilley et al., 1989; Selmane et al., 2003). The MLH complexes interact with the MSH complexes in a similar fashion (Blackwell et al., 2001; Bowers et al., 2000; Raschle et al., 2002). Studies using both the prokaryotic and eukaryotic complexes have demonstrated that the ternary complex requires larger DNA substrates than the MSH complexes to form efficiently (Blackwell et al., 2001; Schofield et al., 2001). The ternary complex can be formed either by adding both complexes together in the presence of ATP to the DNA substrate (Baitinger et al., 2003), or by prebinding MutS with ADP or without nucleotide, washing away unbound protein and then adding in MutL with ATP (Acharya et al., 2003; Selmane et al., 2003). The latter condition demonstrates that MutL can bind directly to MutS that is bound to DNA. Studies with non-hydrolyzable ATP analogues and MutS mutants with ATP hydrolysis defects suggest that ATP hydrolysis is not required for this interaction (Acharya et al., 2003; Selmane et al., 2003), however, there are conflicting reports that suggest otherwise (Baitinger et al., 2003; Galio et al., 1999). In addition, studies with MutL mutants that are defective in ATP binding suggest that the requirement for ATP in ternary complex formation resides within MutS (Acharya et al., 2003; Raschle et al., 2002).

Three major models have been proposed to explain the coordination of mispair recognition with downstream MMR events, such as excision (Figure 1-2). The first model originated from observations made in electron microscopy studies using *E. coli* proteins. DNA loops were formed in the presence of MutS, and further stimulated by MutL, in a manner dependent on ATP hydrolysis (Allen et al., 1997). This result was interpreted as an active translocation mechanism, in analogy to type I and type III restriction enzymes (Bourniquel and Bickle, 2002); here, a MutS-MutL complex forms at the mispair and spools DNA through until it reaches its downstream recognition sequence; in *E. coli*, this is the hemimethylated GATC site.

A second model was based on the observation that MSH complexes can be trapped on DNA in an ATP binding dependent, but ATP hydrolyisis indendent, manner (Gradia et al., 1999). Here, the MLH complex can bind to the ATP-bound "sliding clamp" conformation of the MSH complex after mispair promoted ADP-ATP exchange. This complex is free to diffuse along DNA to signal downstream effector molecules. This process is assisted by the flux of new MSH complexes that load onto the recently vacated mispair, yielding a gradient of complexes that ensure the complexes ahead move away in a unidirectional manner (Acharya et al., 2003).

Both models described above require a continuous DNA helix from the mispair to the downstream effector site on DNA. In contrast, a trans models was proposed where the two distant DNA sites come together in solution; here there is no movement by the MSH-MLH complex away from the mispair (Schofield et al., 2001). This model was based upon experiments showing that the MutS-MutL complex has a

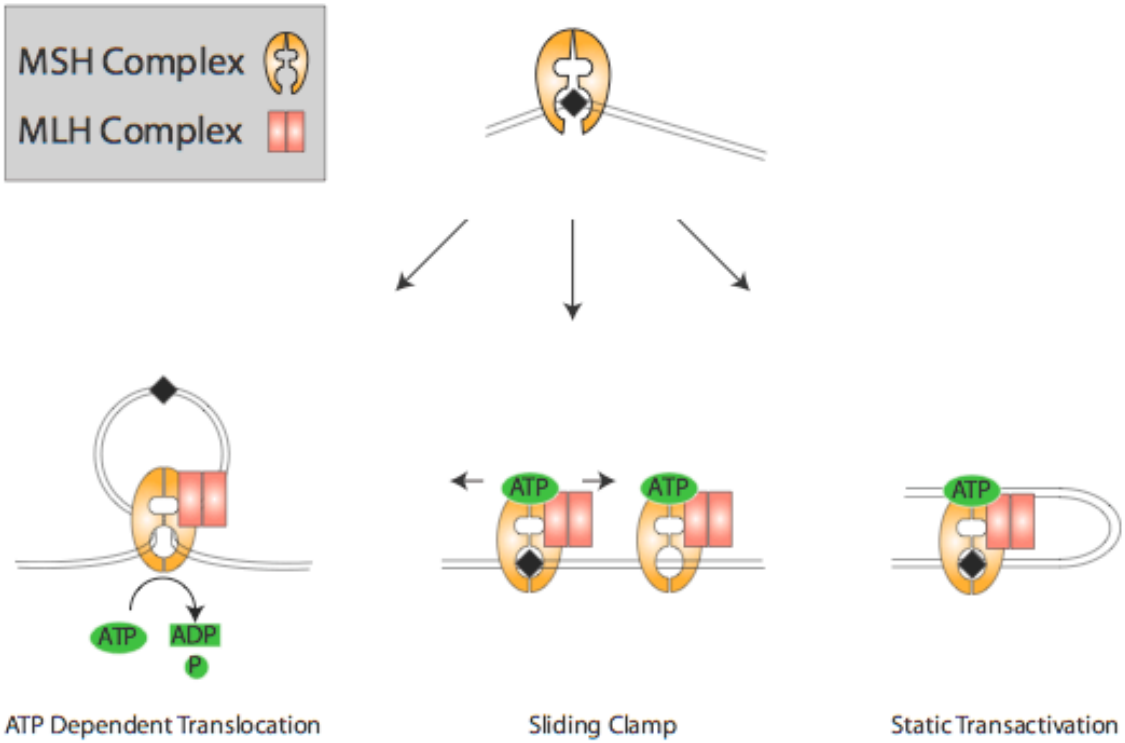

Figure 1-2. Current models of MMR initiation. See text for details.

slower rate of dissociation, compared to MutS, off of DNA (Schofield et al., 2001). Therefore, the MutS-MutL repair complex stays at or near the mispair and reaches for the distant GATC site. Perhaps more direct evidence for this model came from studies demonstrating that MutH activity on short DNA substrates containing a mispair and a hemimethylated GATC sequence were the same as when the mispair and the GATC sequence were located on different substrates (Schofield et al., 2001). Similarly, studies in human cell-free extracts found that substrates containing an Avidin protein or an internal DNA hairpin loop as a blockade between the mispair and the nick, had similar levels of excision as compared to substrates lacking the blocks (Wang and Hays, 2003; Wang and Hays, 2004). This model does not offer an expanation for the mispair-driven directionality of excision. Regardless, further study will be required to truly understand the mechanistic features of MMR.

1.6 SUMMARY AND AIMS

The studies described in this dissertation address the molecular mechanism of the initiation of DNA mismatch repair. In chapter 2, we describe a system that was developed in order to study the mobility of MMR proteins along DNA. In particular, we address whether mobility is due to active transport driven by ATP hydrolysis, or rather from sliding by diffusion, induced by a conformational change driven by ATP binding, but not hydrolysis. In addition, interaction with the MLH complex and its mobility are examined in the same manner. In chapter 3, dominant mutant Msh2-Msh6 complexes are tested for the ability to slide along DNA and interact with Mlh1-Pms1 using the system described in chapter 2. Their ATP binding and hydrolysis properties are characterized as well. In chapter 4, a crosslinking assay is described for the simultaneous detection of the nucleotide occupancy for both subunits of the MSH complex. In addition, its nucleotide occupancy state for the sliding clamp conformation is determined. Lastly, in chapter 5, we determine a model for the full-length MutS protein using small angle X-ray scattering and a crystal structure of the C-terminal tetramerization domain fused to Maltose Binding Protein, and use this information along with mutagenesis and genetic analysis to determine the oligomerization requirements for MMR function *in vivo*.

1.7 REFERENCES

Acharya, S., Foster, P. L., Brooks, P., and Fishel, R. (2003). The coordinated functions of the E. coli MutS and MutL proteins in mismatch repair. Mol Cell *12*, 233-246.

Acharya, S., Wilson, T., Gradia, S., Kane, M. F., Guerrette, S., Marsischky, G. T., Kolodner, R., and Fishel, R. (1996). hMSH2 forms specific mispair-binding complexes with hMSH3 and hMSH6. Proc Natl Acad Sci U S A *93*, 13629-13634.

Alani, E. (1996). The Saccharomyces cerevisiae Msh2 and Msh6 proteins form a complex that specifically binds to duplex oligonucleotides containing mismatched DNA base pairs. Mol Cell Biol *16*, 5604-5615.

Alani, E., Lee, J. Y., Schofield, M. J., Kijas, A. W., Hsieh, P., and Yang, W. (2003). Crystal structure and biochemical analysis of the MutS.ADP.beryllium fluoride complex suggests a conserved mechanism for ATP interactions in mismatch repair. J Biol Chem *278*, 16088-16094.

Allen, D. J., Makhov, A., Grilley, M., Taylor, J., Thresher, R., Modrich, P., and Griffith, J. D. (1997). MutS mediates heteroduplex loop formation by a translocation mechanism. Embo J *16*, 4467-4476.

Antony, E., and Hingorani, M. M. (2003). Mismatch recognition-coupled stabilization of Msh2-Msh6 in an ATP-bound state at the initiation of DNA repair. Biochemistry *42*, 7682-7693.

Antony, E., and Hingorani, M. M. (2004). Asymmetric ATP binding and hydrolysis activity of the Thermus aquaticus MutS dimer is key to modulation of its interactions with mismatched DNA. Biochemistry *43*, 13115-13128.

Au, K. G., Welsh, K., and Modrich, P. (1992). Initiation of methyl-directed mismatch repair. J Biol Chem *267*, 12142-12148.

Baitinger, C., Burdett, V., and Modrich, P. (2003). Hydrolytically deficient MutS E694A is defective in the MutL-dependent activation of MutH and in the mismatch-dependent assembly of the MutS.MutL.heteroduplex complex. J Biol Chem *278*, 49505-49511.

Ban, C., Junop, M., and Yang, W. (1999). Transformation of MutL by ATP binding and hydrolysis: a switch in DNA mismatch repair. Cell *97*, 85-97.

Ban, C., and Yang, W. (1998). Crystal structure and ATPase activity of MutL: implications for DNA repair and mutagenesis. Cell *95*, 541-552.

Biswas, I., Ban, C., Fleming, K. G., Qin, J., Lary, J. W., Yphantis, D. A., Yang, W., and Hsieh, P. (1999). Oligomerization of a MutS mismatch repair protein from Thermus aquaticus. J Biol Chem *274*, 23673-23678.

Bjornson, K. P., Allen, D. J., and Modrich, P. (2000). Modulation of MutS ATP hydrolysis by DNA cofactors. Biochemistry *39*, 3176-3183.

Bjornson, K. P., Blackwell, L. J., Sage, H., Baitinger, C., Allen, D., and Modrich, P. (2003). Assembly and molecular activities of the MutS tetramer. J Biol Chem *278*, 34667-34673.

Blackwell, L. J., Martik, D., Bjornson, K. P., Bjornson, E. S., and Modrich, P. (1998). Nucleotide-promoted release of hMutSalpha from heteroduplex DNA is consistent with an ATP-dependent translocation mechanism. J Biol Chem *273*, 32055-32062.

Blackwell, L. J., Wang, S., and Modrich, P. (2001). DNA chain length dependence of formation and dynamics of hMutSalpha.hMutLalpha.heteroduplex complexes. J Biol Chem *276*, 33233-33240.

Bourniquel, A. A., and Bickle, T. A. (2002). Complex restriction enzymes: NTP-driven molecular motors. Biochimie *84*, 1047-1059.

Bowers, J., Sokolsky, T., Quach, T., and Alani, E. (1999). A mutation in the MSH6 subunit of the Saccharomyces cerevisiae MSH2-MSH6 complex disrupts mismatch recognition. J Biol Chem *274*, 16115-16125.

Bowers, J., Tran, P. T., Liskay, R. M., and Alani, E. (2000). Analysis of yeast MSH2-MSH6 suggests that the initiation of mismatch repair can be separated into discrete steps. J Mol Biol *302*, 327-338.

Burdett, V., Baitinger, C., Viswanathan, M., Lovett, S. T., and Modrich, P. (2001). In vivo requirement for RecJ, ExoVII, ExoI, and ExoX in methyl-directed mismatch repair. Proc Natl Acad Sci U S A *98*, 6765-6770.

Calmann, M. A., Nowosielska, A., and Marinus, M. G. (2005a). The MutS C terminus is essential for mismatch repair activity in vivo. J Bacteriol *187*, 6577-6579.

Calmann, M. A., Nowosielska, A., and Marinus, M. G. (2005b). Separation of mutation avoidance and antirecombination functions in an Escherichia coli mutS mutant. Nucleic Acids Res *33*, 1193-1200.

Constantin, N., Dzantiev, L., Kadyrov, F. A., and Modrich, P. (2005). Human mismatch repair: reconstitution of a nick-directed bidirectional reaction. J Biol Chem *280*, 39752-39761.

Cooper, D. L., Lahue, R. S., and Modrich, P. (1993). Methyl-directed mismatch repair is bidirectional. J Biol Chem *268*, 11823-11829.

Cox, E. C., Degnen, G. E., and Scheppe, M. L. (1972). Mutator gene studies in Escherichia coli: the mutS gene. Genetics *72*, 551-567.

Das Gupta, R., and Kolodner, R. D. (2000). Novel dominant mutations in Saccharomyces cerevisiae MSH6. Nat Genet *24*, 53-56.

de la Chapelle, A. (2004). Genetic predisposition to colorectal cancer. Nat Rev Cancer *4*, 769-780.

Drake, J. W. (1991). Spontaneous mutation. Annu Rev Genet *25*, 125-146.

Drake, J. W., Allen, E. F., Forsberg, S. A., Preparata, R. M., and Greening, E. O. (1969). Genetic control of mutation rates in bacteriophageT4. Nature *221*, 1128-1132.

Drotschmann, K., Yang, W., and Kunkel, T. A. (2002). Evidence for sequential action of two ATPase active sites in yeast Msh2-Msh6. DNA Repair (Amst) *1*, 743-753.

Dutta, R., and Inouye, M. (2000). GHKL, an emergent ATPase/kinase superfamily. Trends Biochem Sci *25*, 24-28.

Fishel, R., Lescoe, M. K., Rao, M. R., Copeland, N. G., Jenkins, N. A., Garber, J., Kane, M., and Kolodner, R. (1993). The human mutator gene homolog MSH2 and its association with hereditary nonpolyposis colon cancer. Cell *75*, 1027-1038.

Flores-Rozas, H., Clark, D., and Kolodner, R. D. (2000). Proliferating cell nuclear antigen and Msh2p-Msh6p interact to form an active mispair recognition complex. Nat Genet *26*, 375-378.

Flores-Rozas, H., and Kolodner, R. D. (1998). The Saccharomyces cerevisiae MLH3 gene functions in MSH3-dependent suppression of frameshift mutations. Proc Natl Acad Sci U S A *95*, 12404-12409.

Galio, L., Bouquet, C., and Brooks, P. (1999). ATP hydrolysis-dependent formation of a dynamic ternary nucleoprotein complex with MutS and MutL. Nucleic Acids Res *27*, 2325-2331.

Genschel, J., Bazemore, L. R., and Modrich, P. (2002). Human exonuclease I is required for 5' and 3' mismatch repair. J Biol Chem *277*, 13302-13311.

Gorbalenya, A. E., and Koonin, E. V. (1990). Superfamily of UvrA-related NTP-binding proteins. Implications for rational classification of recombination/repair systems. J Mol Biol *213*, 583-591.

Gradia, S., Acharya, S., and Fishel, R. (1997). The human mismatch recognition complex hMSH2-hMSH6 functions as a novel molecular switch. Cell *91*, 995-1005.

Gradia, S., Subramanian, D., Wilson, T., Acharya, S., Makhov, A., Griffith, J., and Fishel, R. (1999). hMSH2-hMSH6 forms a hydrolysis-independent sliding clamp on mismatched DNA. Mol Cell *3*, 255-261.

Green, M. M. (1970). The genetics of a mutator gene in Drosophila melanogaster. Mutat Res *10*, 353-363.

Grilley, M., Welsh, K. M., Su, S. S., and Modrich, P. (1989). Isolation and characterization of the Escherichia coli mutL gene product. J Biol Chem *264*, 1000-1004.

Guarne, A., Ramon-Maiques, S., Wolff, E. M., Ghirlando, R., Hu, X., Miller, J. H., and Yang, W. (2004). Structure of the MutL C-terminal domain: a model of intact MutL and its roles in mismatch repair. Embo J *23*, 4134-4145.

Haber, L. T., Pang, P. P., Sobell, D. I., Mankovich, J. A., and Walker, G. C. (1988). Nucleotide sequence of the Salmonella typhimurium mutS gene required for mismatch repair: homology of MutS and HexA of Streptococcus pneumoniae. J Bacteriol *170*, 197-202.

Haber, L. T., and Walker, G. C. (1991). Altering the conserved nucleotide binding motif in the Salmonella typhimurium MutS mismatch repair protein affects both its ATPase and mismatch binding activities. Embo J *10*, 2707-2715.

Hall, M. C., and Matson, S. W. (1999). The Escherichia coli MutL protein physically interacts with MutH and stimulates the MutH-associated endonuclease activity. J Biol Chem *274*, 1306-1312.

Harfe, B. D., and Jinks-Robertson, S. (2000). DNA mismatch repair and genetic instability. Annu Rev Genet *34*, 359-399.

Hess, M. T., Gupta, R. D., and Kolodner, R. D. (2002). Dominant Saccharomyces cerevisiae msh6 mutations cause increased mispair binding and decreased dissociation from mispairs by Msh2-Msh6 in the presence of ATP. J Biol Chem *277*, 25545-25553.

Holland, I. B., and Blight, M. A. (1999). ABC-ATPases, adaptable energy generators fuelling transmembrane movement of a variety of molecules in organisms from bacteria to humans. J Mol Biol *293*, 381-399.

Hopfner, K. P., Karcher, A., Shin, D. S., Craig, L., Arthur, L. M., Carney, J. P., and Tainer, J. A. (2000). Structural biology of Rad50 ATPase: ATP-driven conformational control in DNA double-strand break repair and the ABC-ATPase superfamily. Cell *101*, 789-800.

Hopfner, K. P., and Tainer, J. A. (2003). Rad50/SMC proteins and ABC transporters: unifying concepts from high-resolution structures. Curr Opin Struct Biol *13*, 249-255.

Iaccarino, I., Marra, G., Palombo, F., and Jiricny, J. (1998). hMSH2 and hMSH6 play distinct roles in mismatch binding and contribute differently to the ATPase activity of hMutSalpha. Embo J *17*, 2677-2686.

Iyer, R. R., Pluciennik, A., Burdett, V., and Modrich, P. L. (2006). DNA mismatch repair: functions and mechanisms. Chem Rev *106*, 302-323.

Jiricny, J. (2006). The multifaceted mismatch-repair system. Nat Rev Mol Cell Biol *7*, 335-346.

Jo, W. S., and Carethers, J. M. (2006). Chemotherapeutic implications in microsatellite unstable colorectal cancer. Cancer Biomark *2*, 51-60.

Kolodner, R. (1996). Biochemistry and genetics of eukaryotic mismatch repair. Genes Dev *10*, 1433-1442.

Kolodner, R. D., and Marsischky, G. T. (1999). Eukaryotic DNA mismatch repair. Curr Opin Genet Dev *9*, 89-96.

Kondo, E., Horii, A., and Fukushige, S. (2001). The interacting domains of three MutL heterodimers in man: hMLH1 interacts with 36 homologous amino acid residues within hMLH3, hPMS1 and hPMS2. Nucleic Acids Res *29*, 1695-1702.

Kosinski, J., Steindorf, I., Bujnicki, J. M., Giron-Monzon, L., and Friedhoff, P. (2005). Analysis of the quaternary structure of the MutL C-terminal domain. J Mol Biol *351*, 895-909.

Lahue, R. S., Au, K. G., and Modrich, P. (1989). DNA mismatch correction in a defined system. Science *245*, 160-164.

Lamers, M. H., Georgijevic, D., Lebbink, J. H., Winterwerp, H. H., Agianian, B., de Wind, N., and Sixma, T. K. (2004). ATP increases the affinity between MutS ATPase domains. Implications for ATP hydrolysis and conformational changes. J Biol Chem *279*, 43879-43885.

Lamers, M. H., Perrakis, A., Enzlin, J. H., Winterwerp, H. H., de Wind, N., and Sixma, T. K. (2000). The crystal structure of DNA mismatch repair protein MutS binding to a G x T mismatch. Nature *407*, 711-717.

Lamers, M. H., Winterwerp, H. H., and Sixma, T. K. (2003). The alternating ATPase domains of MutS control DNA mismatch repair. Embo J *22*, 746-756.

Leach, F. S., Nicolaides, N. C., Papadopoulos, N., Liu, B., Jen, J., Parsons, R., Peltomaki, P., Sistonen, P., Aaltonen, L. A., Nystrom-Lahti, M., and et al. (1993). Mutations of a mutS homolog in hereditary nonpolyposis colorectal cancer. Cell *75*, 1215-1225.

Lin, Y. L., Shivji, M. K., Chen, C., Kolodner, R., Wood, R. D., and Dutta, A. (1998). The evolutionarily conserved zinc finger motif in the largest subunit of human replication protein A is required for DNA replication and mismatch repair but not for nucleotide excision repair. J Biol Chem *273*, 1453-1461.

Lu, A. L., Clark, S., and Modrich, P. (1983). Methyl-directed repair of DNA base-pair mismatches in vitro. Proc Natl Acad Sci U S A *80*, 4639-4643.

Lynch, H. T., and de la Chapelle, A. (2003). Hereditary colorectal cancer. N Engl J Med *348*, 919-932.

Malkov, V. A., Biswas, I., Camerini-Otero, R. D., and Hsieh, P. (1997). Photocross-linking of the NH2-terminal region of Taq MutS protein to the major groove of a heteroduplex DNA. J Biol Chem *272*, 23811-23817.

Marsischky, G. T., Filosi, N., Kane, M. F., and Kolodner, R. (1996). Redundancy of Saccharomyces cerevisiae MSH3 and MSH6 in MSH2-dependent mismatch repair. Genes Dev *10*, 407-420.

Marsischky, G. T., and Kolodner, R. D. (1999). Biochemical characterization of the interaction between the Saccharomyces cerevisiae MSH2-MSH6 complex and mispaired bases in DNA. J Biol Chem *274*, 26668-26682.

Modrich, P. (1991). Mechanisms and biological effects of mismatch repair. Annu Rev Genet *25*, 229-253.

Modrich, P., and Lahue, R. (1996). Mismatch repair in replication fidelity, genetic recombination, and cancer biology. Annu Rev Biochem *65*, 101-133.

Mushegian, A. R., Bassett, D. E., Jr., Boguski, M. S., Bork, P., and Koonin, E. V. (1997). Positionally cloned human disease genes: patterns of evolutionary conservation and functional motifs. Proc Natl Acad Sci U S A *94*, 5831-5836.

Obmolova, G., Ban, C., Hsieh, P., and Yang, W. (2000). Crystal structures of mismatch repair protein MutS and its complex with a substrate DNA. Nature *407*, 703-710.

Pang, Q., Prolla, T. A., and Liskay, R. M. (1997). Functional domains of the Saccharomyces cerevisiae Mlh1p and Pms1p DNA mismatch repair proteins and their relevance to human hereditary nonpolyposis colorectal cancer-associated mutations. Mol Cell Biol *17*, 4465-4473.

Peltomaki, P. (2003). Role of DNA mismatch repair defects in the pathogenesis of human cancer. J Clin Oncol *21*, 1174-1179.

Prolla, T. A., Pang, Q., Alani, E., Kolodner, R. D., and Liskay, R. M. (1994). MLH1, PMS1, and MSH2 interactions during the initiation of DNA mismatch repair in yeast. Science *265*, 1091-1093.

Raschle, M., Dufner, P., Marra, G., and Jiricny, J. (2002). Mutations within the hMLH1 and hPMS2 subunits of the human MutLalpha mismatch repair factor affect its ATPase activity, but not its ability to interact with hMutSalpha. J Biol Chem *277*, 21810-21820.

Reenan, R. A., and Kolodner, R. D. (1992). Characterization of insertion mutations in the Saccharomyces cerevisiae MSH1 and MSH2 genes: evidence for separate mitochondrial and nuclear functions. Genetics *132*, 975-985.

Runyon, G. T., Bear, D. G., and Lohman, T. M. (1990). Escherichia coli helicase II (UvrD) protein initiates DNA unwinding at nicks and blunt ends. Proc Natl Acad Sci U S A *87*, 6383-6387.

Rydberg, B. (1978). Bromouracil mutagenesis and mismatch repair in mutator strains of Escherichia coli. Mutat Res *52*, 11-24.

Schofield, M. J., Nayak, S., Scott, T. H., Du, C., and Hsieh, P. (2001). Interaction of Escherichia coli MutS and MutL at a DNA mismatch. J Biol Chem *276*, 28291-28299.

Selmane, T., Schofield, M. J., Nayak, S., Du, C., and Hsieh, P. (2003). Formation of a DNA mismatch repair complex mediated by ATP. J Mol Biol *334*, 949-965.

Spampinato, C., and Modrich, P. (2000). The MutL ATPase is required for mismatch repair. J Biol Chem *275*, 9863-9869.

Stojic, L., Brun, R., and Jiricny, J. (2004). Mismatch repair and DNA damage signalling. DNA Repair (Amst) *3*, 1091-1101.

Su, S. S., Lahue, R. S., Au, K. G., and Modrich, P. (1988). Mispair specificity of methyl-directed DNA mismatch correction in vitro. J Biol Chem *263*, 6829-6835.

Su, S. S., and Modrich, P. (1986). Escherichia coli mutS-encoded protein binds to mismatched DNA base pairs. Proc Natl Acad Sci U S A *83*, 5057-5061.

Takamatsu, S., Kato, R., and Kuramitsu, S. (1996). Mismatch DNA recognition protein from an extremely thermophilic bacterium, Thermus thermophilus HB8. Nucleic Acids Res *24*, 640-647.

Tishkoff, D. X., Boerger, A. L., Bertrand, P., Filosi, N., Gaida, G. M., Kane, M. F., and Kolodner, R. D. (1997). Identification and characterization of Saccharomyces cerevisiae EXO1, a gene encoding an exonuclease that interacts with MSH2. Proc Natl Acad Sci U S A *94*, 7487-7492.

Tran, P. T., and Liskay, R. M. (2000). Functional studies on the candidate ATPase domains of Saccharomyces cerevisiae MutLalpha. Mol Cell Biol *20*, 6390-6398.

Umar, A., Buermeyer, A. B., Simon, J. A., Thomas, D. C., Clark, A. B., Liskay, R. M., and Kunkel, T. A. (1996). Requirement for PCNA in DNA mismatch repair at a step preceding DNA resynthesis. Cell *87*, 65-73.

Von Borstel, R. C., Cain, K. T., and Steinberg, C. M. (1971). Inheritance of spontaneous mutability in yeast. Genetics *69*, 17-27.

Wang, H., and Hays, J. B. (2003). Mismatch repair in human nuclear extracts: effects of internal DNA-hairpin structures between mismatches and excision-initiation nicks on mismatch correction and mismatch-provoked excision. J Biol Chem *278*, 28686-28693.

Wang, H., and Hays, J. B. (2004). Signaling from DNA mispairs to mismatch-repair excision sites despite intervening blockades. Embo J *23*, 2126-2133.

Wang, T. F., Kleckner, N., and Hunter, N. (1999). Functional specificity of MutL homologs in yeast: evidence for three Mlh1-based heterocomplexes with distinct roles during meiosis in recombination and mismatch correction. Proc Natl Acad Sci U S A *96*, 13914-13919.

Welsh, K. M., Lu, A. L., Clark, S., and Modrich, P. (1987). Isolation and characterization of the Escherichia coli mutH gene product. J Biol Chem *262*, 15624-15629.

Worth, L., Jr., Bader, T., Yang, J., and Clark, S. (1998). Role of MutS ATPase activity in MutS,L-dependent block of in vitro strand transfer. J Biol Chem *273*, 23176-23182.

Wu, T. H., and Marinus, M. G. (1994). Dominant negative mutator mutations in the mutS gene of Escherichia coli. J Bacteriol *176*, 5393-5400.

Yamaguchi, M., Dao, V., and Modrich, P. (1998). MutS and MutL activate DNA helicase II in a mismatch-dependent manner. J Biol Chem *273*, 9197-9201.

Yamamoto, A., Schofield, M. J., Biswas, I., and Hsieh, P. (2000). Requirement for Phe36 for DNA binding and mismatch repair by Escherichia coli MutS protein. Nucleic Acids Res *28*, 3564-3569.

Zhang, Y., Yuan, F., Presnell, S. R., Tian, K., Gao, Y., Tomkinson, A. E., Gu, L., and Li, G. M. (2005). Reconstitution of 5'-directed human mismatch repair in a purified system. Cell *122*, 693-705.

CHAPTER 2

Analysis of the interaction between the *Saccharomyces cerevisiae* Msh2-Msh6 and Mlh1-Pms1 complexes with DNA using a reversible DNA end blocking system

2.1 ABSTRACT

The Lac Repressor-Operator interaction was used as a reversible DNA end blocking system in conjunction with an IAsys biosensor instrument, which detects total internal reflectance and allows monitoring of binding and dissociation in real-time, to develop a system for studying the ability of MMR repair proteins to move along DNA. The Msh2-Msh6 complex bound to a mispaired base was found to be converted by ATP binding to a form that showed rapid sliding along the DNA and dissociation via the DNA ends and also showed slow, direct dissociation from the DNA. In contrast, the Msh2-Msh6 complex bound to a basepair containing DNA only showed direct dissociation from the DNA. The Mlh1-Pms1 complex formed both mispair-dependent and mispair-independent ternary complexes with the Msh2-Msh6 complex on DNA. The mispair-independent ternary complexes were formed most efficiently on DNA molecules with free ends under conditions where ATP hydrolysis did not occur, and only exhibited direct dissociation from the DNA. The mispair-dependent ternary complexes were formed in the highest yield on DNA molecules with blocked ends, required ATP and Magnesium for formation and showed both dissociation via the DNA ends and direct dissociation from the DNA.

2.2 INTRODUCTION

Errors that occur during DNA replication result in base-base mismatches and small insertion/deletion mismatches that if left uncorrected are fixed in the DNA as mutations by subsequent rounds of DNA replication. The DNA mismatch repair (MMR) system normally corrects such errors in the cell and is highly conserved from bacteria to humans (Harfe and Jinks-Robertson, 2000; Kolodner, 1996; Kolodner and Marsischky, 1999; Modrich, 1991; Modrich and Lahue, 1996). Defects in the system lead to increased rates of accumulation of mutations and in humans, inherited and somatic defects in MMR result in increased development of cancer (Lynch and de la Chapelle, 1999; Lynch and de la Chapelle, 2003; Peltomaki, 2003; Wheeler et al., 2000). The mechanism of MMR is best understood in the bacteria *Escherichia coli* (Harfe and Jinks-Robertson, 2000; Modrich, 1991; Modrich and Lahue, 1996). In *E. coli* the MutS protein, which appears to function as a homodimer, serves as the mispair recognition factor (Joshi et al., 2000; Mazurek et al., 2002; Schofield et al., 2001; Su et al., 1988). MutL, another homodimer, interacts with the MutS complex in the presence of a mispair and ATP and activates the endonucleolytic activity of MutH (Acharya et al., 2003; Au et al., 1992; Baitinger et al., 2003; Galio et al., 1999; Grilley et al., 1989; Hall and Matson, 1999; Schofield et al., 2001; Selmane et al., 2003). MutH makes single strand breaks in the newly synthesized daughter strand at transiently unmethylated GATC sequences allowing the unwinding of the DNA by UvrD coupled with the degradation of the error-containing strand by one of at least

four redundant exonucleases (Burdett et al., 2001; Welsh et al., 1987). Then DNA polymerase III holoenzyme can resynthesize the DNA strand leaving a nick that is subsequently sealed by DNA ligase (Lahue et al., 1989). In eukaryotic cells, three different MutS-homologues form two different heterodimeric complexes, called Msh2-Msh6 (MutSα) and Msh2-Msh3 (MutSβ) that together recognize base-base mispairs and insertion/deletion loops (Acharya et al., 1996; Alani, 1996; Drummond et al., 1995; Genschel et al., 1998; Gradia et al., 1997; Hess et al., 2002; Kolodner, 1996; Kolodner and Marsischky, 1999; Marsischky et al., 1996; Marsischky and Kolodner, 1999; Palombo et al., 1995; Palombo et al., 1996; Reenan and Kolodner, 1992a; Reenan and Kolodner, 1992b). Similarly, three different MutL-homologues form two different heterodimeric complexes, called Mlh1-Pms1 (MutLa; Pms1 *Saccharomyces cerevisiae* is Pms2 in humans) and Mlh1-Mlh3, that function in MMR (Flores-Rozas and Kolodner, 1998; Prolla et al., 1994; Wang et al., 1999). Like their bacterial homologues, the MSH and MLH complexes have been shown to interact on DNA in a reaction dependent on ATP, where they presumably can activate downstream effecter proteins (Blackwell et al., 2001b; Bowers et al., 2001; Bowers et al., 2000; Habraken et al., 1998; Kijas et al., 2003; Plotz et al., 2002; Raschle et al., 2002). However, at present little is known about how the MLH complexes interact with the MSH complexes, and how this activates the other proteins that function in MMR.

Three major models have been proposed to describe the initial steps of MMR in eukaryotes. Some groups postulate that, upon addition of ATP, the MSH complex can form a “sliding clamp” which can diffuse along DNA where downstream

signaling can take place (Gradia et al., 1999). The MLH complex presumably interacts with this sliding clamp and participates in the signaling process. This diffusion is assisted by the constant flux of new MSH complexes that load onto the recently vacated mispair, yielding a gradient of complexes that ensures the complexes ahead move away in a unidirectional manner, as has been suggested for bacterial *MutS* (Acharya et al., 2003) . Others argue for a second model, deemed the active translocation model. In this scenario, the Msh2-Msh6 complex binds a mispair and translocates off of the mispair in a manner dependent on ATP hydrolysis (Blackwell et al., 1998). By analogy to observations made in the *E. coli* system, this could result in the looping of DNA as the DNA is spooled through the Msh2-Msh6 complex and coordination of the other proteins that function in MMR with the mispair and the sites where excision initiates (Allen et al., 1997). Lastly, a static transactivation model has been described, predominantly based on studies of bacterial proteins. Here, the MLH complex stabilizes the MSH complex at the mispair and this static complex can then interact in trans with other MMR proteins located at different sites to initiate mispair dependent excision reactions (Selmane et al., 2003).

Many of the studies that provide the basis for the above models of the initial steps of MMR are based on data from biochemical studies with the Msh2-Msh6 (or MutS) complex and DNA in isolation. While there does seem to be movement of Msh2-Msh6 off the mispair along the DNA in the presence of ATP, it is not clear if this occurs in the presence of the Mlh1-Pms1 complex. Furthermore, while there is general agreement that the Msh2-Msh6 complex has a 20-30 fold higher specificity for

DNA containing a mispair compared with homoduplex DNA, it is not well established if, beyond its role as a downstream signaling complex, the Mlh1-Pms1 complex provides any additional mispair recognition specificity (Blackwell et al., 2001b; Kolodner and Marsischky, 1999; Marsischky and Kolodner, 1999).

The *lac* repressor-*lac* operator system has been used previously in studies of replication proteins tracking along DNA (Fu et al., 1996). Here this system was used in conjunction with an IAsys biosensor instrument, which detects total internal reflectance and allows monitoring of binding and dissociation in real-time, to develop a system for studying the ability of MMR proteins to move along DNA. In contrast to all previous MMR studies, use of the *lac* repressor-*lac* operator interaction as a method for blocking DNA ends allows for rapid dissociation of the blocking protein; addition of the allolactose analogue isopropylthiogalactoside (IPTG) induces dissociation of *lac* repressor (LacI) essentially instantaneously. We find that the Msh2-Msh6 complex has multiple modes of association onto a mispair and dissociation off of a mispair. Mlh1-Pms1 binds to Msh2-Msh6 that has been bound to a mispair in a specific, high affinity manner that is dependent on ATP and Magnesium (Mg^{2+}). It appears that the Msh2-Msh6-Mlh1-Pms1 ternary complex retains the ability to diffuse along DNA, although the affinity of the complex for DNA ends confounds the analysis of the rate of its movement along DNA. We have also defined reaction conditions under which the Msh2-Msh6 complex and the Mlh1-Pms1 complex undergo mispair-independent ternary complex formation, which raises implications concerning studies that have been reported previously.

2.3 RESULTS

The Msh2-Msh6 and Mlh1-Pms1 complexes form a mispair-independent ternary complex with DNA in buffer containing ATP -Mg^{2+}

Most studies demonstrating interactions between the Msh2-Msh6 mispair recognition complex and the Mlh1-Pms1 (Pms2 in humans) complex have utilized gel mobility shift assays. In addition, as discussed below, most observed interactions between Msh2-Msh6 and Mlh1-Pms1 (Pms2 in humans) on DNA have been documented in reactions containing ATP -Mg^{2+} or non-hydrolyzable ATP analogs, which may not represent physiological conditions. Because gel mobility shift assays do not allow straightforward determination of the amounts of individual proteins present in complexes an immunoprecipitation assay was used to analyze MMR protein-DNA interactions. A functionally tagged Mlh1-Pms1 complex was incubated with different combinations of Msh2-Msh6 and a DNA substrate containing a central GT mispair or GC basepair and either ADP or ATP with or without Mg^{2+}. The reaction products were then captured on antibody linked beads and analyzed by SDS-PAGE (Figure 2-1A). Under all reaction conditions, the Mlh1-Pms1 complex was quantitatively recovered. In the absence of DNA, no Msh2-Msh6 was co-precipitated regardless of whether the reactions contained ATP or ADP +/- Mg^{2+} (Figure 2-1A and data not shown). Little if any Msh2-Msh6 co-precipitated with Mlh1-Pms1 in reactions containing GT mispair DNA and either ADP +/- Mg^{++} or ATP +Mg^{2+}. However, in reactions containing the GT mispair DNA and ATP -Mg^{2+}, Msh2-Msh6

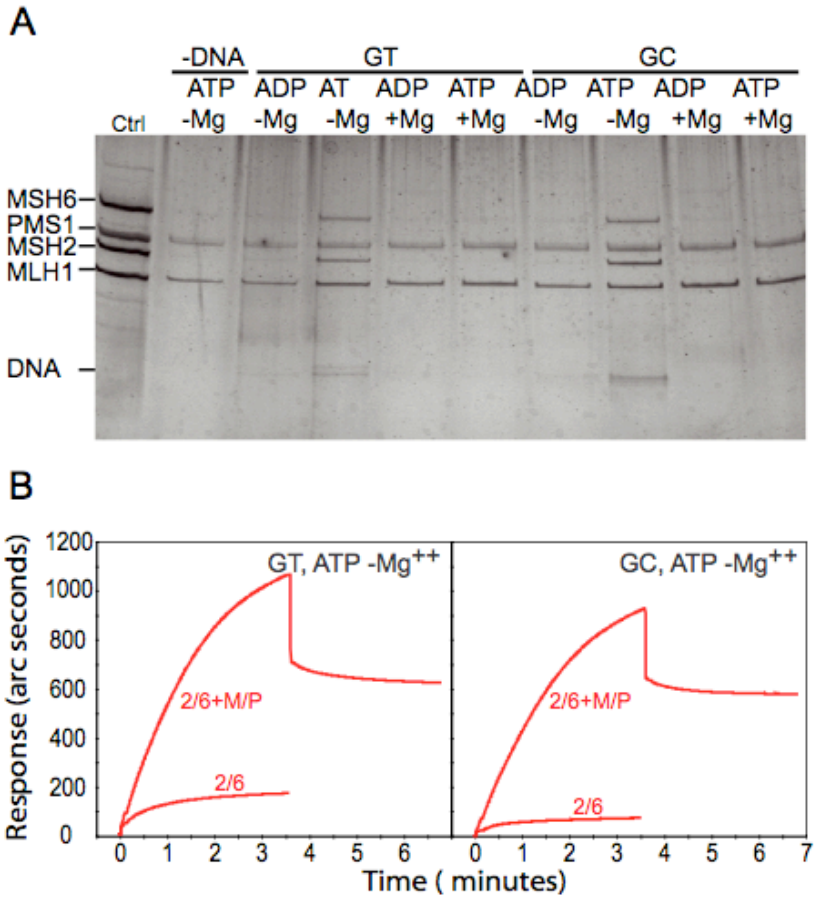

Figure 2-1. The Msh2-Msh6 and Mlh1-Pms1 complexes form a ternary complex with DNA independent of a mispair in buffer containing ATP but without Mg^{2+}. A. Reactions containing Msh2-Msh6, Mlh1-Pms1, DNA (duplex, GC or mispaired, GT), nucleotide (ADP or ATP) and Mg^{2+} (as indicated) were incubated and Mlh1-Pms1 containing complexes were recovered as described under "Experimental Procedures", separated by SDS-PAGE and the resulting gels silver stained. The positions of proteins (Mlh1, Msh2, Pms1, Msh6) and DNA are indicated on the left. Lane 1 (Ctrl) contains denatured Msh2-Msh6 and Mlh1-Pms1 proteins and was included as a size standard. B. Biosensor analysis of the association and dissociation of the Msh2-Msh6- Mlh1-Pms1 ternary complex formed on a DNA substrate containing a GT mispair or a GC basepair under standard conditions as described under "Materials and Methods," except that the 10 mM Mg^{2+} in the running buffer was replaced with 2 mM EDTA. In addition, 50 nM Msh2-Msh6 alone or 50 nM Msh2-Msh6 and 50 nM Mlh1-Pms1 were included as indicated along with 250 μM ATP in the running buffer. Association was monitored for 3.5 minutes, after which the protein-containing buffer was replaced with an equivalent buffer lacking protein, allowing dissociation of complex from the DNA.

co-precipitated in a 1:1 ratio with Mlh1-Pms1, and the DNA was also co- precipitated. Exactly the same results were obtained in parallel control experiments containing GC basepair DNA indicating that formation of this ternary complex did not require a mispaired base for assembly. To confirm this result, a similar experiment was performed using an IAsys biosensor instrument with immobilized DNA containing either a central GT mispair or GC basepair; these substrates are described in greater detail in subsequent sections (Figure 2-1B). In the presence of ATP -Mg^{2+} there was a 2 to 3-fold greater level of association of Msh2-Msh6 with GT mispair DNA compared to GC basepair DNA, although only a low level of association was seen, consistent with previous studies of the interaction of Msh2-Msh6 and DNA in the presence of ATP (data not shown) (Blackwell et al., 2001a; Gradia et al., 1997; Hess et al., 2002). Mlh1-Pms1 did not associate with either DNA in the absence of Msh2-Msh6 (data not shown). In contrast, under the same conditions there was a high level of protein association observed when the reactions contained an equimolar mixture of Msh2-Msh6 and Mlh1-Pms1 and there was little if any difference in the level of association with the GT DNA compared to the GC DNA. When the protein-containing buffer was removed from the reaction chamber and the same buffer but without protein was added, approximately 30% of the bound protein rapidly dissociated and the remaining protein did not dissociate from the DNA over a 4 min period. Consistent with the immunoprecipitation results, there was no difference between the level of stable association of protein with either the GT mispair or the GC basepair DNA.

On review of the literature we observed that many studies that have used gel shift assays to demonstrate ternary complex formation between Msh2-Msh6, Mlh1-Pms1 (or human Pms2) and mispair DNA only observed efficient ternary complex formation in reactions containing ATP -Mg^{2+} or in binding reactions stopped by the addition of a solution containing EDTA, which effectively adds an incubation step in buffer containing ATP -Mg^{2+} (Blackwell et al., 2001b; Bowers et al., 2001; Bowers et al., 2000; Kijas et al., 2003; Raschle et al., 2002). Surprisingly, several studies did not directly test whether ternary complex formation requires a mispair (Bowers et al., 2001; Bowers et al., 2000; Raschle et al., 2002). In four studies we could identify that directly tested mispair dependence, one concluded that ternary complex formation did not require a mispair (Plotz et al., 2002). The second concluded that even though ternary complexes were formed in the absence of a mispair, they were relevant to mismatch repair because they were not formed when a mismatch repair defective mutant protein was tested (Kijas et al., 2003). The third observed essentially equal levels of binding to both mispair and basepair containing substrates and suggested that the binding to the basepair substrate might be due to end binding (Blackwell et al., 2001b). A separate experiment in this study using a Biacore instrument to detect real-time binding, under conditions containing ATP and Mg^{2+}, apparently detected only mispair specific ternary complex formation and did not detect end affects (Blackwell et al., 2001b). The last was the only study using a gel-shift that observed efficient mispair specific ternary complex formation, but unlike other studies, this study did not detect ternary complex formation on DNA substrates that did not contain a mispair

despite the addition of EDTA at the end of the reaction (Habraken et al., 1998). These results in combination with the results presented in Figure 2-1 have led us to systematically reexamine the interaction between the Msh2-Msh6 and Mlh1-Pms1 complexes.

The *lac* repressor-*lac* operator interaction provides a reversible DNA end blocking system for use in studying interactions between MMR proteins and DNA

Previous studies utilizing both bacterial and eukaryotic MMR proteins, including both gel mobility shift and real-time binding and dissociation analysis (Biacore or IAsys) assays, have shown that blocking DNA ends limits the dissociation of MutS or the Msh2-Msh6 complex from DNA substrates containing a mispaired base upon addition of ATP (Acharya et al., 2003; Blackwell et al., 1998; Gradia et al., 1999; Schofield et al., 2001). All of these studies blocked the DNA substrate in an irreversible manner, by binding either avidin or an antibody to the DNA ends or by incorporating some type of DNA secondary structure at the DNA ends. The *lac* repressor-*lac* operator interaction has been extensively characterized and has been used previously to block various replication proteins from tracking along DNA (Fu et al., 1996; Matthews and Nichols, 1998). We took advantage of this system as a means to reversibly block DNA ends during analysis of the interaction of the Msh2-Msh6 and Mlh1-Pms1 complexes with DNA immobilized on an IAsys affinity biosensor. Briefly, the *lac* O_1 operator sequence was incorporated at one end of a 236-nucleotide

dsDNA fragment, containing either a central GT mispair or GC basepair, while the other end was biotinlyated and permanently blocked via its interaction with the avidin-coated cuvette surface. Control experiments demonstrated that LacI binding resulted in an increase of response of up to 60 arc seconds, which was dependent on the presence of the *lac* O_1 operator sequence. Upon addition of IPTG, LacI dissociated rapidly and completely, with the response dropping by a similar 60 arc seconds, with a half time of dissociation ~1.6 sec (Supplemental Figure 2-1). As will be discussed below, binding of LacI to the operator sequence at the DNA end provided a block that was completely reversible upon addition of IPTG.

Characterization of the Real-Time Reversible End-blocking System with the Msh2-Msh6 complex

The system was initially characterized by analyzing the steady-state levels of binding and dissociation of the Msh2-Msh6 complex with DNA under various conditions in the absence of LacI. In many cases, the dissociation data were fit to single- and multi-phase dissociation models and the results from the best fit are also reported (Table 2-1).

When association with the GT substrate was analyzed in the presence of different nucleotides, the highest level of Msh2-Msh6 binding was observed in ADP followed by progressively lower levels of binding in ATP and ATP-γS (Figure 2-2A). When Msh2-Msh6 was bound to the GT substrate in the presence of ADP and the protein-containing buffer was replaced with buffer containing different nucleotides,

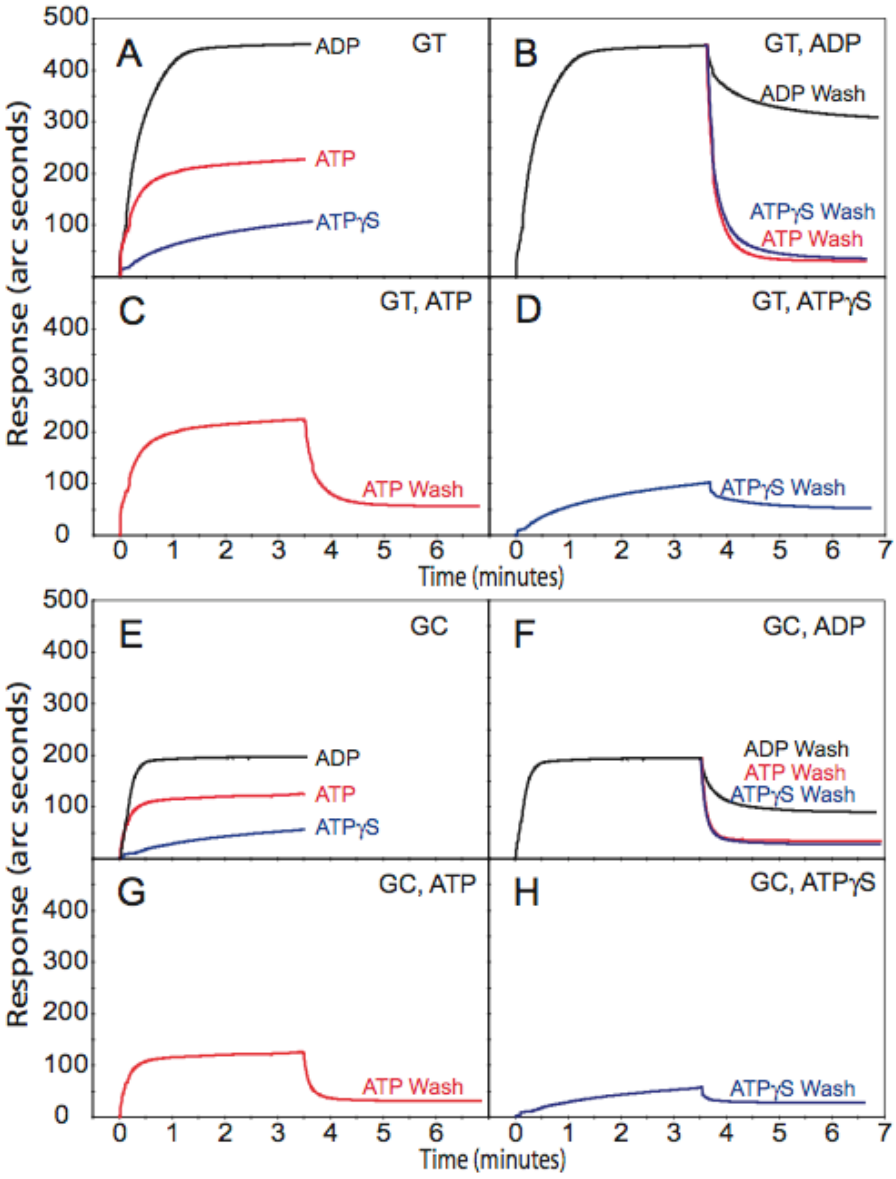

Figure 2-2. Msh2-Msh6 binds specifically to a mispair in the presence of ADP and rapidly dissociates in the presence of ATP or ATP-γS. Biosensor analysis of the association and dissociation of the Msh2-Msh6 complex with a DNA substrate containing a GT mispair (A, B, C, D) or a GC basepair (E, F, G, H) under standard conditions as described under "Experimental Procedures." A. Binding of 50 nM Msh2-Msh6 to a DNA substrate containing a GT mispair with either 250 μM ATP (*red line*), 250 μM ATP-γS (*blue line*) or no nucleotide (*black line*) in addition to the 25 μM ADP present in the standard running buffer. B. 50 nM Msh2-Msh6 was bound in running buffer on a DNA substrate containing a GT mispair. Dissociation was observed by replacing the protein-containing buffer with running buffer containing the nucleotide as indicated according to the color scheme described in "A". C. 50 nM Msh2-Msh6 was bound in running buffer containing 250 μM ATP on a DNA substrate containing a GT mispair. Dissociation was observed by replacing the protein-containing buffer with running buffer containing 250 μM ATP. D. Same as "C", except ATP-γS was used in place of ATP. E, F, G and H were same as A, B, C and D respectively, except a DNA substrate containing a GC basepair was used in place of the substrate containing a GT mispair.

Table 2-1. Half-times of dissociation for the Msh2/6 and Msh2/6+Mlh1/Pms1 complexes. Association and dissociation conditions are described under "Materials and Methods" and in the legends to individual figures. Note that when the dissociation conditions indicate IPTG alone, IPTG was added thus freeing the end of the DNA substrate while leaving the concentration of proteins in solution essentially unchanged. The results reported are the average of the half-times of dissociation from three or more independent experiments ± the standard deviation (SD). As indicated under "Materials and Methods", the half-times were calculated by fitting the dissociation data to either a single exponential or double exponential decay model; the R^2 values for the fit were always greater than 95%. In the case where a double exponential decay model was used, a second half-time of dissociation is reported ($t_{1/2}$ (B)) and the average percent of the total amplitude that each phase constitutes is reported in brackets.

Protein	Substrate	ON	OFF	$T_{1/2}$ (A) ± SD	$T_{1/2}$ (B) ± SD	R^2
				s		
Msh2/6						
	GT Unblocked	ADP	ADP	27.0 ± 9.5	-	0.98
		ADP	ATP	8.0 ± 2.7	-	0.99
		ADP	ATPγS	10.8 ± 3.2	-	0.98
		ATP	ATP	9.3 ± 3.6	-	0.97
		ATPγS	ATPγS	29.3 ± 0.6	-	0.98
	GT Blocked	ADP	ATP	23.7 ± 7.3	-	0.99
		ADP	ATPγS	27.8 ± 0.2	-	0.98
		ADP	ATP+IPTG	10.2 ± 2.3	-	0.99
		ADP	ATPγS+IPTG	13.1 ± 1.3	-	0.99
		ATP	ATP	20.9 ± 4.5	-	0.99
		ATP	IPTG	5.6 ± 2.8	-	0.99
		ATP	ATP+IPTG	8.4 ± 3.8	-	0.99
		ATPγS	ATPγS	28.3 ± 11.1	-	0.99
Msh2/6+Mlh1/Pms1						
	GT Unblocked	ATP	ATP	26.2 ± 0.3 [75]	0.6 ± 0.2 [25]	0.99
	GT Blocked	ATP	ATP	31.9 ± 6.1	-	0.99
		ATP	IPTG	21.3 ± 0.4	-	0.98
		ATP	ATP+IPTG	21.6 ± 0.5	-	0.99
Msh2/6*						
	GC Unblocked	ADP	ADP	17.0 ± 9.9	-	0.98
		ADP	ATP	5.0 ± 1.9	-	0.99
		ATP	ATP	8.4 ± 3.2	-	0.96
	GC Blocked	ADP	ATP	6.6 ± 4.0	-	0.96
		ATP	ATP	10.0 ± 2.6	-	0.96
Msh2/6+Mlh1/Pms1						
	GC Unblocked	ATP	ATP	16.3 ± 1.0 [86]	0.5 ± 0.1 [14]	0.99
	GC Blocked	ATP	ATP	13.8 ± 5.7	-	0.99
		ATP	ATP+IPTG	16.0 ± 8.3	-	0.99

*, The dissociation conditions of ATP+IPTG were not analyzed in the case of Msh2-Msh6 bound to end-blocked GC substrate because the additional dissociation seen relative to ATP alone was entirely attributable to dissociation of the LacI protein and the fraction of dissociation attributable to LacI is large enough to confound the dissociation analysis.

ATP and ATP-γS caused identical, virtually complete rapid mono-phasic dissociation with half-times of dissociation of ~8 to 11 sec, whereas ADP caused much less dissociation at a slower apparent rate ($t_{1/2}$ ~27 sec; Figure 2-2B and Table 2-1). The remaining protein appeared to be stably bound as further ADP washes resulted in little additional dissociation; similar results have been seen in other studies with *S. cerevisiae* and human Msh2-Msh6, as well as with *E. coli* MutS (Acharya et al., 2003; Antony and Hingorani, 2003; Hess et al., 2002; Selmane et al., 2003). When Msh2-Msh6 was bound to the GT substrate in the presence of ATP, less binding was observed than in the presence of ADP; ATP-induced dissociation under this condition was as rapid as ATP-induced dissociation observed when binding occurred in the presence of ADP, and the amount of binding that was resistant to ATP-induced dissociation was the same in both cases (Figure 2-2C and Table 2-1). When Msh2-Msh6 was bound to the GT substrate in the presence of ATP-γS, only a low level of binding was observed and most of the bound protein was resistant to dissociation in buffer containing ATP-γS (Figure 2-2D). A parallel series of experiments was performed using a GC containing control DNA substrate (Figures 2-2E to H). Virtually the same results were obtained with the GT and GC containing substrates with two exceptions: regardless of the nucleotide present, the level of binding to the GC substrate was ~40% that observed with the GT substrate, which presumably reflects the mispair binding specificity of Msh2-Msh6; and ADP induced a greater overall extent of dissociation from the GC substrate compared to the GT substrate (additional features of the dissociation from GC basepair substrates are discussed

below). Consistent with this, it has previously been suggested that ADP contributes to mispair specificity of human Msh2-Msh6 by reducing non-specific DNA binding (Blackwell et al., 1998).

A parallel series of experiments was then performed in the presence of LacI protein to block the ends of the substrates. The presence of LacI or IPTG was not found to have any effect on Msh2-Msh6 binding to or dissociation off of DNA substrates lacking the *lac* O_1 operator sequence (data not shown). When association with the GT substrate was analyzed in the presence of LacI, the level of Msh2-Msh6 binding observed in ADP was slightly lower than observed on the unblocked substrate (compare Figure 2-3A to Figure 2-2A) consistent with the idea that LacI may prevent a small amount of binding of Msh2-Msh6 to DNA ends. When ATP was present, the level of association was greater than two-fold higher than observed with the unblocked GT substrate (see inset and compare Figure 2-3A to Figure 2-2A) consistent with the idea that blocking the DNA ends reduces dissociation under these reaction conditions (Blackwell et al., 1998; Gradia et al., 1999). In contrast, the level of binding observed in ATP-γS was essentially the same on the blocked and unblocked substrates (Figures 2-2A, D and 2-3A, D). When Msh2-Msh6 was bound to the end-blocked GT substrate in the presence of ADP and IPTG was added, a small amount of dissociation was observed that was equivalent to the amount of LacI bound (Figure 2-3B). When Msh2-Msh6 was bound to the GT substrate in the presence of ADP and LacI and the protein-containing buffer was replaced with buffer containing LacI and different nucleotides, ATP and ATP-γS caused identical, slow single phase ($t_{1/2}$ ranging from 24

Figure 2-3. Steady-state binding of the Msh2-Msh6 complex is dramatically increased on an end-blocked DNA substrate containing a GT mispair in buffer containing ATP and Mg^{2+}.
Biosensor analysis of the association and dissociation of the Msh2-Msh6 complex with a DNA substrate containing a GT mispair (A, B, C, D) or a GC basepair (E, F, G, H), end-blocked with 100 nM LacI (unless otherwise indicated) under standard conditions as described under "Experimental Procedures." A. Binding of 50 nM Msh2-Msh6, with either 250 μM ATP (*red line*), 250 μM ATP-γS (*blue line*) or no nucleotide (*black line*) in addition to the 25 μM ADP present in the standard running buffer, to a DNA substrate containing a GT mispair, end blocked with LacI. Binding of 50 nM Msh2-Msh6 with 250 μM ATP on an unblocked GT mispair *(dotted red line)* is included for comparison. B. 50 nM Msh2-Msh6 was bound in running buffer (ADP) to a DNA substrate containing a GT mispair and end blocked with LacI. After association for 3.5 minutes, dissociation was observed under one of five following conditions. Either 5 μL of running buffer containing 10 mM IPTG (1 mM final concentration) was added to the microcuvette to release LacI from DNA (*green line*), or the protein containing buffer was replaced with running buffer containing 250 μM ATP and LacI (*red line*), 250 μM ATP and 1 mM IPTG (*dashed red line*), 250 μM ATP-γS and LacI (*blue line*), or 250 μM ATP-γS and 1 mM IPTG (*dashed blue line*). C. 50 nM Msh2-Msh6 was bound in running buffer containing 250 μM ATP to a DNA substrate containing a GT mispair, end blocked with LacI. Binding of 50 nM Msh2-Msh6 with 250 μM ATP on an unblocked GT mispair *(dotted red line)* is included for comparison. Various methods of dissociation are shown, as indicated according to the scheme in "B". D. Same as "C", except ATP-γS was used in place of ATP. E, F, G and H were same as A, B, C and D respectively, except a DNA substrate containing a GC basepair was used in place of the substrate containing a GT mispair. Note the small IPTG induced decrease (B, D, F, G and H) is due to LacI dissociation, while the larger decrease (C) is mainly due to rapid Msh2-Msh6 dissociation from newly freed ends.

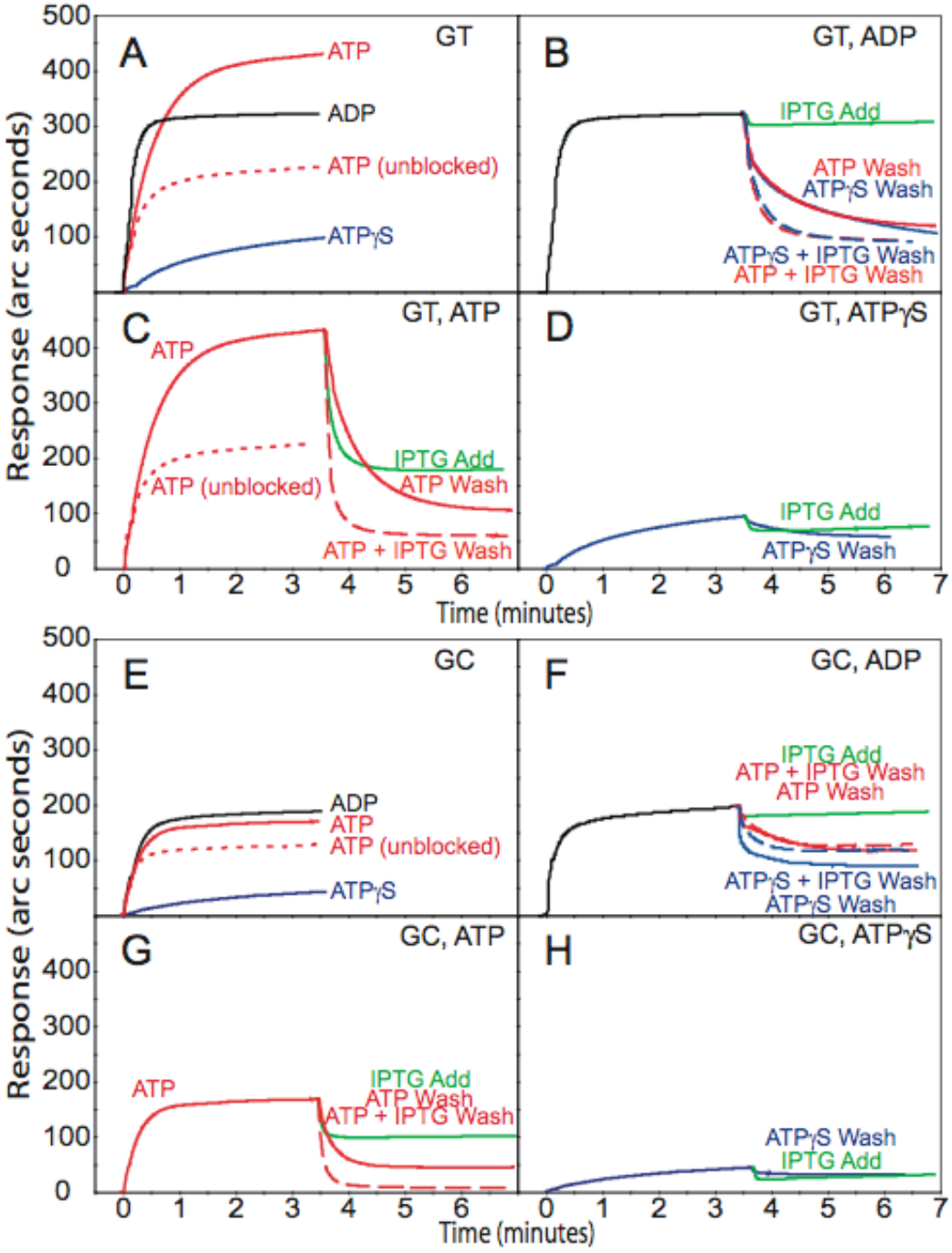
A
GT
ATP
ADP
ATP (unblocked)
ATPγS
B
GT, ADP
IPTG Add
ATP Wash
ATPγS Wash
ATPγS + IPTG Wash
ATP + IPTG Wash
C
GT, ATP
ATP
ATP (unblocked)
IPTG Add
ATP Wash
ATP + IPTG Wash
D
GT, ATPγS
IPTG Add
ATPγS Wash
Response (arc seconds)
Time (minutes)
E
GC
ADP
ATP
ATP (unblocked)
ATPγS
F
GC, ADP
IPTG Add
ATP + IPTG Wash
ATP Wash
ATPγS + IPTG Wash
ATPγS Wash
G
GC, ATP
ATP
IPTG Add
ATP Wash
ATP + IPTG Wash
H
GC, ATPγS
ATPγS Wash
IPTG Add
Response (arc seconds)
Time (minutes)

to 28 sec) partial dissociation (Figure 2-3B and Table 2-1); after the dissociation under these conditions reached a plateau, addition of IPTG induced a rapid single phase dissociation ($t_{1/2}$ ranging from 5 to 7 sec) of the remaining bound protein (data not shown). Dissociation induced by replacing the protein-containing buffer with buffer containing IPTG and either ATP or ATP-γS was the same (single phase; $t_{1/2}$ ranging from 10 to 13 sec) and was more rapid than dissociation induced by ATP or ATP-γS inthe presence of LacI (Figure 2-3B and Table 2-1). The dissociation of Msh2-Msh6 bound to the GT substrate in the presence of LacI and ATP was also analyzed (Figure 2-3C). After binding under these conditions, addition of IPTG resulted in rapid mono-phasic dissociation of Msh2-Msh6 ($t_{1/2}$ of ~6 sec; Table 2-1) and reestablishment of equilibrium binding levels that were the same as observed during the association of Msh2-Msh6 with unblocked GT substrate in the presence of ATP (see inset and compare Figures 2-2A, 2-2C and 2-3C). When the bound protein was challenged with buffer containing ATP and LacI, extensive mono-phasic dissociation was observed but the apparent rate was reduced ($t_{1/2}$ of ~21 sec; Table 2-1). In contrast, when the bound protein was challenged with buffer containing ATP and IPTG, there was yet more extensive mono-phasic dissociation at a more rapid rate ($t_{1/2}$ of ~8 sec; Table 2-1). Binding and dissociation of Msh2-Msh6 from the end-blocked GT substrate in the presence of ATP-γS was the same as observed with the unblocked GT substrate (compare Figures 2-2D and 2-3D). As will be discussed in greater detail below, these results are consistent with the view that when Msh2-Msh6 binds to a GT mispair in the presence of ADP and is challenged with ATP or ATP-γS or binds in the presence

of ATP (under hydrolysis conditions) but not when binding occurs in the presence of ATP-γS, it is converted to a form that exhibits rapid, end-dependent dissociation.

A similar series of experiments was performed using a end-blocked GC control DNA substrate (Figures 2-3E to 2-H). Blocking the end of the GC substrate had much less affect on Msh2-Msh6 binding than blocking the end of the GT substrate and there were only small differences in binding to blocked vs. unblocked GC substrate DNA. Binding to the blocked GC substrate in the presence of ATP resulted in a small increase in binding compared to the unblocked substrate, but not to the extent seen with the GT substrates (compare Figure 2-3E to 2-3A). Addition of IPTG after binding to the blocked GC substrate in the presence of ATP and LacI resulted in a small but significant amount of dissociation of Msh2-Msh6 beyond the amount of dissociation attributable to LacI, but not to the extent seen with the GT substrates (compare Figure 2-3G to 2-3C). Finally, challenging the protein bound to the blocked GC substrate in the presence of ATP and LacI with buffer containing ATP and IPTG resulted in somewhat more dissociation than seen with buffer containing ATP and LacI; however, the difference between these two dissociation conditions was not as large as seen for the blocked GT substrate and was primarily attributable to dissociation of LacI (compare Figures 2-3G with 2-3C). Kinetic analysis of ATP induced dissociation of Msh2-Msh6 that had been loaded onto either unblocked or end blocked GC basepair substrates in the presence of ADP or ATP (Table 2-1; also see Figures 2-2F and G and 2-3F and G) showed that there was no significant difference between the half-times of dissociation under these different conditions; this is in

marked contrast to the results seen with the GT mispair substrate. These results indicate that binding of Msh2-Msh6 to GC basepair substrate does not result in the conversion of Msh2-Msh6 to a form that shows end-dependent dissociation.

The Msh2-Msh6 and Mlh1-Pms1 complexes form a mispair-dependent, dynamic ternary complex on end-blocked DNA

Immunoprecipitation assays and fractionation of potential protein complexes by gel-filtration failed to show any evidence of interaction between Msh2-Msh6 and Mlh1-Pms1 complexes in buffer containing Mg^{2+} with or without ATP (data not shown). These assays can probably only reliably detect relatively stable interactions. However, we were able to demonstrate such interactions using the IAsys affinity biosensor system, which allows monitoring binding and dissociation in real-time.

Msh2-Msh6 and Mlh1-Pms1 were incubated at equimolar concentrations with various nucleotides and the immobilized GT mispair or GC basepair substrates described above. When incubated with ADP, there was virtually no increased complex formation, as the observed association levels were equivalent to that seen with Msh2-Msh6 alone, regardless of the presence of a mispair (Figures 2-4A, B, E and F). There was little if any binding of Mlh1-Pms1 to DNA under any of the assay conditions used (Figures 2-4 and 2-5). Upon inclusion of ATP in the buffer with Msh2-Msh6 and Mlh1-Pms1, there was significantly increased binding to both the GT mispair and GC basepair substrates (Figures 2-4A, C, E and G); a ~five-fold increase in binding was observed compared with Msh2-Msh6 + ATP and DNA alone (also

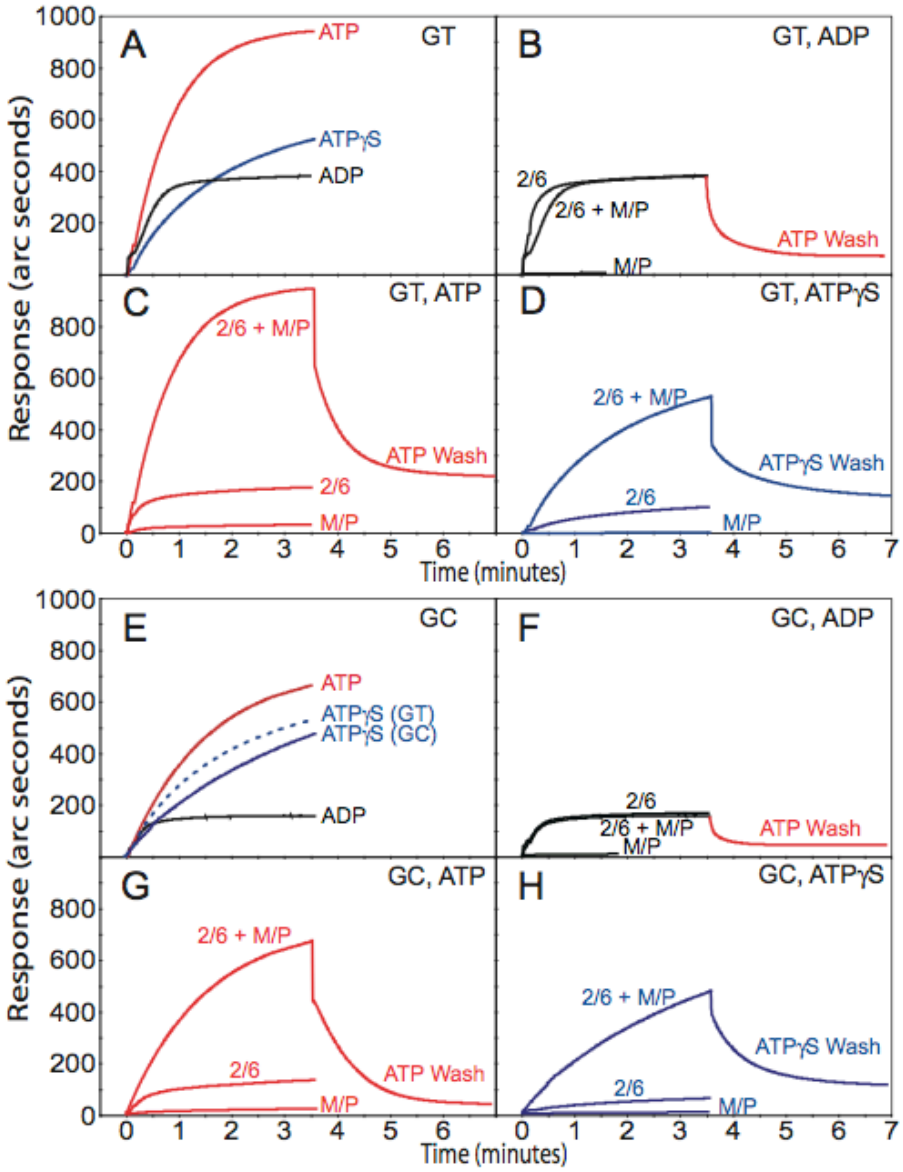

Figure 2-4. The Mlh1-Pms1 complex can form a ternary complex with the Msh2-Msh6 complex and DNA in buffer containing ATP. Biosensor analysis of the association and dissociation of the Mlh1-Pms1-Msh2-Msh6 ternary complex with a DNA substrate containing a GT mispair (A, B, C, D) or a GC basepair (E, F, G, H) under standard conditions as described under "Experimental Procedures." A. Binding of 50 nM Msh2-Msh6 and 50 nM Mlh1-Pms1 with either 250 μM ATP (*red line*), 250 μM ATP-γS (*blue line*) or no nucleotide (*black line*) in addition to the 25 μM ADP present in the standard running buffer on a DNA substrate containing a GT mispair. B. 50 nM Mlh1-Pms1 and 50 nM Msh2-Msh6 were bound in running buffer on a DNA substrate containing a GT mispair. Dissociation was observed by replacing the protein-containing buffer with running buffer containing 250 μM ATP. Association reactions consisting of 50 nM Msh2-Msh6 alone or 50 nM Mlh1-Pms1 alone were included as controls. C & D. Reactions were performed as in "B", except 250 μM ATP (C) or 250 μM ATP-γS (D) was included in all buffers. E, F, G and H were same as A, B, C and D respectively, except a DNA substrate containing a GC basepair was used in place of the substrate containing a GT mispair. Binding of 50 nM Msh2-Msh6 and 50 nM Mlh1-Pms1 with 250 μM ATP-γS on a GT mispair *(dotted blue line)* is included for comparison in "E".

compare with Figure 2-2). In binding reactions containing Msh2-Msh6, Mlh1-Pms1 and ATP, there was ~30% more binding to the GT mispair substrate compared to the GC basepair substrate (compare Figures 2-4A and 2-4C to 2-4E and 2-4G). Increased binding of Msh2-Msh6 and Mlh1-Pms1 in the presence of ATP-γS was observed compared to Msh2-Msh6 alone, although there was only a small if any increase in binding to the GT mispair substrate compared to the GC basepair substrate (Figure 2-4D and H).

Regardless of whether ATP or ATP-γS was present in the binding reaction, the complex that assembled on either the GT mispair or GC basepair substrates was dynamic and dissociated when the binding buffer was exchanged with buffer without Msh2-Msh6 and Mlh1-Pms1, but containing the nucleotide present in the original binding reaction. There was an initial phase of rapid dissociation in both cases followed by a slower phase (Table 2-1). The rapid dissociation phase was only seen when binding occurred on substrates that had free ends; however, we have little insight into the nature of the proteins that make up this rapid dissociation phase. It should be noted that the rapid ($t_{1/2}$ of ~1 sec) and slow ($t_{1/2}$ of ~26 sec) phases of dissociation of Msh2-Msh6 and Mlh1-Pms1 off of the GT mispair in the presence of ATP were more rapid and more slow, respectively, than observed for Msh2-Msh6 alone ($t_{1/2}$ of ~9 sec) (Table 2-1) making it unlikely that either phase of dissociation was due to dissociation of Msh2-Msh6 alone.

A series of experiments was performed to determine if blocking the ends of the DNA substrates would prevent end-dependent dissociation of the ternary complex

between Msh2-Msh6, Mlh1-Pms1 and DNA, as it had with Msh2-Msh6 bound to GT mispair substrate DNA. Similar to their behavior on DNA with unblocked ends, incubating Msh2-Msh6 and Mlh1-Pms1 with the DNA in the presence of LacI to block the ends in binding buffer containing ADP failed to produce any significant association beyond that observed with Msh2-Msh6 alone (Figure 2-5A, B, E and F). However, compared to the results seen with the unblocked DNA substrates, incubating the proteins in the presence of LacI and ATP resulted in a small increase in complex formation on the GT mispair substrate compared to a 25% decrease in complex formation on the GC basepair substrate (Figure 2-5A, C, E and G). This resulted in a two-fold preference for complex formation on the GT mispair substrate vs. the GC basepair substrate and further suggests that Msh2-Msh6 and Mlh1-Pms1 can assemble onto the ends of DNA. Blocking the ends of the GT mispair and GC basepair substrates with LacI when the binding reactions were performed in the presence of ATP-γS (Figure 2-5D and H) resulted in a modest preference for the GT mispair substrate and an ~50% reduction in binding compared to the unblocked substrates (see inset and compare Figures 2-5D and H with Figures 2-4D and H); furthermore, in the case of both end-blocked substrates there was considerably less binding in the presence of ATP-γS compared to ATP.

Dissociation of the complex formed by Msh2-Msh6 and Mlh1-Pms1 with DNA under conditions where the ends were blocked with LacI was studied using the same three conditions as described above for dissociation of the Msh2-Msh6-DNA complex. When Msh2-Msh6 and Mlh1-Pms1 were bound to the end-blocked GT

Figure 2-5. Mispair specificity of Mlh1-Pms1-Msh2-Msh6 ternary complex is improved upon blocking the end of the DNA substrate.
Biosensor analysis of the association and dissociation of the Mlh1-Pms1-Msh2-Msh6 complex with a DNA substrate containing a GT mispair (A, B, C, D) or a GC basepair (E, F, G, H), end-blocked with 100 nM LacI (unless otherwise indicated) under standard conditions as described under "Experimental Procedures." A. Binding of 50 nM Msh2-Msh6 and 50 nM Mlh1-Pms1 with either 250 μM ATP (*red line*), 250 μM ATP-γS (*blue line*) or no nucleotide (*black line*) in addition to the 25 μM ADP present in the standard running buffer on a DNA substrate containing a GT mispair, end blocked with LacI. Binding of 50 nM Msh2-Msh6 and 50 nM Mlh1-Pms1 with 250 μM ATP on an unblocked GT mispair substrate *(dotted red line)* is included for comparison. B. 50 nM Msh2-Msh6 and 50 nM Mlh1-Pms1 was bound in running buffer (ADP) on a DNA substrate containing a GT mispair and end blocked with LacI. After association was allowed to proceed, dissociation was observed under one of two following conditions. Either 5 μL of running buffer containing 10 mM IPTG (1 mM final concentration) was added to the microcuvette to release LacI from DNA (*green line*), or the protein-containing buffer was replaced with buffer containing 250 μM ATP and 100 nM LacI (*red line*). Association reactions consisting of 50 nM Msh2-Msh6 alone or 50 nM Mlh1-Pms1 alone were included as controls. C & D. Reactions were performed as in "B", except 250 μM ATP (C) or 250 μM ATP-γS (D) was included in all buffers. Binding of 50 nM Msh2-Msh6 and 50 nM Mlh1-Pms1 with 250 μM ATP-γS on an unblocked GT mispair substrate *(dotted blue line)* is included for comparison. Also, an additional dissociation reaction was observed by replacing the protein containing buffer with running buffer containing ATP (C) or ATP-γS (D) and 1 mM IPTG (*dashed lines*). E, F, G and H were same as A, B, C and D respectively, except a DNA substrate containing a GC basepair was used in place of the substrate containing a GT mispair.

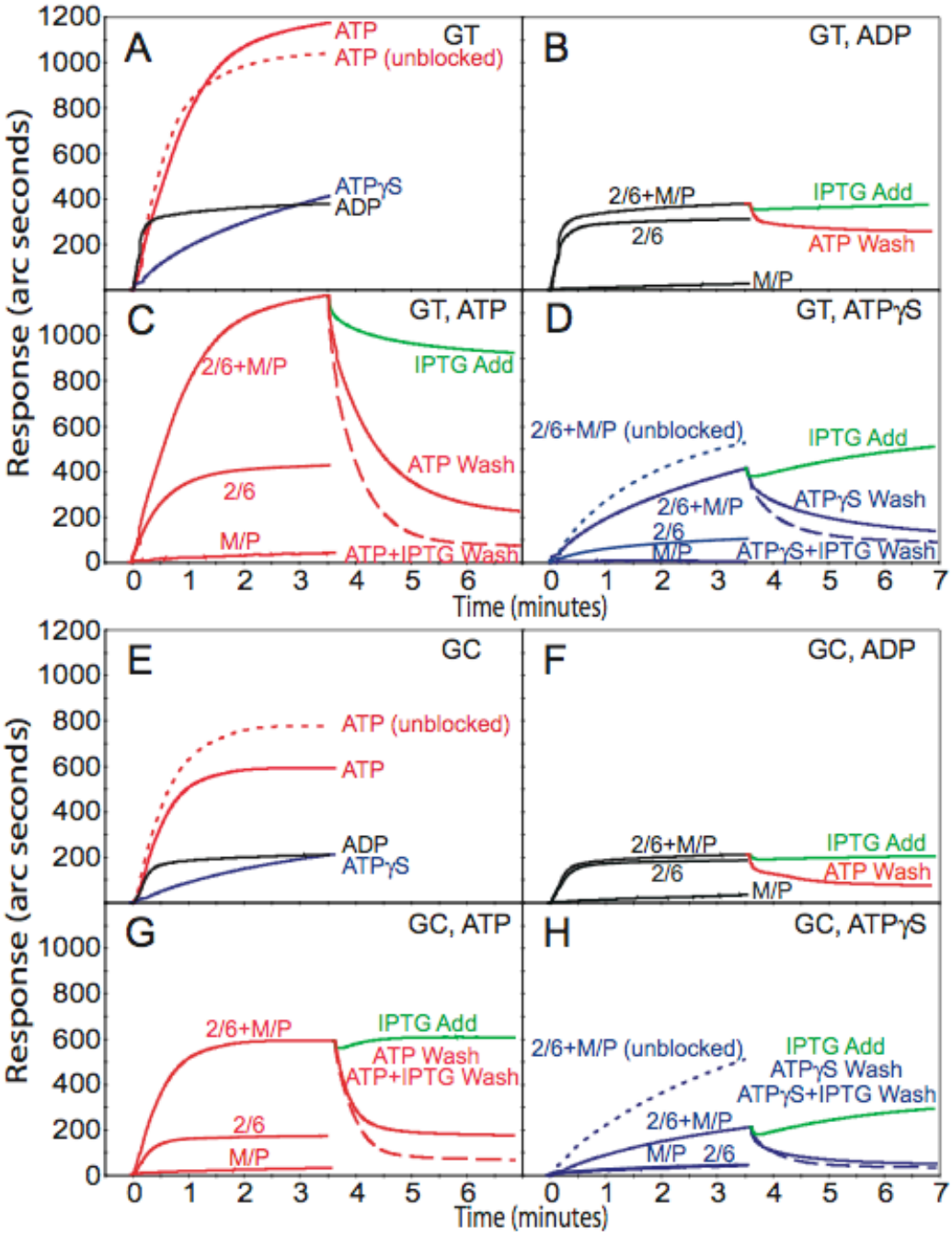
A
GT
ATP
ATP (unblocked)
ATPγS
ADP
B
GT, ADP
2/6+M/P
2/6
M/P
IPTG Add
ATP Wash
C
GT, ATP
2/6+M/P
2/6
M/P
IPTG Add
ATP Wash
ATP+IPTG Wash
D
GT, ATPγS
2/6+M/P (unblocked)
2/6+M/P
2/6
M/P
IPTG Add
ATPγS Wash
ATPγS+IPTG Wash
E
GC
ATP (unblocked)
ATP
ADP
ATPγS
F
GC, ADP
2/6+M/P
2/6
M/P
IPTG Add
ATP Wash
G
GC, ATP
2/6+M/P
2/6
M/P
IPTG Add
ATP Wash
ATP+IPTG Wash
H
GC, ATPγS
2/6+M/P (unblocked)
2/6+M/P
M/P
2/6
IPTG Add
ATPγS Wash
ATPγS+IPTG Wash
Response (arc seconds)
Time (minutes)

mispair substrate in the presence of ADP (note that Mlh1-Pms1 does not interact with Msh2-Msh6 under these conditions), addition of IPTG to dissociate LacI did not result in decreased binding beyond that predicted to be due to dissociation of LacI (Figure 2-5B). Challenging the bound protein with buffer containing ATP and LacI resulted in a modest amount of dissociation of bound protein, but not to the extent seen when just Msh2-Msh6 had been bound (Figure 2-3B); this limited dissociation may be due to residual protein left in the cuvette after washing away the majority of the free protein (~5 to 10% of the protein remains in the cuvette), that now, upon addition of ATP is able to form ternary complex, yielding conditions similar to those seen when the proteins are incubated together in the presence of ATP and then washed away (Figure 2-5B and 2-5C).

When Msh2-Msh6 and Mlh1-Pms1 were bound to the end-blocked GT mispair substrate in the presence of ATP, addition of IPTG to dissociate LacI resulted in a small but significant decrease in the amount of protein bound, which was greater than the amount of bound LacI (Figure 2-5C), but not to the extent seen when Msh2-Msh6 alone was analyzed under these conditions (Figure 2-3C). This dissociation occurred at a much slower apparent rate ($t_{1/2}$ of ~21 sec) compared with the dissociation of Msh2-Msh6 alone under the same conditions ($t_{1/2}$ of ~6 sec) (Table 2-1). When the bound protein was challenged with buffer containing ATP and LacI, extensive dissociation was observed; however, when the bound protein was challenged with buffer containing ATP and IPTG, more extensive dissociation was observed and the apparent rate of dissociation was greater ($t_{1/2}$ of ~22 sec vs. ~32 sec) (Figure 2-5C and

Table 2-1). These results are consistent with the view that when Msh2-Msh6 and Mlh1-Pms1 assemble onto an end-blocked GT mispair substrate, the resulting ternary complex can undergo both direct and end-dependent dissociation; however, the rate of end-dependent dissociation of the ternary complex appears to be slower than the rate of end-dependent dissociation of Msh2-Msh6 alone.

When Msh2-Msh6 and Mlh1-Pms1 were bound to the end-blocked GT mispair substrate in the presence of ATP-γS, addition of IPTG to dissociate LacI caused increased binding in contrast to the dissociation seen when binding occurred in the presence of ATP consistent with the idea that under these conditions Msh2-Msh6 and Mlh1-Pms1 bind to DNA ends (compare Figure 2-5C and 2-5D). In contrast, challenging the bound protein with buffer containing ATP-γS and LacI or ATP-γS and IPTG (these buffers do not contain Msh2-Msh6 or Mlh1-Pms1) resulted in extensive dissociation, with modestly more dissociation seen under conditions where the bound LacI was released. Virtually the same dissociation properties were observed when Msh2-Msh6 and Mlh1-Pms1 were bound to the end-blocked GC basepair substrate in the presence of ATP-γS (Figure 2-5H) with the exception that there was less initial binding to the GC substrate. This dissociation behavior combined with the observations that Msh2-Msh6 does not appear to bind to a mispaired base in the presence of ATP-γS and the low level of ternary complex formation seen on end blocked substrates compared to that seen in the presence of ATP suggests that the ternary complex that forms in the presence of ATP-γS is a nonspecific or non-productive complex.

Finally, when Msh2-Msh6 and Mlh1-Pms1 were bound to the end-blocked GC basepair substrate in the presence of ATP, addition of IPTG to dissociate LacI resulted in a small increase in binding (Figure 2-5G). In contrast, challenging the bound protein with buffer containing ATP and LacI or ATP and IPTG resulted in extensive dissociation, with modestly more dissociation seen when the bound LacI was released (this is primarily attributable to the release of the bound LacI); the $t_{1/2}$ of dissociation was similar under these later conditions (~14 sec vs. ~16 sec; Table 2-1) but dissociation was more rapid than seen with the GT substrate ($t_{1/2}$ of ~32 sec for ATP + LacI and ~22 sec for ATP + IPTG). This difference in dissociation behavior is consistent with the idea that the ternary complex formed on the GC basepair substrate is a nonspecific complex that only undergoes direct dissociation in contrast to the distinctly different properties of the ternary complex that formed on end blocked GT mispair substrates.

ATP dependent association of the Mlh1-Pms1 complex with the Msh2-Msh6 complex previously bound at a mispair in the presence of ADP

We next determined if Mlh1-Pms1 would bind to Msh2-Msh6 that was pre-bound to DNA. In these experiments (Figure 2-6), Msh2-Msh6 was added to microcuvettes containing either bound GT mispair or GC basepair substrate in buffer containing ADP +/- LacI to block the ends of the substrate. After association of the Msh2-Msh6 complex with the substrate, Mlh1-Pms1 was added along with ADP, ATP or ATP-γS. In experiments with both substrates with or without LacI, there was no

additional protein bound when Mlh1-Pms1 was added in combination with ADP (data not shown). However, when Mlh1-Pms1 was added in combination with ATP or ATP-γS in the absence of LacI there was significant additional binding, although there was only a small preference for the GT mispair substrate compared to the GC basepair substrate (Figure 2-6A vs. 2-6C and 2-6B vs. 2-6D). When the ends of the DNA substrate were blocked with LacI and Mlh1-Pms1 was added in the presence of either ATP or ATP-γS there was significant additional protein binding on the GT mispair substrate and to a lesser extent on the GC basepair substrate (see inset; Figure 2-6E, F, G and H). In addition, specificity for the GT mispair was significantly enhanced due to a reduction of binding to the GC-basepair substrate (compare Figure 2-6C to 2-6G). In the presence of ATP-γS there was a significant reduction in overall binding to the blocked end substrates compared to the unblocked substrates suggesting there is significant end binding in the presence of ATP-γS (see inset; compare Figure 2-6B to 2-6F and 2-6D to 2-6H); this effect was not seen to the same extent when binding reactions were performed with the GT mispair substrate in the presence of ATP (compare Figure 2-6A to 2-6E and 2-6C to 2-6G). The net complex formation was about the same when Mlh1-Pms1 and ATP were added to Msh2-Msh6 that was prebound in the presence of ADP compared with both complexes mixed together in the presence of ATP (see inset; compare Figure 2-6 with Figures 2-4 and 2-5). In contrast, there was only a small amount of ternary complex formation when both complexes were incubated with the end-blocked GT mispair substrate in the presence of ATP-γS (Figure 2-5D), whereas when Mlh1-Pms1 and ATP-γS were added to

Figure 2-6. Mlh1-Pms1 can bind to the Msh2-Msh6-DNA complex in buffer containing ATP.
Biosensor analysis of the association of the Msh2-Msh6 complex with a DNA substrate containing a GT mispair (A, B, E, F) or a GC basepair (C, D, G, H), that had a free end (A, B, C, D) or was end-blocked with 100 nM LacI (E, F, G, H) under standard conditions was performed as described under "Experimental Procedures." Mlh1-Pms1 was then added to the Msh2-Msh6 solution and association was observed, followed by analysis of the dissociation of the ternary complex. A. 100 nM Msh2-Msh6 was bound in running buffer on a DNA substrate containing a GT mispair *(black line)*. An equal volume of 100 nM Mlh1-Pms1 in running buffer containing 500 μM ATP was then added to the Msh2-Msh6 mixture yielding final concentrations of 50 nM of both protein complexes and 250 μM ATP. Dissociation was observed by replacing the protein-containing buffer with running buffer containing 250 μM ATP. B. Reactions were performed as in "A", except ATP was replaced by ATP-γS. C & D were same as A & B respectively, except a DNA substrate containing a GC basepair was used in place of the substrate containing a GT mispair. E, F, G & H were the same as A, B, C & D respectively, except the DNA ends were blocked with LacI. Binding of 50 nM Msh2-Msh6 and 50 nM Mlh1-Pms1 mixed together with 250 μM ATP *(dotted red lines)* are included for comparison in "E" and "G". In E, F, G and H, in addition to the above dissociation reaction, additional disassociation reactions were performed as indicated, including either addition of 5 μL of running buffer containing 10 mM IPTG (1 mM final concentration) to the microcuvette to release LacI from DNA (*green lines*), replacing the protein containing buffer with running buffer containing 250 μM ATP and 1 mM IPTG (*red dashed lines*) or replacing the protein containing buffer with running buffer containing 250 μM ATP-γS and 1 mM IPTG (*blue dashed lines*).

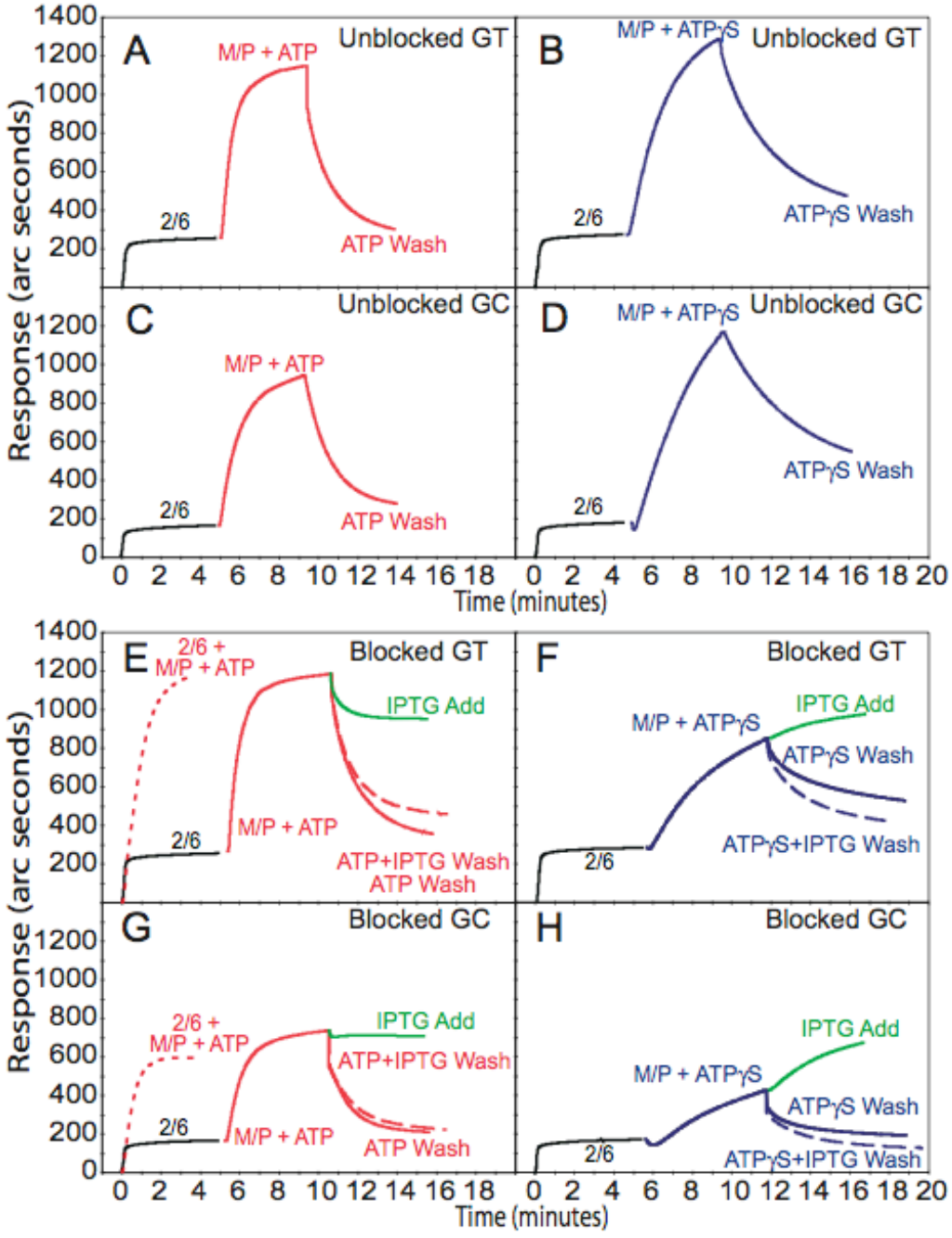
A
Unblocked GT
M/P + ATP
2/6
ATP Wash
B
Unblocked GT
M/P + ATPγS
2/6
ATPγS Wash
C
Unblocked GC
M/P + ATP
2/6
ATP Wash
D
Unblocked GC
M/P + ATPγS
2/6
ATPγS Wash
Response (arc seconds)
Time (minutes)
E
Blocked GT
2/6 + M/P + ATP
IPTG Add
M/P + ATP
2/6
ATP+IPTG Wash
ATP Wash
F
Blocked GT
IPTG Add
M/P + ATPγS
ATPγS Wash
2/6
ATPγS+IPTG Wash
G
Blocked GC
2/6 + M/P + ATP
IPTG Add
ATP+IPTG Wash
2/6
M/P + ATP
ATP Wash
H
Blocked GC
IPTG Add
M/P + ATPγS
ATPγS Wash
2/6
ATPγS+IPTG Wash
Response (arc seconds)
Time (minutes)

Msh2-Msh6 that was prebound in the presence of ADP (Figure 2-6F), ternary complex formation was more robust but appeared to form more slowly and did not reach the same levels compared to that formed in the presence of ATP. This reduced level of ternary complex formation likely results because additional binding of Msh2-Msh6 to the mispair during the time course of the experiment is limited in ATP-γS (see Figure 2-3D) in comparison to considerable additional binding by Msh2-Msh6 in the presence of ATP (see Figure 2-3C).

The dissociation behavior of the Mlh1-Pms1 complexes formed on prebound Msh2-Msh6 in the presence of ATP on blocked or unblocked GT mispair or GC basepair substrates was essentially the same as the complexes formed when Msh2-Msh6 and Mlh1-Pms1 were incubated together (compare Figures 2-4C, 2-4G, 2-5C and 2-5G with figures 2-6A, 2-6E, 2-6C and 2-6G). The complexes formed in ATP-γS on blocked or unblocked substrates displayed similar dissociation behavior (Figures 2-6B, 2-6D, 2-6F and 2-6H); however, this dissociation behavior was somewhat different than that of the complexes formed in the presence of ATP. When IPTG alone was added to the complex formed in the presence of ATP-γS, significantly increased binding was observed on both the GT mispair and GC basepair substrates (Figure 2-6F, H) compared to, for example, the dissociation seen when IPTG was added to similar complexes formed on the GT mispair substrate in the presence of ATP (Figure 2-5C), consistent with an end-binding reaction in the presence of ATP-γS. When the protein-containing buffer was removed from reactions with end-blocked substrates and replaced with buffer containing LacI and ATP-γS or buffer containing

IPTG and ATP-γS, significant dissociation was observed (Figure 2-6F, H); this dissociation behavior was similar to that observed for the complexes formed when Msh2-Msh6 and Mlh1-Pms1 were incubated together with the DNA substrate in the presence of ATP-γS (Figure 2-5D, H). In addition, this latter dissociation seemed to occur at a lower apparent rate than dissociation in the presence of ATP (compare Figure 2-6E with 2-6F and 2-6G with 2-6H).

Taken together, these results suggest that recognition of Msh2-Msh6 bound to a mispair in buffer containing ADP by Mlh1-Pms1 to form a ternary complex requires ATP binding to either Msh2-Msh6 or Mlh1-Pms1 or both; the reduced apparent rate of association in ATP-γS compared to ATP may also suggest that ATP hydrolysis plays a role in stable ternary complex formation or is required for turnover and rebinding of Mlh1-Pms1. In addition, the seemingly reduced apparent rate of dissociation of the ternary complex in the presence of ATP-γS compared to ATP suggests that ATP hydrolysis may play an additional role in dissociation; However, this could also reflect the increased end binding that occurs in the presence of ATP-γS compared to ATP (Figure 2-5C, D), either directly or during dissociation via the DNA ends.

2.4 DISCUSSION

In this study, we have used LacI protein to reversibly block the ends of substrate DNA molecules in order to investigate the interaction of Msh2-Msh6 and Mlh1-Pms1 with DNA. This approach has allowed the analysis of multiple modes of association and dissociation with DNA. Msh2-Msh6 can bind to both basepair and mispair containing substrates and exhibits only direct dissociation from basepair containing substrates and both direct and end-dependent dissociation from mispair containing substrates; the formation of a complex that moves along the DNA and undergoes end-dependent dissociation accounts for the increased association seen on end-blocked mispair containing substrates. Mlh1-Pms1 can bind to Msh2-Msh6 on mispair and basepair containing substrates and at the ends of DNA molecules. The interaction of Mlh1-Pms1 with Msh2-Msh6 at a mispair results in ternary complexes that show both direct and end-dependent dissociation whereas the interaction of Mlh1-Pms1 with Msh2-Msh6 on basepair containing substrates results in a ternary complex that appears to only show direct dissociation; the ternary complex formed on GC basepair substrates also dissociates more rapidly than either the direct or end-dependent dissociation modes of the ternary complex formed on GT mispair substrates.

The interaction between Mlh1-Pms1 and Msh2-Msh6 at DNA ends, particularly under conditions where ATP is present but cannot be hydrolyzed, is a mispair independent interaction that confounds the analysis of Mlh1-Pms1 interactions

with Msh2-Msh6; because of this, the interaction between Mlh1-Pms1 with Msh2-Msh6 at a mispair can best be studied on DNA substrates which have blocked DNA ends. A consequence of this is that most studies of Msh2-Msh6 interactions with Mlh1-Pms1 (Pms2 in humans) using gel shift methods have likely studied a non-mispair dependent interaction (Bowers et al., 2001; Bowers et al., 2000; Kijas et al., 2003; Raschle et al., 2002). It should also be noted that because we cannot precisely monitor the binding of additional Msh2-Msh6 to the DNA substrate during the ternary complex formation experiments containing ATP using the IAsys biosensor, we have not attempted to measure the stoichiometry of the interaction of Msh2-Msh6 and Mlh1-Pms1; however, in the immunoprecipitation experiments presented here and in unpublished experiments, the observed stoichiometry was 1:1.

The binding of Msh2-Msh6 to DNA fits the model presented in Figure 2-7. When Msh2-Msh6 binds to DNA containing a mispair in the presence of ADP or in the absence of nucleotide, it primarily binds to the mispair due to the higher affinity for mispairs compared to basepairs (Acharya et al., 1996; Fishel et al., 1994; Hess et al., 2002; Marsischky and Kolodner, 1999; Mu et al., 1997). Under these conditions, Msh2-Msh6 only directly dissociates from DNA. On addition of either ATP or ATP-γS to the complex formed in the presence of ADP, essentially all of the Msh2-Msh6 is converted to a form that rapidly dissociates from the DNA but can be trapped on the DNA by blocking the ends, consistent with a study of human Msh2-Msh6 (Gradia et al., 1999). Our conclusions differ from those of another study of Msh2-Msh6 mispair complexes formed in the absence of nucleotide that concluded that ATP, but not

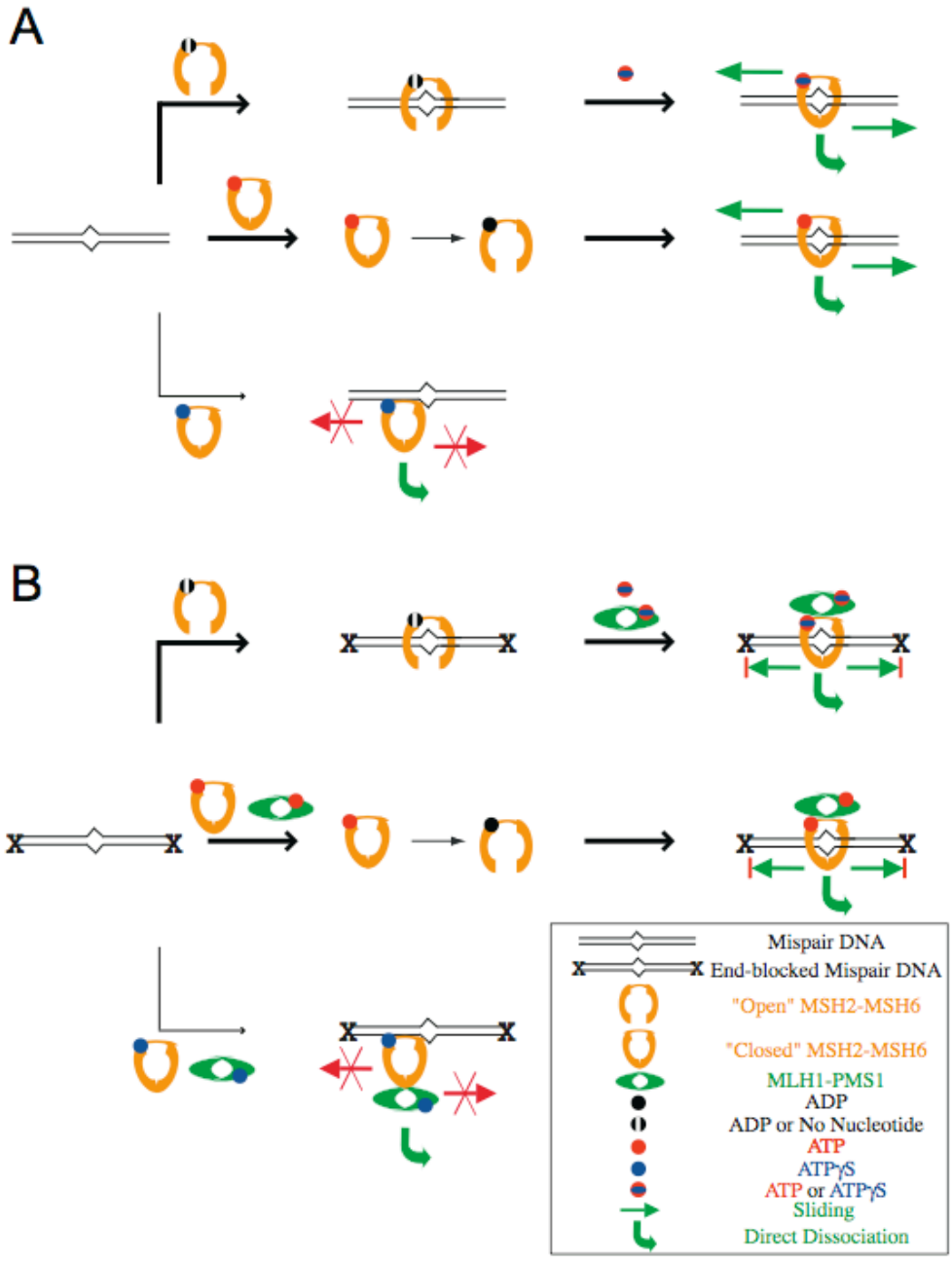

Figure 2-7. Model of interactions of Msh2-Msh6 and Mlh1-Pms1 on DNA containing a mispair. A. Multiple modes of association of Msh2-Msh6 onto a mispair and dissociation off of a mispair. B. Interaction of Mlh1-Pms1 with Msh2-Msh6 on end-blocked DNA containing a mispair. In the absence of blocked ends, the ternary complex can also form on DNA ends. See "Discussion" for explanation.

nonhydrolyzable ATP analogs, could convert human Msh2-Msh6 to a form that could be trapped on end-blocked DNA substrates (Blackwell et al., 1998); however, our results predict the observed lower level of complex seen in the presence of ATP-γS vs. ATP (Blackwell et al., 1998) because while both ATP and ATP-γS induce the movement of Msh2-Msh6 off of the mispair as well as direct dissociation from the blocked DNA substrates, only ATP but not ATP-γS, because it can be hydrolyzed, allows the rebinding of Msh2-Msh6 (present in the binding buffer) to the mispair (see below).

We have confirmed that Msh2-Msh6 bound to a mispair in the absence of any nucleotide shows the same ATP induced conversion to a form that can be trapped on the DNA by blocking the ends (data not shown). Msh2-Msh6 that has been trapped on DNA in this way rapidly dissociates from the DNA when the block is reversed and more slowly dissociates from the DNA when the ends remain blocked; these results indicate that the end-dependent dissociation form undergoes slower direct dissociation when it is trapped on the DNA by blocking the ends.

Although Msh2-Msh6 shows a small amount of increased binding to mispair containing DNA in the presence of ATP-γS relative to basepair containing DNA, blocking the end of the substrate DNA does not increase binding suggesting that ATP bound Msh2-Msh6 is in a conformation that cannot productively recognize mispairs (Gradia et al., 1999). When Msh2-Msh6 is incubated with mispair containing DNA substrate in the presence of ATP, a low level of mispair binding at steady-state occurs when the ends are not blocked and a much higher level of binding is seen when the

ends are blocked; Msh2-Msh6 that is trapped on the DNA when the ends are blocked rapidly and completely dissociates when the block is reversed. These results are consistent with the view that bound ATP is hydrolyzed to ADP by Msh2-Msh6 allowing Msh2-Msh6 to bind to the mispair and that subsequent binding of ATP converts the Msh2-Msh6 to a ring or clamped form that dissociates rapidly by moving along the DNA (Gradia et al., 1999); conversion to this form accounts for the increased levels of binding seen in the presence of ATP on blocked GT mispair substrates compared to GT substrates with out a block. The observation that ATP and ATP-γS induce the same dissociation behavior of mispair bound Msh2-Msh6 (bound in ADP or no nucleotide) and that ATP induced dissociation of mispair-bound Msh2-Msh6 loaded in ADP or ATP results in complete dissociation (on unblocked DNA or end-blocked DNA followed by block reversal) rather than trapping of a portion of the protein on the DNA between the mispair and the cuvette surface (or on a single end-blocked DNA substrate) as seen for MutS (Blackwell et al., 2001a) is consistent with the view that the clamped form diffuses along the DNA (Gradia et al., 1999) rather than translocating along the DNA in a manner dependent on ATP hydrolysis (Blackwell et al., 1998).

Binding of Msh2-Msh6 to GC basepair substrate DNA in the presence of ADP or ATP results in a low level of bound protein (relative to that seen on GT mispair substrates) that appears to only exhibit end-independent direct dissociation whereas binding in ATP-γS results in low level, stable binding. The net result of blocking the ends of a mispair containing substrate is that mispair binding of Msh2-Msh6 followed

by ATP binding induces conversion to a form that is trapped on the DNA allowing much higher levels of Msh2-Msh6 to stably associate with the DNA than is seen on unblocked DNA. This loading reaction does not occur in the absence of a mispair and hence blocking the end of the DNA substrates increases the apparent specificity of Msh2-Msh6 for mispaired bases.

Our analysis indicates that Mlh1-Pms1 can specifically assemble onto Msh2-Msh6 in a mispair-mediated reaction as described in the model illustrated in Figure 2-7. However, as will be discussed in more detail below, the analysis of this interaction is confounded by non-specific interactions between these two complexes on basepairs and at DNA ends; blocking the DNA ends was therefore critical to characterizing the mispair-mediated reaction.

Mlh1-Pms1 can assemble onto Msh2-Msh6 at a mispair under two conditions: when the two proteins are incubated together with the substrate and ATP, or when Msh2-Msh6 is preloaded onto the mispair in the presence of ADP and the Mlh1-Pms1 is then added along with ATP or ATP-γS. In the presence of ATP-γS the extent of binding of Mlh1-Pms1 to Msh2-Msh6 prebound on end-blocked GT mispair substrates is higher than when Msh2-Msh6 is prebound on end-blocked GC basepair substrates; this indicates that the interaction of Mlh1-Pms1 with Msh2-Msh6 at a mispair is a specific interaction distinct from the interaction of Mlh1-Pms1 with Msh2-Msh6 at a basepair.

The dissociation behavior of the ternary complexes also supports the view that the ternary complex formed on mispair substrates is different from the ternary

complex formed on basepair substrates. The ternary complex loaded onto end-blocked mispaired base substrate under either of the specific interaction conditions showed direct dissociation. Several observations suggest that the complexes also show movement along the DNA and end-dependent dissociation. First, blocking the DNA ends results in increased accumulation of complex and removing the block by addition of IPTG results in increased dissociation. Second, the ternary complex dissociated more rapidly from the mispaired base substrate when the end blocks were released than from the blocked mispaired base substrate (compare dissociation in ATP + IPTG to ATP alone; Table 2-1). There is, however, less effect of blocking or unblocking the ends of GT mispair substrates on the Mlh1-Pms1-Msh2-Msh6 complex as compared to Msh2-Msh6 alone. This could be because either the ternary complex has a reduced apparent rate of end-dependent dissociation relative to the apparent rate of direct dissociation than seen for Msh2-Msh6 alone or that the sliding form of the ternary complex moves as rapidly along the DNA but is retarded at the ends due to the end binding reaction. This affect could explain the observation that the presence of human Mlh1-Pms2 appears to increase the affinity of Msh2-Msh6 for mispairs (Blackwell et al., 2001b). It is also possible that the apparent increased dissociation seen in the absence of end blocks is due to a small amount of Msh2-Msh6 loaded onto the mispair substrate that did not then bind Mlh1-Pms1 or is present on the DNA alone if some of the Mlh1-Pms1 disassembles from the ternary complex; we do not favor these latter possibilities because the protein that dissociates on addition of IPTG alone

appears to dissociate more slowly than Msh2-Msh6 alone ($t_{1/2}$ of ~21 sec vs. ~6 sec; Table 2-1). Additional experimentation will be required to resolve these possibilities.

In contrast, when Mlh1-Pms1 was assembled with Msh2-Msh6 on GC basepair substrate under either of the two binding conditions, there was no evidence of an end-dependent dissociation form that could be trapped on the substrate by blocking the substrate ends. In addition, the complex formed on end-blocked basepair substrate appeared to show more rapid dissociation than the complex formed on end-blocked mispaired base substrate ($t_{1/2}$ of ~14 sec vs. ~32 sec; Table 2-1). These results again indicate that the assembly of Mlh1-Pms1 on Msh2-Msh6 on mispaired base containing substrate is a different reaction than that seen on basepair containing substrates and that basepair-mediated assembly likely represents some type of non-specific interaction.

The experiments performed with ATP-γS have revealed additional mechanistic details of ternary complex formation on a mispair. Incubation of Mlh1-Pms1, Msh2-Msh6 and ATP-γS together with GT mispair substrates resulted in much less ternary complex binding, no evidence of end-dependent dissociation and much less discrimination between GT mispair vs. GC basepair substrates compared to binding reactions containing ATP. Because Msh2-Msh6 cannot bind to a mispair in the presence of ATP-γS (This study and Ref. (Gradia et al., 1999), these results indicate that ternary complex formation requires that Msh2-Msh6 first bind to a mispair (Figure 2-7). When Mlh1-Pms1 and ATP-γS were added to Msh2-Msh6 prebound to an end-blocked mispair substrate in ADP, ternary complex formation occurred more

slowly than when ATP was present in the binding reaction containing Mlh1-Pms1. In addition, the level of complex formed was also lower in the presence of ATP-γS; this is in part because ATP-γS prevents the additional binding of Msh2-Msh6 to the mispair that occurs during the course of such experiments containing ATP due to ATP hydrolysis by Msh2-Msh6. Once the ternary complex formed, it dissociated more slowly than when complex formation occurred in the presence of ATP. These results suggest that ATP hydrolysis might have an additional role in promoting both association and dissociation of the complex. That mutations predicted to alter ATP binding and hydrolysis by the Pms1 ATP binding site have little affect on MMR suggest that the Pms1 ATP binding site may be of lesser importance than the other three ATP binding sites (Tran and Liskay, 2000). Additional experimentation will be required to determine which of the four ATP binding sites present in these two protein complexes must bind and/or hydrolyze ATP during ternary complex formation and dissociation.

Our results on ternary complex formation in the presence of ATP-γS explain the apparent discrepancy between two studies that analyzed ternary complex formation between MutL and the same ATP hydrolysis defective mutant MutS protein. In one study when the two proteins were co-incubated with ATP and a mispair containing substrate, no ternary complex was observed (Baitinger et al., 2003); our results predict that no ternary complex should be formed because the mutant MutS protein would not be able to hydrolyze ATP to ADP and hence would not bind to a mispair. In contrast, in the other study when the MutS protein was

preloaded onto the mispair substrate, ternary complex formation was observed when MutL and ATP were added (Selmane et al., 2003); our results predict that once the mutant MutS protein is bound to a mispair in the absence of ATP, addition of ATP, even in the absence of hydrolysis, would allow MutL to interact with MutS at the mispair.

The results presented here clearly show that Mlh1-Pms1 can interact with Msh2-Msh6 in the presence of ATP or ATP-γS on DNA substrates that do not contain mispaired bases. There appear to be two types of interactions; those on basepairs and those at DNA ends. The latter interaction has also been suggested by a gel shift but not a Biacore experiment performed with human MutLα (Blackwell et al., 2001b). On the end-blocked GC basepair substrates, the interaction that occurs in the presence of ATP appears to be a lower affinity interaction between Mlh1-Pms1 and Msh2-Msh6 that only undergoes direct dissociation from DNA that appears to be more rapid than that seen with ternary complexes assembled onto end-blocked GT mispair substrate; this GC basepair ternary complex appears to be due to a non-specific interaction and is distinct from the more stable complex that forms in the presence of a mispair. When the GC basepair substrates do not have blocked ends or when the end blocks are removed, increased binding is seen and the affinity of the interaction between Mlh1-Pms1 and Msh2-Msh6 appears to be higher. This end binding is most striking when the binding reactions are performed in the presence of ATP-γS or ATP -Mg^{2+}; indeed the ternary complexes formed in the IAsys instrument under the latter conditions could not be dissociated by high NaCl or Mg^{2+} and NaDOD-SO_4 (SDS) was required for

their disruption. End binding can also be significant on substrates containing a mispair and hence the need to block the DNA ends to detect significant mispair dependent ternary complex formation. Interestingly, most studies that have used gel mobility shift assays to study interactions between Msh2-Msh6 and Mlh1-Pms1 (human Pms2) have used reactions conditions ATP -Mg^{2+} or ATP +Mg^{2+} followed by incubation with an EDTA-containing stop buffer, which we have demonstrated to yield high affinity mispair independent interactions, suggesting these studies may have not detected mispair-dependent interactions (Blackwell et al., 2001b; Bowers et al., 2001; Bowers et al., 2000; Kijas et al., 2003; Raschle et al., 2002). Our studies clearly show that blocking the ends of DNA substrates is required to reliably reveal mispair-dependent interactions between Msh2-Msh6 and Mlh1-Pms1 (human Pms2). However, it should be noted that during MMR, interactions with other proteins might significantly alter the character of Msh2-Msh6-Mlh1-Pms1 ternary complexes.

2.5 EXPERIMENTAL PROCEDURES

DNA substrates

Biotinylated oligonucleotides were synthesized by Midland Certified Reagent Company Inc., (Midland, Texas). All other oligonucleotides were synthesized by MWG, (www.mwgbiotech.com). The GT mispair and the GC basepair were 236 nucleotide PCR-derived substrates and were prepared in the following manner. The biotinylated "G" strand was prepared by PCR amplification of a 236 basepair product, using the forward 5'-biotinylated oligonucleotide (5' BIOT-ACCATGATTACGCCAAGCTC) and the reverse 5'-phosphorylated oligonucleotide (5' PHOS-TCACACATCaattgttatccgctcacaattGGGTAACGCCAGGGTTTTC), which has the *lac* O_1 operator sequence incorporated (lowercase) with plasmid RDK3686 as template DNA. The "C" strand, for the GC basepair, was made by amplifying the plasmid template RDK3687 with oligonucleotides having the same sequence, except the forward primer was 5'-phosphorylated and the reverse primer was not phosphorylated. The "T" strand for the GT mispair substrate was made by amplifying the plasmid template RDK3688 with the same primers used to create the "C" strand. The plasmid RDK3688 has the same sequence as RDKY3687 except for a single nucleotide change which places an AT basepair instead of a GC basepair 100 bases from the 5' end of the forward primer. The three PCR products (GbCp, GpC and ApT) were then digested with lambda exonuclease (New England Biolabs), which is specific for the 5'phosphorylated strand of dsDNA; thus digestion of these PCR

products with lambda exonuclease produces the biotinylated “G” top strand, as well as the “C” and “T” bottom strands. The “G” and “C” strands were mixed together and annealed by heating to 95° C and cooling slowly to create the GC basepair and the “G” and “T” strands were similarly annealed to create the GT mispair. The dsDNA was then purified using the QIAGEN PCR purification kit (QIAGEN). Quality control of the DNA substrates was performed by restriction endonuclease digestion analysis as follows. The PCR product that was derived from RDK3687 has an Xho1 site that would be lost upon formation of the mispair with the bottom strand of RDK3688, which has an NsiI site that is lost upon formation of the mispair with the top strand from RDK3687. Therefore, GC basepair DNA has a functional XhoI site, while the GT mispair DNA has neither the XhoI site nor the NsiI site. By this analysis, all GT substrates used were greater than 90% pure. The 150 bp GT mispair and GC basepair substrates used in the immunoprecipitation assays were similarly constructed except that the oligonucleotides (5’-BIOT-ACCATGATTACGCCAAGCTC) and (5’ PHOS-TACGACTCACTATAGGGCG) were used for PCR amplification of the template DNAs.

Proteins

The Msh2-Msh6 complex was purified as described previously (Hess et al., 2002) and did not contain prebound ADP or ATP (unpublished results of M. Hess and RDK). A detailed description of the overproduction and purification of the Mlh1-Pms1 complex will be described elsewhere. Briefly, Mlh1 was co-expressed in the *S.*

cerevisiae strain RDKY1293 with a fully biologically functional Pms1 containing a FLAG peptide sequence using two different 2μ-based plasmids that each contain a different selectable marker and a GAL10 promoter. The protein from 20 liters of cells was purified by sequential chromatography on a Hi-Trap Heparin column, anti-flag antibody resin eluted with FLAG peptide (Sigma) and a Mono S column. SDS-PAGE analysis indicated the resulting protein preparation was >95% pure and had an equimolar ratio of the two subunits (see Figure 2-1). The protein was frozen in liquid nitrogen and stored frozen in small aliquots at –75° C. LacI protein was kindly provided by Dr. Kathleen Matthews (Rice University).

Immunoprecipitation assay

Binding reactions (10 μl) containing 2 picomoles Msh2-Msh6, 2 picomoles Mlh1-Pms1 and 1 picomole duplex or mispair containing DNA (150 bp) were performed in binding buffer containing 50 mM Tris pH 7.5, 110 mM NaCl, 1 mM dithiolthreitol, 10% glycerol, 0.01% IGEPAL CA-630 (NP-40) and, as indicated, 10 mM $MgCl_2$ and 1 mM ADP, ATP or ATP-γS. Initial incubations were performed on ice for 10 minutes followed by the addition of 25 μl anti-flag beads (Sigma); resuspended in appropriate binding buffer) for 20 minutes. Samples were centrifuged for 20 seconds at 5,000 RPM (2,800 RCF) in an Eppendorf microfuge and resuspended 2 times with 250 μl ice cold binding buffer containing the appropriate nucleotide at 100 μM. Bound protein and protein DNA complexes were eluted with

100 μl of binding buffer containing 200 μg/ml FLAG peptide. The eluted proteins were separated by SDS-PAGE, and the resulting gels were silver stained.

Total Internal Reflectance measurements

Interaction of the Msh2-Msh6 complex and the Msh2-Msh6-Mlh1-Pms1 ternary complex with DNA were measured by total internal reflectance using the IAsys Auto Plus system (Thermo Affinity Sensors) (Hess et al., 2002). IAsys Auto Plus microcuvettes with two biotin-coated reaction cells were treated with a solution containing neutravidin (Pierce). After washing away unbound neutravidin with 4 washes of 50 μL of phosphate-buffered saline + 0.05% Tween20 (PBST), 3 μg of the indicated biotinylated DNA substrates was bound to the neutravidin-coated cell and excess DNA was then washed away with PBST. DNA binding resulted in ~130 arc second increase in response. Individual experiments were then performed as described below.

Experiments analyzing either Msh2-Msh6 or the Msh2-Msh6-Mlh1-Pms1 ternary complex formation on the GT mispair or GC basepair substrates were performed as follows. The IAsys cuvettes containing the indicated DNA substrate were equilibrated two times with running buffer consisting of 25 mM Tris, (pH 8.0), 110 mM NaCl, 0.5 mM dithiothreitol, 2% Glycerol, 0.05% IGEPAL CA-630 (NP-40) and 25 μM ADP. 10 mM $MgCl_2$ was also included, unless indicated otherwise. Additional nucleotides were added to the binding buffer as indicated in individual experiments. The equilibration buffer was then washed away and replaced with the

same buffer, but containing 50 nM of the indicated proteins. Incubation was carried out for approximately 3.5 minutes or until equilibrium was reached. Binding increased with increasing concentrations of protein added to the cuvette with saturation being reached at high protein concentrations; a representative titration showing saturation binding has been published elsewhere (Hess et al., 2002) and therefore such data are not specifically presented here. Based on the known relationship between arc seconds and protein mass (Saenko et al., 1998) we calculated that no more than 3.2% of any individual protein added to the cuvette bound to the DNA substrate in any experiment. Representative experiments were also performed using buffers that did not contain ADP and identical results were obtained, consistent with the fact that ADP is fully exchangeable by ATP (Gradia et al., 1997).

To analyze complex dissociation, the protein-containing buffer was subsequently replaced with buffer containing the indicated nucleotide; modifications to this basic procedure are discussed below and in individual experiments. Dissociation conditions in which running buffer is replaced with a different buffer are annotated with the term "wash" in individual figures. Control experiments showed that this “wash” step removed 90 to 95% of the unbound protein initially present in the cuvette. Dissociation was monitored for at least 4 minutes. The DNA substrate was regenerated and prepared for additional binding reactions by incubation in 3 M NaCl for 2 minutes, followed by extensive washing in PBST. All experiments were performed at 25° C.

Rate constants for dissociation were determined by fitting the data to mono-phasic and bi-phasic dissociation models by nonlinear regression using GraphPad Prism version 4.0 (Graphpad) to fit the dissociation data to the following Equations 2.1 and 2.2,

$$Y = (\text{top} - \text{bottom})*e^{(-k*X)} + \text{bottom} \qquad \text{(Eq. 2.1)}$$

and

$$Y = (\text{top} - \text{bottom})*(f*e^{(-k_1*X)} + (1 - f)*\exp^{(-k_2*X)}) + \text{bottom} \qquad \text{(Eq. 2.2)}$$

where X is time, in seconds; Y is response, in arc seconds; f is the fraction of complexes that dissociate with the rate constant k_1; top is response, in arc seconds, after binding reaction reaches equilibrium, just prior to the initiation of dissociation and bottom is response, in arc seconds, after dissociation is complete and reaction reaches a new equilibrium. The dissociation model that best fit the data was determined by considering the precision of the following features of the data: visual comparison of the raw data points to the dissociation model; the R^2 values for the fit; the standard deviation of the fit of the data points to k, the rate constant(s) of the model (these standard deviations were always less than 2% in the case of the best-fit model); and the standard deviation of the average of the amplitude for each phase from multiple independent experiments. We also considered more complex multi-phasic models but the fits to these models were never better than to mono-phasic and bi-phasic models. Once the best-fit model was determined as the model to which the

data fit with the greatest precision, the data from individual experiments were converted to a $t_{1/2}$ (half-time) of dissociation by Equation 2.3,

$$t_{1/2} = 0.693/k_{off} \qquad \text{(Eq. 2.3)}$$

The data reported in the text and Table 2-1 are the average and standard deviation of the $t_{1/2}$ values from multiple independent experiments, the R^2 values for the fits and, for bi-phasic fits, the average of the amplitude values from multiple independent experiments. The standard deviation of the fit of the data points to k, the rate constant(s) of the model is not reported because this value was always smaller than the standard deviation of the average of the k values obtained from multiple independent experiments.

Experiments examining either Msh2-Msh6 or the Msh2-Msh6-Mlh1-Pms1 ternary complex formation on the blocked GT mispair or the blocked GC basepair were performed as follows. After equilibration in running buffer, 100 nM LacI in running buffer was bound to the DNA substrates bound to IAsys microcuvettes. Under these conditions, binding of LacI resulted in an increase of ~60 arc seconds, which was dependent on the presence of the *lac* O_1 operator sequence (Supplement Figure 2-1). Subsequent association of the complexes was performed as described above except that 100 nM LacI was included in the running buffer in all steps. The baseline of the association curves of mismatch repair proteins depicted was taken after LacI was bound to the DNA substrates, so the binding curves reflect association of

mismatch repair proteins only. Dissociation was monitored in the following three ways. First, 5 μl of running buffer containing 10 mM IPTG was added to the 50 μL of protein-containing buffer in the cuvette to allow dissociation of LacI bound at the ends of the DNA substrate without significantly altering the concentrations of protein in solution. Second, the protein-containing buffer was replaced with running buffer containing 100 nM LacI and the indicated nucleotide resulting in dissociation while maintaining the blocked end on the DNA substrate. In the third method, the protein-containing buffer was replaced with running buffer containing 10 mM IPTG and the indicated nucleotide resulting in dissociation in the absence of any proteins in solution or LacI at the end of the DNA substrate. Addition of IPTG resulted in complete dissociation of LacI with a half-time of ~1.6 sec (Supplemental Figure 2-1). Again, dissociation was monitored for at least 4 minutes.

Analysis of Mlh1-Pms1 binding to the Msh2-Msh6-DNA complex was performed as follows. DNA bound to IAsys microcuvettes was equilibrated in running buffer two times. 25 μL of running buffer containing 100 nM Msh2-Msh6 was added and binding was monitored for approximately five minutes. Next, 25 μl of running buffer containing 100 nM Mlh1-Pms1 and 500 μM ATP (or other nucleotides, as indicated) was added to the cuvette, resulting in the presence of both complexes at 50 nM and a final concentration of ATP at 250 μM. The association of Mlh1-Pms1 to the pre-bound Msh2-Msh6 complex was monitored for five minutes or until equilibrium was reached. Dissociation was monitored by replacing the protein-containing buffer with running buffer containing the indicated nucleotide for

approximately five minutes. The Mlh1-Pms1 association to the Msh2-Msh6-DNA complex was also analyzed under conditions in which the DNA substrate was blocked with LacI. In this case, LacI was bound to the DNA substrate initially and included in the running buffer at a concentration of 100 nM in all steps. Dissociation of the complex that was formed in the presence of blocked ends was analyzed using the same three methods discussed above.

2.6 ACKNOWLEDGEMENTS

The authors would like to thank Chris Putnam and Scarlet Shell for helpful discussions and comments on the manuscript and Rick Fishel and Paul Modrich for communication of results and helpful discussions. We are especially grateful to Peter Geiduschek for suggesting the use of LacI and Kathleen Matthews for generously providing the LacI protein used in these studies. This work was supported by NIH Grant GM50006 to RDK and a postdoctoral fellowship from the American Cancer Society to DJM.

Chapter 2, in full, is a reprint of the material as it appears in Mendillo, M. L., Mazur, D. J. and Kolodner R. D. "Analysis of the interaction between the *Saccharomyces cerevisiae* Msh2-Msh6 and Mlh1-Pms1 complexes with DNA using a reversible DNA end-blocking system," *Journal of Biological Chemistry* (2005) Jun 10; 280(23): 22245-57. The dissertation author was the primary author of this paper.

2.7 SUPPLEMENTARY MATERIALS

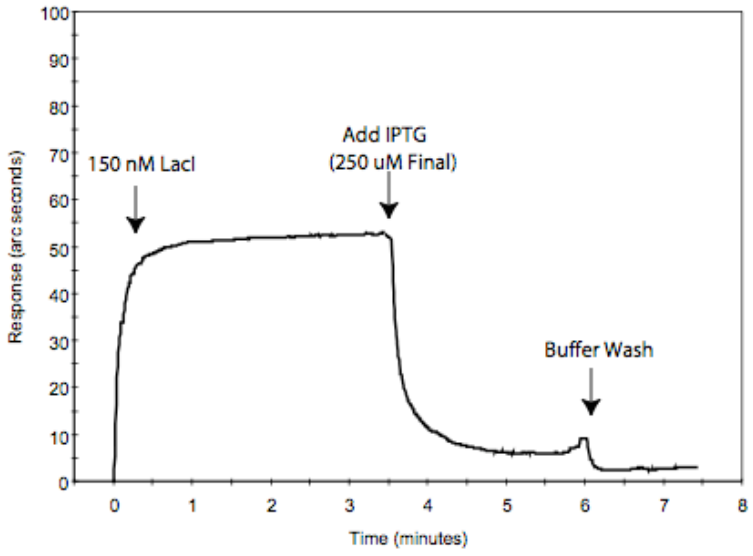

Supplementary Figure 2-S1. LacI protein bound to DNA containing the *lac* O_1 operator sequence dissociates rapidly and completely upon addition of IPTG.

2.8 REFERENCES

Acharya, S., Foster, P. L., Brooks, P., and Fishel, R. (2003). The coordinated functions of the E. coli MutS and MutL proteins in mismatch repair. Mol Cell *12*, 233-246.

Acharya, S., Wilson, T., Gradia, S., Kane, M. F., Guerrette, S., Marsischky, G. T., Kolodner, R., and Fishel, R. (1996). hMSH2 forms specific mispair-binding complexes with hMSH3 and hMSH6. Proc Natl Acad Sci U S A *93*, 13629-13634.

Alani, E. (1996). The Saccharomyces cerevisiae Msh2 and Msh6 proteins form a complex that specifically binds to duplex oligonucleotides containing mismatched DNA base pairs. Mol Cell Biol *16*, 5604-5615.

Allen, D. J., Makhov, A., Grilley, M., Taylor, J., Thresher, R., Modrich, P., and Griffith, J. D. (1997). MutS mediates heteroduplex loop formation by a translocation mechanism. Embo J *16*, 4467-4476.

Antony, E., and Hingorani, M. M. (2003). Mismatch recognition-coupled stabilization of Msh2-Msh6 in an ATP-bound state at the initiation of DNA repair. Biochemistry *42*, 7682-7693.

Au, K. G., Welsh, K., and Modrich, P. (1992). Initiation of methyl-directed mismatch repair. J Biol Chem *267*, 12142-12148.

Baitinger, C., Burdett, V., and Modrich, P. (2003). Hydrolytically deficient MutS E694A is defective in the MutL-dependent activation of MutH and in the mismatch-dependent assembly of the MutS.MutL.heteroduplex complex. J Biol Chem *278*, 49505-49511.

Blackwell, L. J., Bjornson, K. P., Allen, D. J., and Modrich, P. (2001a). Distinct MutS DNA-binding modes that are differentially modulated by ATP binding and hydrolysis. J Biol Chem *276*, 34339-34347.

Blackwell, L. J., Martik, D., Bjornson, K. P., Bjornson, E. S., and Modrich, P. (1998). Nucleotide-promoted release of hMutSalpha from heteroduplex DNA is consistent with an ATP-dependent translocation mechanism. J Biol Chem *273*, 32055-32062.

Blackwell, L. J., Wang, S., and Modrich, P. (2001b). DNA chain length dependence of formation and dynamics of hMutSalpha.hMutLalpha.heteroduplex complexes. J Biol Chem *276*, 33233-33240.

Bowers, J., Tran, P. T., Joshi, A., Liskay, R. M., and Alani, E. (2001). MSH-MLH complexes formed at a DNA mismatch are disrupted by the PCNA sliding clamp. J Mol Biol *306*, 957-968.

Bowers, J., Tran, P. T., Liskay, R. M., and Alani, E. (2000). Analysis of yeast MSH2-MSH6 suggests that the initiation of mismatch repair can be separated into discrete steps. J Mol Biol *302*, 327-338.

Burdett, V., Baitinger, C., Viswanathan, M., Lovett, S. T., and Modrich, P. (2001). In vivo requirement for RecJ, ExoVII, ExoI, and ExoX in methyl-directed mismatch repair. Proc Natl Acad Sci U S A *98*, 6765-6770.

Drummond, J. T., Li, G. M., Longley, M. J., and Modrich, P. (1995). Isolation of an hMSH2-p160 heterodimer that restores DNA mismatch repair to tumor cells. Science *268*, 1909-1912.

Fishel, R., Ewel, A., Lee, S., Lescoe, M. K., and Griffith, J. (1994). Binding of mismatched microsatellite DNA sequences by the human MSH2 protein. Science *266*, 1403-1405.

Flores-Rozas, H., and Kolodner, R. D. (1998). The Saccharomyces cerevisiae MLH3 gene functions in MSH3-dependent suppression of frameshift mutations. Proc Natl Acad Sci U S A *95*, 12404-12409.

Fu, T. J., Sanders, G. M., O'Donnell, M., and Geiduschek, E. P. (1996). Dynamics of DNA-tracking by two sliding-clamp proteins. Embo J *15*, 4414-4422.

Galio, L., Bouquet, C., and Brooks, P. (1999). ATP hydrolysis-dependent formation of a dynamic ternary nucleoprotein complex with MutS and MutL. Nucleic Acids Res *27*, 2325-2331.

Genschel, J., Littman, S. J., Drummond, J. T., and Modrich, P. (1998). Isolation of MutSbeta from human cells and comparison of the mismatch repair specificities of MutSbeta and MutSalpha. J Biol Chem *273*, 19895-19901.

Gradia, S., Acharya, S., and Fishel, R. (1997). The human mismatch recognition complex hMSH2-hMSH6 functions as a novel molecular switch. Cell *91*, 995-1005.

Gradia, S., Subramanian, D., Wilson, T., Acharya, S., Makhov, A., Griffith, J., and Fishel, R. (1999). hMSH2-hMSH6 forms a hydrolysis-independent sliding clamp on mismatched DNA. Mol Cell *3*, 255-261.

Grilley, M., Welsh, K. M., Su, S. S., and Modrich, P. (1989). Isolation and characterization of the Escherichia coli mutL gene product. J Biol Chem *264*, 1000-1004.

Habraken, Y., Sung, P., Prakash, L., and Prakash, S. (1998). ATP-dependent assembly of a ternary complex consisting of a DNA mismatch and the yeast MSH2-MSH6 and MLH1-PMS1 protein complexes. J Biol Chem *273*, 9837-9841.

Hall, M. C., and Matson, S. W. (1999). The Escherichia coli MutL protein physically interacts with MutH and stimulates the MutH-associated endonuclease activity. J Biol Chem *274*, 1306-1312.

Harfe, B. D., and Jinks-Robertson, S. (2000). DNA mismatch repair and genetic instability. Annu Rev Genet *34*, 359-399.

Hess, M. T., Gupta, R. D., and Kolodner, R. D. (2002). Dominant Saccharomyces cerevisiae msh6 mutations cause increased mispair binding and decreased dissociation from mispairs by Msh2-Msh6 in the presence of ATP. J Biol Chem *277*, 25545-25553.

Joshi, A., Sen, S., and Rao, B. J. (2000). ATP-hydrolysis-dependent conformational switch modulates the stability of MutS-mismatch complexes. Nucleic Acids Res *28*, 853-861.

Kijas, A. W., Studamire, B., and Alani, E. (2003). Msh2 separation of function mutations confer defects in the initiation steps of mismatch repair. J Mol Biol *331*, 123-138.

Kolodner, R. (1996). Biochemistry and genetics of eukaryotic mismatch repair. Genes Dev *10*, 1433-1442.

Kolodner, R. D., and Marsischky, G. T. (1999). Eukaryotic DNA mismatch repair. Curr Opin Genet Dev *9*, 89-96.

Lahue, R. S., Au, K. G., and Modrich, P. (1989). DNA mismatch correction in a defined system. Science *245*, 160-164.

Lynch, H. T., and de la Chapelle, A. (1999). Genetic susceptibility to non-polyposis colorectal cancer. J Med Genet *36*, 801-818.

Lynch, H. T., and de la Chapelle, A. (2003). Hereditary colorectal cancer. N Engl J Med *348*, 919-932.

Marsischky, G. T., Filosi, N., Kane, M. F., and Kolodner, R. (1996). Redundancy of Saccharomyces cerevisiae MSH3 and MSH6 in MSH2-dependent mismatch repair. Genes Dev *10*, 407-420.

Marsischky, G. T., and Kolodner, R. D. (1999). Biochemical characterization of the interaction between the Saccharomyces cerevisiae MSH2-MSH6 complex and mispaired bases in DNA. J Biol Chem *274*, 26668-26682.

Matthews, K. S., and Nichols, J. C. (1998). Lactose repressor protein: functional properties and structure. Prog Nucleic Acid Res Mol Biol *58*, 127-164.

Mazurek, A., Berardini, M., and Fishel, R. (2002). Activation of human MutS homologs by 8-oxo-guanine DNA damage. J Biol Chem *277*, 8260-8266.

Modrich, P. (1991). Mechanisms and biological effects of mismatch repair. Annu Rev Genet *25*, 229-253.

Modrich, P., and Lahue, R. (1996). Mismatch repair in replication fidelity, genetic recombination, and cancer biology. Annu Rev Biochem *65*, 101-133.

Mu, D., Tursun, M., Duckett, D. R., Drummond, J. T., Modrich, P., and Sancar, A. (1997). Recognition and repair of compound DNA lesions (base damage and mismatch) by human mismatch repair and excision repair systems. Mol Cell Biol *17*, 760-769.

Palombo, F., Gallinari, P., Iaccarino, I., Lettieri, T., Hughes, M., D'Arrigo, A., Truong, O., Hsuan, J. J., and Jiricny, J. (1995). GTBP, a 160-kilodalton protein essential for mismatch-binding activity in human cells. Science *268*, 1912-1914.

Palombo, F., Iaccarino, I., Nakajima, E., Ikejima, M., Shimada, T., and Jiricny, J. (1996). hMutSbeta, a heterodimer of hMSH2 and hMSH3, binds to insertion/deletion loops in DNA. Curr Biol *6*, 1181-1184.

Peltomaki, P. (2003). Role of DNA mismatch repair defects in the pathogenesis of human cancer. J Clin Oncol *21*, 1174-1179.

Plotz, G., Raedle, J., Brieger, A., Trojan, J., and Zeuzem, S. (2002). hMutSalpha forms an ATP-dependent complex with hMutLalpha and hMutLbeta on DNA. Nucleic Acids Res *30*, 711-718.

Prolla, T. A., Pang, Q., Alani, E., Kolodner, R. D., and Liskay, R. M. (1994). MLH1, PMS1, and MSH2 interactions during the initiation of DNA mismatch repair in yeast. Science *265*, 1091-1093.

Raschle, M., Dufner, P., Marra, G., and Jiricny, J. (2002). Mutations within the hMLH1 and hPMS2 subunits of the human MutLalpha mismatch repair factor affect its ATPase activity, but not its ability to interact with hMutSalpha. J Biol Chem *277*, 21810-21820.

Reenan, R. A., and Kolodner, R. D. (1992a). Characterization of insertion mutations in the Saccharomyces cerevisiae MSH1 and MSH2 genes: evidence for separate mitochondrial and nuclear functions. Genetics *132*, 975-985.

Reenan, R. A., and Kolodner, R. D. (1992b). Isolation and characterization of two Saccharomyces cerevisiae genes encoding homologs of the bacterial HexA and MutS mismatch repair proteins. Genetics *132*, 963-973.

Saenko, E. L., Scandella, D., Yakhyaev, A. V., and Greco, N. J. (1998). Activation of factor VIII by thrombin increases its affinity for binding to synthetic phospholipid membranes and activated platelets. J Biol Chem *273*, 27918-27926.

Schofield, M. J., Nayak, S., Scott, T. H., Du, C., and Hsieh, P. (2001). Interaction of Escherichia coli MutS and MutL at a DNA mismatch. J Biol Chem *276*, 28291-28299.

Selmane, T., Schofield, M. J., Nayak, S., Du, C., and Hsieh, P. (2003). Formation of a DNA mismatch repair complex mediated by ATP. J Mol Biol *334*, 949-965.

Su, S. S., Lahue, R. S., Au, K. G., and Modrich, P. (1988). Mispair specificity of methyl-directed DNA mismatch correction in vitro. J Biol Chem *263*, 6829-6835.

Tran, P. T., and Liskay, R. M. (2000). Functional studies on the candidate ATPase domains of Saccharomyces cerevisiae MutLalpha. Mol Cell Biol *20*, 6390-6398.

Wang, T. F., Kleckner, N., and Hunter, N. (1999). Functional specificity of MutL homologs in yeast: evidence for three Mlh1-based heterocomplexes with distinct roles during meiosis in recombination and mismatch correction. Proc Natl Acad Sci U S A *96*, 13914-13919.

Welsh, K. M., Lu, A. L., Clark, S., and Modrich, P. (1987). Isolation and characterization of the Escherichia coli mutH gene product. J Biol Chem *262*, 15624-15629.

Wheeler, J. M., Bodmer, W. F., and Mortensen, N. J. (2000). DNA mismatch repair genes and colorectal cancer. Gut *47*, 148-153.

CHAPTER 3

Biochemical basis for dominant mutations in the *Saccharomyces cerevisiae MSH6* gene

3.1 ABSTRACT

Here, the ATP binding, ATP hydrolysis, mispair binding, sliding clamp formation and Mlh1-Pms1 complex interaction properties of dominant mutant Msh2-Msh6 complexes have been characterized. The results demonstrate two mechanisms for dominance. In one, seen with the Msh6-S1036P and Msh6-G1067D mutant complexes, the mutant complex binds mispaired bases, is defective for ATP induced sliding clamp formation and assembly of ternary complexes with Mlh1-Pms1 and occludes mispaired bases from other mismatch repair (MMR) pathways. In the second, seen with the Msh6-G1142D complex, the mutant complex binds mispaired bases and is defective for ATP induced sliding clamp formation but assembles ternary complexes with Mlh1-Pms1 that either occlude the mispaired base or prevent Mlh1-Pms1 from acting in alternate MMR pathways.

3.2 INTRODUCTION

Errors during DNA replication that result in base-base mismatches and small insertion/deletion mismatches can lead to mutations in DNA. The MMR system corrects such errors, and is highly conserved from bacteria to humans (Harfe and Jinks-Robertson, 2000; Kolodner, 1996; Kolodner and Marsischky, 1999; Modrich, 1991; Modrich and Lahue, 1996). MMR defects cause increased mutation rates and in humans, inherited and somatic defects in MMR result in increased development of cancer (Lynch and de la Chapelle, 1999; Lynch and de la Chapelle, 2003; Peltomaki, 2003; Wheeler et al., 2000). In eukaryotic MMR, mispair recognition is performed by two different heterodimeric complexes, Msh2-Msh6 and Msh2-Msh3, whose subunits are homologues of the bacterial MutS protein (Acharya et al., 1996; Drummond et al., 1995; Marsischky et al., 1996; Palombo et al., 1996; Reenan and Kolodner, 1992; Sia et al., 1997). The Msh2-Msh6 complex recognizes base-base mispairs and insertion/deletion loops and is the dominant mismatch recognition complex (Acharya et al., 1996; Alani, 1996; Gradia et al., 1997; Hess et al., 2002; Marsischky and Kolodner, 1999; Palombo et al., 1995). The Msh2-Msh3 complex primarily recognizes insertion/deletion loops and can partially substitute for Msh2-Msh6 (Acharya et al., 1996; Genschel et al., 1998; Marsischky and Kolodner, 1999; Palombo et al., 1996). Similarly, eukaryotic MMR utilizes heterodimeric complexes of proteins related to the bacterial MutL protein of which the Mlh1-Pms1 complex (Pms1 *S. cerevisiae* is Pms2 in humans) is the dominant complex (Flores-Rozas and

Kolodner, 1998; Prolla et al., 1994; Wang et al., 1999). Like their bacterial homologues, the Msh and Mlh complexes form a ternary complex on mispaired bases in DNA, where they presumably interact with downstream effector proteins (for a discussion see (Acharya et al., 2003; Mendillo et al., 2005).

The MutS and Msh2-Msh6 proteins form a ring around DNA when they bind to a mispair (Lamers et al., 2000; Obmolova et al., 2000). On ATP binding, in a reaction that does not require ATP hydrolysis, the Msh2-Msh6 complex is converted to a form that slides along DNA (Gradia et al., 1999; Mendillo et al., 2005). These Msh2-Msh6 sliding clamps have two modes of dissociation from DNA: slow direct dissociation and rapid sliding dependent dissociation off of the ends of linear DNA substrates (Mendillo et al., 2005). The Mlh1-Pms1-Msh2-Msh6 ternary complex that forms at mispairs also appears to exhibit sliding behavior (Mendillo et al., 2005). However, the role of these sliding protein complexes in the mechanism of MMR is not well understood. Sliding of MMR proteins along DNA plays a critical mechanistic role in only one of the major MMR models (Acharya et al., 2003; Gradia et al., 1999) whereas the other two models do not propose a role for sliding (Blackwell et al., 1998; Selmane et al., 2003).

We previously described dominant mutant Msh2-Msh6 complexes that appear to prevent mispaired bases in DNA from being acted on by Msh2-Msh3 (Das Gupta and Kolodner, 2000; Hess et al., 2002). Two of the dominant amino acid substitutions, S1036P and G1067D, are located in Msh6 near the γ-phosphate of ATP in the Msh2 binding site and the third dominant amino acid substitution, G1142D, is in

a C-terminal helix-turn-helix of Msh6 that contacts Msh2 near the Msh6 ATP binding site; S1036P probably contacts ATP in the Msh2 site whereas G1067D and G1142D probably do not contact bound ATP (Hess et al., 2002). Biochemical analysis of these three mutant Msh2-Msh6 complexes showed that they exhibited altered ATP-induced dissociation from mispaired bases (Hess et al., 2002). A fourth Msh6 amino acid substitution, H1096A, that results from a weak dominant *msh6* mutation changes an amino acid predicted to help activate the water that attacks the γ-phosphate of ATP in the Msh6 ATP binding site; however, this amino acid substitution had little effect on the biochemical properties of Msh2-Msh6. Here, we have performed a detailed biochemical analysis of these mutant Msh2-Msh6 complexes. Our results indicate that the three strong dominant Msh6 amino acid substitutions alter the interaction between ATP binding and downstream conformational changes within Msh2-Msh6 and result in trapping of different intermediates in the process of assembly of the Msh2-Msh6-Mlh1-Pms1 ternary complex.

3.3 RESULTS

Dominant mutant Msh2-Msh6 complexes show altered kinetics of ATP hydrolysis

Previous studies showed that three of the dominant mutant Msh2-Msh6 complexes had reduced ATPase activity in the presence of some mispaired bases in contrast to stimulation of wild-type Msh2-Msh6 (Hess et al., 2002). To extend these results, a kinetic analysis of ATP hydrolysis was performed and the kinetic constants are presented in Table 3-1. Compared to wild-type Msh2-Msh6, the strong dominant Msh6-S1036P and Msh6-G1067D complexes showed a lower k_{cat} under most reaction conditions, which was most pronounced in the presence of the GT mispair and +A substrates. This reduced rate of ATP hydrolysis likely reflects a defect in turnover from mispaired bases rather than a general inability to bind ATP given the nucleotide binding data presented below and that these two mutant complexes show reduced ATP-induced dissociation from mispaired bases (Hess et al., 2002). Compared to wild-type Msh2-Msh6, the strong dominant Msh6-G1142D complex generally showed a significantly reduced k_{cat} in the presence DNA that was most pronounced in the presence of the GT mispair and +A substrates. This combined with the nucleotide binding data presented below suggests that an ATP binding defect may underlie the ATP hydrolysis defect of the Msh6-G1142D complex. Finally, compared to wild-type Msh2-Msh6, the weakly dominant Msh6-H1096A complex showed a generally reduced k_{cat} that was somewhat more pronounced in the presence of the GT mispair

Table 3-1: Kinetic parameters of ATP hydrolysis by wild-type and mutant Msh2-Msh6 complexes.

	Protein				
	WT	S1036P	G1067D	H1096A	G1142D
			K_m (μM)		
-	14 ± 1.4	4 ± 2.4	18 (17-19)	8 (7-10)	90 ± 7.5
GC	31 ± 5.6	10 ± 1.2	25 (25-25)	22 (18-26)	85 ± 11.2
GT	81 ± 7.9	18 ± 3.1	32 (26-39)	84 (83-85)	357 ± 104.0
+A	52 ± 6.6	17 ± 0.5	31 (25-36)	35 (28-42)	122 ± 17.3
			k_{cat} (min^{-1})		
-	4.2 ± 0.8	2.0 ± 0.3	5.1 (4.9-5.3)	2.4 (2.3-2.5)	7.2 ± 2.6
GC	9.2 ± 0.9	3.5 ± 0.9	6.1 (5.9-6.3)	4.1 (3.3-4.8)	5.5 ± 1.9
GT	16.2 ± 2.3	0.9 ± 0.3	1.4 (1.3-1.6)	6.6 (6.1-7.1)	6.9 ± 2.7
+A	18.4 ± 1.6	5.9 ± 1.7	7.8 (6.7-9.0)	5.7 (4.7-6.7)	5.5 ± 0.9
			k_{cat}/K_m ($\mu M^{-1} \bullet min^{-1}$)		
-	0.30 ± 0.06	0.54 ± 0.28	0.28 (0.28-0.29)	0.30 (0.24-0.35)	0.08 ± 0.03
GC	0.30 ± 0.07	0.37 ± 0.13	0.24 (0.24-0.25)	0.19 (0.19-0.19)	0.06 ± 0.02
GT	0.20 ± 0.04	0.05 ± 0.01	0.05 (0.04-0.05)	0.08 (0.07-0.09)	0.02 ± 0.01
+A	0.36 ± 0.07	0.36 ± 0.11	0.26 (0.25-0.26)	0.16 (0.16-0.17)	0.05 ± 0.01

dsDNA substrates are as follows: GC, base pair; GT, base mispair; and +A, insertion (see *Experimental Procedures*). The values presented are the mean ± SD of the values obtained in independent experiment when three or more experiments were performed, in parenthesis, the range of values when only two experiments were performed.

and +A substrates. These results suggest that a general ATP hydrolysis defect results in the weakly dominant Msh6-H1096A complex.

Filter binding assays reveal that dominant mutant Msh2-Msh6 complexes have reduced ATP binding

Previous studies have shown that the *S. cerevisiae* Msh2-Msh6 complex has a high-affinity ATP binding site with a K_D of ATPγS binding of ~3.7 μM and a low-affinity ATP binding site with a K_D of ATPγS binding of ~17 μM (Antony and Hingorani, 2003). We have used filter binding to evaluate the ability of the mutant Msh2-Msh6 complexes to bind ATP in the absence of DNA and in the presence of 5-fold excess of DNA to protein of either a base paired DNA, a GT mispair DNA or a +A substrate. Two basic conditions were studied: binding to [α-^{32}P]ATP in the presence of EDTA to eliminate ATP hydrolysis and binding of [^{35}S]ATPγS in the presence of Mg^{++}. We also evaluated the effect of the order of addition of ATP and DNA and the time course of binding including short binding times as short as 10 sec. However, none of the modified binding conditions yielded results that were significantly different than obtained with the representative conditions presented in Figure 3-1.

First, binding to [α-^{32}P]ATP in the presence of EDTA was evaluated as a function of ATP concentration in the presence or absence of different DNA substrates with the DNA added before addition of nucleotide (Figure 3-1A-D). The highest levels of ATP binding were seen for the wild-type protein and there was little effect of

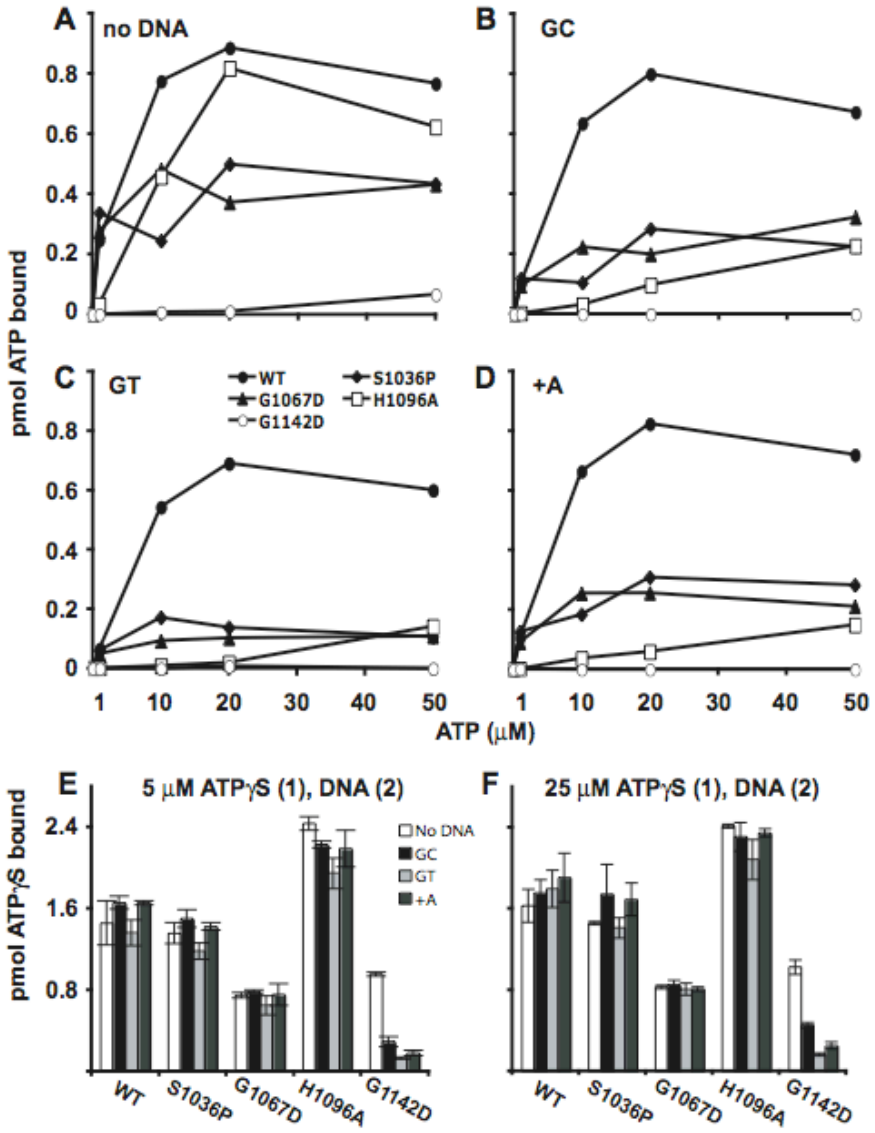

Figure 3-1. Filter binding analysis of ATP binding to mutant Msh2-Msh6 complexes. In the first series of experiments, the indicated Msh2-Msh6 complexes (4 pmole/200 nM) were incubated in the absence of DNA (A) or in the presence of GC (B), GT (C) or +A (D) DNA substrate in EDTA containing buffer followed by the addition of [α-^{32}P]ATP and measurement of the amount of ATP bound. In the second series of experiments, the indicated Msh2-Msh6 complexes were incubated in Mg^{2+} containing buffer and either 5 μM (E) or 25 μM (F) [^{35}S]ATPγS followed by the addition of the indicated DNA and measurement of the amount of ATP bound.

the addition of GC basepair, GT mispair or +A insertion/deletion mispair DNA on ATP binding compared to no DNA. In all reaction conditions with the wild-type Msh2-Msh6, the ATP binding detected is probably a measure of ATP bound to protein that is not bound to DNA. This is because under conditions where ATP cannot be hydrolyzed, ATP binding causes Msh2-Msh6 to dissociate from both basepairs and mispairs and ATP-bound Msh2-Msh6 cannot rebind to the DNA substrates (Mendillo et al., 2005). In the case of the Msh6-S1036P and Msh6-G1067D complexes, ATP binding in the absence of DNA was reduced by ~50% compared to wild-type Msh2-Msh6 and each of the DNAs further reduced the level of ATP binding observed to approximately 25% of that seen for the wild-type Msh2-Msh6. These results suggest that the Msh6-S1036P and Msh6-G1067D complexes have some sort of ATP binding defect but can still bind ATP to a significant extent. In addition, because the concentrations of proteins and DNA in these reactions are 10- and 50-fold higher, respectively, than the K_D of binding of the Msh6-S1036P complex to a GT mispair in the presence of ATP (note that the Msh6-G1067D complex showed GT binding kinetics that are virtually identical to those of the Msh6-S1036P complex) and these two protein complexes show stable binding to mispaired bases in the presence of ATP (Hess et al., 2002), these results suggest that they can likely bind ATP while bound to mispaired bases. In the case of the Msh6-H1096A complex, ATP binding in the absence of DNA was similar to that of wild-type Msh2-Msh6 whereas each of the DNAs significantly reduced ATP binding. This suggests that the Msh6-H1096A exhibits an ATP binding defect in the presence of DNA, which parallels the reduced

catalytic efficiency of the Msh6-H1096A complex in the presence of the three DNA substrates (Table 3-1). Finally, the Msh6-G1142D complex exhibited very low ATP binding under all four conditions. However, addition of ATP both decreases the binding of the Msh6-G1142D complex to mispaired bases and increases the dissociation of prebound Msh6-G1142D complex so the Msh6-G1142D complex cannot be completely defective for ATP binding (Hess et al., 2002).

Second, binding of [^{35}S]ATPγS in the presence of Mg^{2+} was evaluated at two different ATPγS concentrations, a low concentration (5 μM) that was slightly above the reported K_D of the high affinity ATP-binding site and a high concentration (25 μM) that was slightly above the reported K_D of the low affinity ATP-binding site (Antony and Hingorani, 2003). In the examples shown (Figure 3-1E & F), the ATPγS was added to the protein before the DNA was added; however, similar results were obtained when the DNA was added before the ATPγS (data not shown). In the case of wild-type Msh2-Msh6, the same level of ATPγS binding was observed in the absence of DNA or in the presence of the three different DNA substrates, and possibly slightly higher binding was observed at 25 μM ATPγS than at 5 μM ATPγS. In the case of the Msh6-S1036P, Msh6-G1067D and Msh6-H1096A complexes, the level of ATPγS binding observed was the same, ~50% lower and ~50% higher, respectively than seen for wild-type Msh2-Msh6. Similar levels of binding were seen at 25 μM ATPγS and 5 μM ATPγS, and addition of the three different DNA substrates had no effect on ATPγS binding. In the case of the Msh6-G1142D complex there was significantly reduced ATPγS binding in the absence of DNA compared to wild-type Msh2-Msh6

and addition of the three DNA substrates further reduced the binding of ATPγS with the mispaired DNAs having the greatest effect. Again, similar results were obtained with 25 μM ATPγS and 5 μM ATPγS. This shows that the Msh6-G1142D complex has a reduced ability to bind ATP, particularly in the presence of DNA.

There were significant differences in the results obtained with [α-^{32}P]ATP in the presence of EDTA and [^{35}S]ATPγS in the presence of Mg^{2+} which suggests that either the absence of Mg^{2+} destabilizes ATP binding or that ATPγS and ATP have different binding characteristics. Regardless, the filter binding experiments reveal that each of the four mutant Msh2-Msh6 complexes has distinct defects in ATP binding.

UV-crosslinking reveals that dominant mutant Msh2-Msh6 complexes have different ATP binding defects

UV-crosslinking was used to analyze the interaction of the mutant Msh2-Msh6 proteins with ATP under conditions (-Mg^{2+}) where ATP hydrolysis cannot occur (Figure 3-2). The concentration of ATP used, 100 μM is well above the K_D of binding to the Msh2 and Msh6 ATP binding sites and induces both mispair-dependent sliding of Msh2-Msh6 and ternary complex formation with Mlh1-Pms1 (unpublished). When the wild type protein was analyzed, both the Msh2 and Msh6 subunits were labeled; ATP titration studies (not shown) indicated that this level of labeling represents 80% binding saturation for Msh2 and 97% binding saturation for Msh6. In addition, the individual Walker A amino acid substitutions Msh2-K694M and Msh6-K988M that change critical residues within the ATP binding pockets of the Msh2 and Msh6 ATP

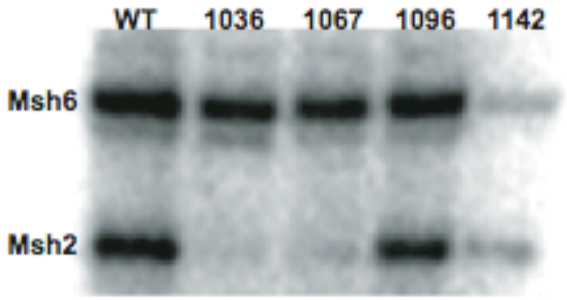

Figure 3-2. UV crosslinking of ATP to mutant Msh2-Msh6 complexes. Crosslinking reactions (20 μl) containing 4 pmoles (200 nM) of the indicated Msh2-Msh6 complexes and 100 μM [γ-^{32}P]ATP were prepared, UV-irradiated and analyzed by SDS-PAGE as described under "Experimental Procedures."

sites, respectively, reduced crosslinking to Msh2 and Msh6 respectively (unpublished). These latter results support the view that these ATP cross-linking experiments provide a useful method for characterization of the nucleotide binding properties of Msh2 and Msh6.

The S1036P and G1067D Msh6 mutants contain amino acid substitutions in a region of Msh6 that is adjacent to the Msh2 ATP binding site. These two amino acid substitutions eliminated ATP crosslinking to Msh2 and had no apparent effect on ATP crosslinking to Msh6. The Msh6 amino acid substitution H1096A changes a residue predicted to help coordinate the γ-phosphate of ATP in the Msh6 ATP binding site. Under the UV-crosslinking conditions this amino acid substitution had little effect on ATP crosslinking to either subunit. The Msh6 amino acid substitution G1142D is adjacent to the Msh6 ATP binding site. This amino acid substitution almost completely eliminated ATP crosslinking to both Msh2 and Msh6; the level of ATP crosslinking observed was 20% and 14% of that seen for Msh2 and Msh6 in the wild-type protein complex, respectively. These results show that the three strong dominant *msh6* mutations affect ATP binding by Msh2-Msh6 and define at least two classes of ATP binding defects.

Dominant mutant Msh2-Msh6 complexes are defective in sliding clamp formation

In a previous study we developed a method using an IAsys biosensor to evaluate binding Msh2-Msh6 to a mispaired base and conversion to a sliding form that

undergoes end-dependent dissociation on binding ATP or ATP analogs (Mendillo et al., 2005). DNA substrates are attached at one end to the surface of an IAsys cuvette and the free end of the DNA, depending on the experiment, is blocked with LacI protein, which can be dissociated ($t_{1/2}$ = 1.6 sec) on addition of IPTG. When Msh2-Msh6 is incubated with either GT or +A mispair containing substrates in the presence of ATP, bound ATP is hydrolyzed to ADP allowing Msh2-Msh6 to bind to the mispair. When ATP then binds to the Msh2-Msh6, it is converted to a form that dissociates from the mispair by sliding off of the end of the DNA. Under these conditions, a steady-state level of binding is reached that is higher on mispair containing DNA (Figure 3-3A & F) than basepair containing DNA (Figure 3-3K). In the presence of LacI protein, a higher level of Msh2-Msh6 binding is seen on the mispair substrates (Figure 3-3A & F) because while the Msh2-Msh6 slides away from the mispair allowing additional Msh2-Msh6 to bind, the end-block prevents its rapid dissociation off of the ends (note that on end-blocked substrates, Msh2-Msh6 undergoes a slower direct mode of dissociation). In contrast, blocking the ends of basepair containing substrates did not lead to increased binding (Figure 3-3K) because dissociation by sliding is mispair dependent. Finally, when Msh2-Msh6 was bound to end-blocked mispair containing substrates and IPTG was added to dissociate the LacI, rapid dissociation of Msh2-Msh6 by sliding off of the ends was seen (Figure 3-3A & F); no IPTG-induced dissociation of Msh2-Msh6 was seen on basepair containing substrates, because dissociation by sliding is mispair dependent (Figure 3-3K).

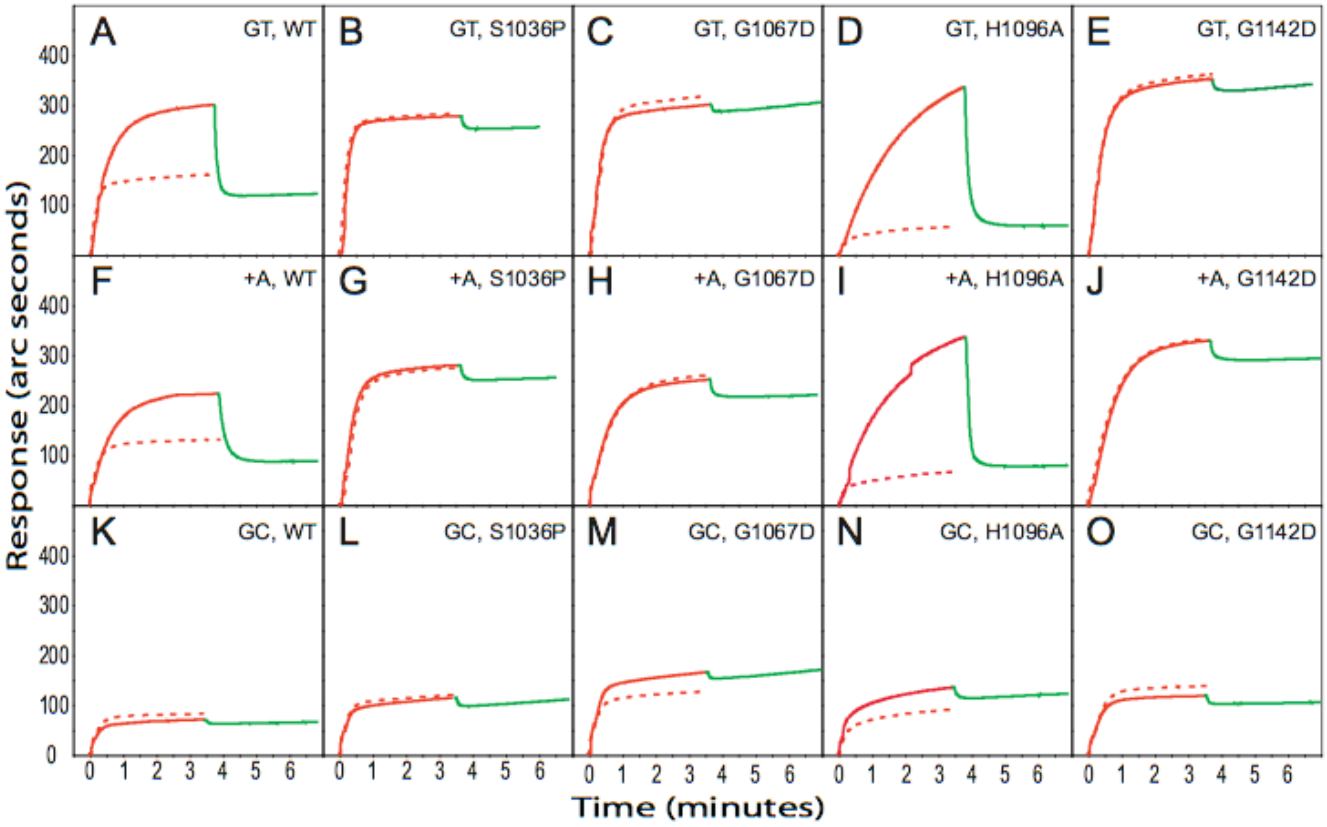

Figure 3-3. Analysis of mutant Msh2-Msh6 complexes for sliding clamp formation. Biosensor analysis of the association and dissociation of the indicated Msh2-Msh6 complexes with a DNA substrate containing a GT mispair (A, B, C, D, E), +A insertion (F, G, H, I, J) or a GC basepair (K, L, M, N, O) is shown. The dashed red line indicates association with DNA substrates with a free end, the solid red line indicates association with DNA substrates with a LacI-blocked end and the solid green line indicates dissociation on addition of IPTG to complexes formed on LacI-blocked DNA substrates. Note the small IPTG induced decrease (B, C, E, G, H, J, K, L, M, N and O) is due to LacI dissociation, while the larger decrease (A, D, F and I) is mainly due to rapid Msh2-Msh6 dissociation from newly freed ends.

The Msh6-S1036P (Figure 3-3B, G & L), Msh6-G1067D (Figure 3-3C, H & M) and Msh6-G1142D (Figure 3-3E, J & O) complexes all showed higher binding to the unblocked GT and +A mispair containing substrates in the presence of ATP compared to the wild-type protein consistent with previous observations that ATP does not induce rapid dissociation of these mutant complexes from mispairs (Hess et al., 2002). In contrast to wild-type Msh2-Msh6, blocking the ends of the mispair containing substrates did not increase the steady-state levels of binding of the Msh6-S1036P, Msh6-G1067D and Msh6-G1142D complexes relative to binding to the unblocked substrates and addition of IPTG to dissociate the LacI did not induce dissociation of these three mutant complexes. The binding behavior of Msh6-S1036P, Msh6-G1067D and Msh6-G1142D complexes on the basepair containing substrate was the same as the wild-type complex. These results show that while the Msh6-S1036P, Msh6-G1067D and Msh6-G1142D complexes recognize mispairs in DNA, they are defective for ATP induced conversion to the sliding configuration. Analysis of the Msh6-H1096A complex (Figure 3-3D, I & N) revealed a binding behavior that was similar to wild-type Msh2-Msh6 (Figure 3-3A, F & K) indicating that this mutant complex was proficient for ATP induced sliding. Interestingly, the Msh6-H1096A complex showed lower binding to unblocked GT or +A mispair containing substrates and slower, but higher binding to the blocked mispair containing substrates than wild-type Msh2-Msh6. These results indicate that the relatively minor ATP binding/hydrolysis defect of the Msh6-H1096A complex alters its mispair binding and dissociation dynamics.

Dominant mutant Msh2-Msh6 complexes exhibit different defects in assembly of ternary complexes with Mlh1-Pms1

To examine the ability of mutant Msh2-Msh6 complexes to form ternary complexes with Mlh1-Pms1, the Msh2-Msh6 complexes were incubated with immobilized LacI blocked substrate in the presence of ADP or ADP + Mlh1-Pms1 to allow Msh2-Msh6 mispair binding to occur (Figure 3-4); ternary complexes do not form in the absence of ATP (Mendillo et al., 2005). Then the Msh2-Msh6-DNA complexes were challenged by the addition of ATP to allow assembly with Mlh1-Pms1; the level of Mlh1-Pms1 binding observed was determined by subtracting the Msh2-Msh6 only curve from the Msh2-Msh6 + Mlh1-Pms1 curve (Figure 3-4 inserts). The LacI end-block was necessary to prevent assembly of Msh2-Msh6-Mlh1-Pms1 complexes on the ends of DNA. In the case of wild-type Msh2-Msh6, robust ternary complex formation was observed on GT and +A mispair containing substrates (Figure 3-4A & F) compared with lower level ternary complex formation on the basepair substrate (Figure 3-4K); prior studies have shown that the ternary complex formed on basepair substrates exhibits distinctly different dissociation behavior than ternary complexes formed on mispair DNA (Mendillo et al., 2005). The significant increase in ternary complex formation above that predicted for loading of one Mlh1-Pms1 complex per prebound wild-type Msh2-Msh6 complex (Figure 3-4F) has been attributed to sliding of the wild-type ternary complex off of the mispair allowing additional Msh2-Msh6 complexes and hence ternary complexes to assemble. Ternary

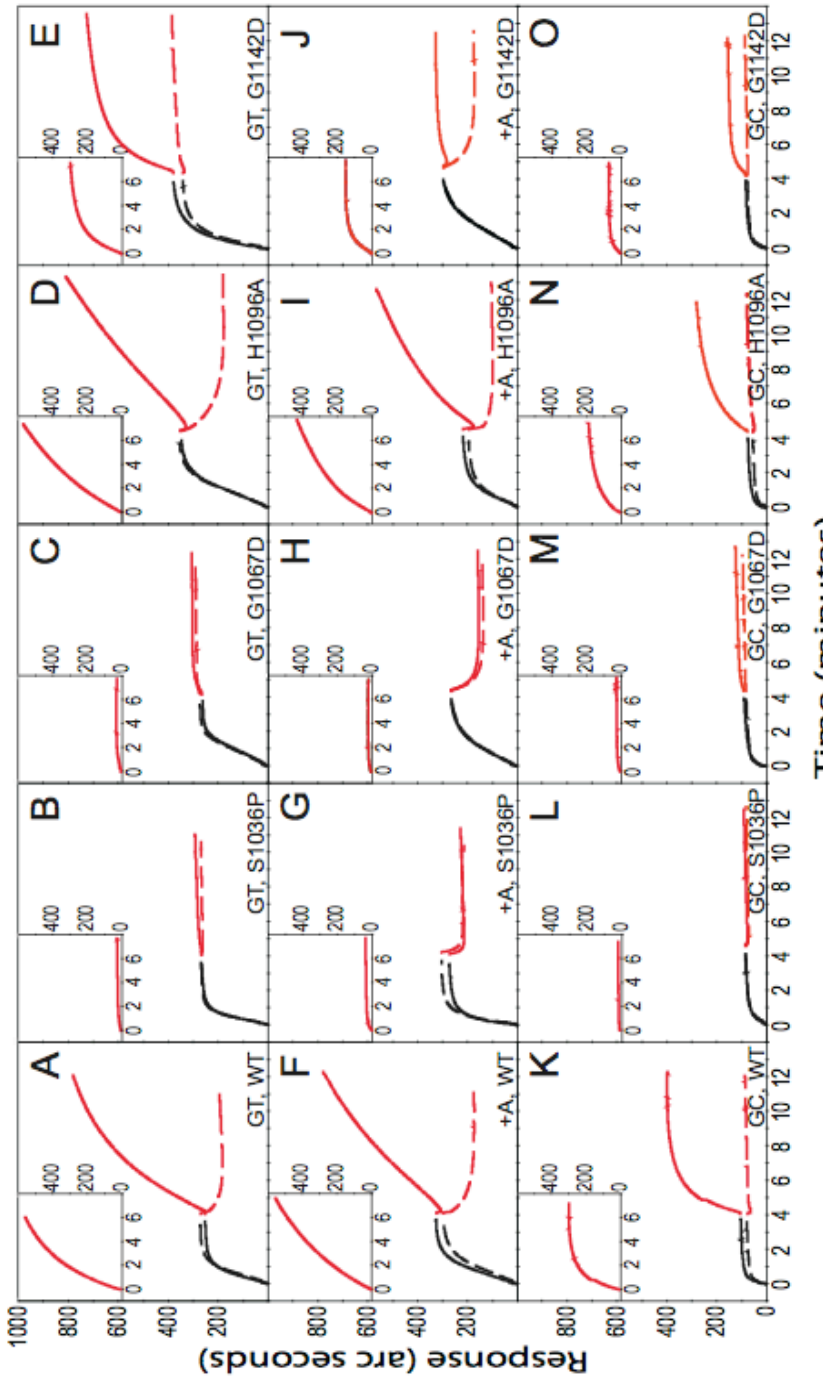

Figure 3-4. Analysis of mutant Msh2-Msh6 complexes for assembly of ternary complexes with Mlh1-Pms1. Biosensor analysis of the association of the indicated Msh2-Msh6 complexes with a DNA substrate containing a GT mispair (A, B, C, D, E), +A insertion (F, G, H, I, J) or a GC basepair (K, L, M, N, O) end-blocked with 30 nM LacI is shown. Mlh1-Pms1 was present in the association (solid black line) buffer, but the Mlh1-Pms1-Msh2-Msh6-DNA ternary complex formed only after addition of ATP (solid red line). A control lacking Mlh1-Pms1 was included for comparison (dashed black line) to determine the effect of adding ATP on Msh2-Msh6 (dashed red line). The level of Mlh1-Pms1 binding was determined by subtracting the Msh2-Msh6 only curve from the Msh2-Msh6 + Mlh1-Pms1 curve (insets).

complex formation with the Msh6-H1096A complex (Figure 3-4D, I & N) was essentially the same as the wild-type Msh2-Msh6 complex.

The strong dominant mutant Msh2-Msh6 complexes exhibited two distinctly different ternary complex formation behaviors. The Msh6-S1036P (Figure 3- 4B, G & L) and Msh6-G1067D (Figure 3-4C, H & M) complexes did not support ternary complex formation with Mlh1-Pms1 on any DNA substrate. Thus, these mutant complexes appear to be defective for one or more ATP induced conformational changes required for sliding clamp formation and ternary complex formation. In contrast, the Msh6-G1142D complex was proficient for ternary complex formation on the GT and +A mispair containing substrates (Figure 3-4E & J) and exhibited ~25% of wild type levels of ternary complex formation on the basepair substrate (Figure 3-4O). However, in comparison to ternary complex formation with wild-type Msh2-Msh6, mispair dependent ternary complex formation with the Msh6-G1142D complex reached a plateau at a lower level consistent with loading of one Mlh1-Pms1 complex per prebound Msh2-Msh6 complex. This result is predicted if the Msh6-G1142D complex, in contrast to the wild-type Msh2-Msh6 complex (see above) is defective for sliding away from the mispair preventing the binding of more Msh2-Msh6 and hence preventing the assembly of additional ternary complexes. These results indicate that the Msh6-G1142D substitution allows ternary complex formation even though the mutant Msh2-Msh6 complex is defective for ATP binding and sliding clamp formation.

3.4 DISCUSSION

Here, we have performed a detailed biochemical analysis of four dominant mutant Msh2-Msh6 complexes. The strongly dominant mutant Msh6-S1036P and Msh6-G1067D complexes had a lower k_{cat} for ATP hydrolysis in the presence of mispaired bases, only bound ATP in the Msh6 ATP binding site, bound to mispaired bases but were defective for conversion to sliding clamps and were defective for assembly of ternary complexes with Mlh1-Pms1. These results indicate that these two mutant complexes remain bound to mispairs in the presence of ATP because they are defective for ATP binding in the Msh2 site and as a consequence do not undergo some type of ATP induced conformational change. The strongly dominant Msh6-G1142D complex had a reduced k_{cat} for ATP hydrolysis particularly in the presence of mispaired bases, only weakly bound ATP, which was further reduced by DNA containing mispaired bases, and bound to mispaired bases but was defective for conversion to rapidly dissociating sliding clamps. These results show this mutant complex remains bound to mispairs in the presence of ATP because it is defective for ATP binding. Remarkably, the Msh6-G1142D complex did support mispair dependent, ATP dependent assembly of ternary complexes with Mlh1-Pms1. These results demonstrate at least two mechanisms for dominance, one in which the mutant Msh2-Msh6 complex binds and occludes mispaired bases and the other in which the mutant Msh2-Msh6 complex binds mispaired bases and assembles a Msh2-Msh6-Mlh1-Pms1 ternary complex that also occludes mispaired bases. The Msh6-H1096A

complex had a relatively minor ATP binding/hydrolysis defect and a subtle alteration of its mispair binding and dissociation dynamics; however, additional experimentation will be required to determine how this results in a weak dominant mutator phenotype.

The Msh6-S1036P and Msh6-G1067D mutants have amino acid changes near the Msh2 ATP binding site and the Msh6-G1142D mutant has an amino acid change near the Msh6 ATP binding site. Based on studies of proteins like Rad50 (Hopfner et al., 2000; Jones and George, 1999; Nikaido and Ames, 1999), these amino acid substitutions would likely affect ATP-binding-induced or ADP-ATP-exchange-induced conformational changes across the Msh2-Msh6 interface. These amino acid changes may also affect mispair induced conformational changes transmitted to this region of the protein (Junop et al., 2001; Lamers et al., 2000; Obmolova et al., 2000; Sixma, 2001). The observation that the Msh6-S1036P and Msh6-G1067D amino acid substitutions prevent ATP binding in the Msh2 site suggests that they either alter the structure of the Msh2 ATP binding site or they block a conformational change at the Msh2-Msh6 interface that allows ATP binding in the Msh2 site. These results further indicate that this conformational change and/or ATP binding in the Msh2 site are required for both sliding clamp formation and ternary complex formation with Mlh1-Pms1. Finally, these results indicate that the interaction with ATP in the Msh2 site is critical for inhibition of mispair binding by prebound ATP (Mendillo et al., 2005). The observation that the Msh6-G1142D amino acid substitution inhibits binding in both sites, which is further diminished by mispair binding suggests that this amino acid substitution stabilizes a conformation that cannot bind ATP but is still competent

for mispair binding and induced conformational changes; these results further suggest that ATP binding in the Msh6 site affects ATP binding in the Msh2 site.

Remarkably, the Msh6-G1142D complex can assemble mispair dependent ternary complexes with Mlh1-Pms1 even though the Msh6-G1142D complex is significantly defective for binding ATP at the Msh2 and Msh6 sites. This observation raises several hypotheses. First, it is possible that a critical mispair induced conformational change at an interface between Msh2-Msh6 and Mlh1-Pms1 is required for ternary complex formation rather than a mispair-induced alteration of ATP bound states or ATP hydrolysis. Second, it is possible that either ATP binding by Msh2-Msh6 is not required for ternary complex formation or the Msh6-G1142D amino acid substitution stabilizes a conformational state in the absence of ATP binding that is normally induced by ATP binding, thus preventing the mutant complexes from binding ATP but allowing assembly of Mlh1-Pms1; in this regard, it should be noted that addition of DNA substrates significantly inhibits the already reduced ATP binding exhibited by the Msh6-G1142D complex (Figure 3-1). However, since ternary complex formation with the Msh6-G1142D complex requires ATP, these first two possibilities would place the ATP requirement on the Mlh1-Pms1 complex. Finally, because Msh2-Msh6 is in large excess over DNA in the ternary complex formation experiments, it is possible that the fraction of Msh6-G1142D complex that binds mispairs and forms ternary complexes is the fraction of Msh6-G1142D complex that binds ATP, but that this ATP-bound form does not support sliding. In the context of each hypothesis, it is tempting to speculate that *msh6-*

G1142D is a separation-of-function mutation resulting in a sliding clamp defective but otherwise MMR competent form of Msh2-Msh6 supporting the view that sliding clamp formation is needed for MMR (Gradia et al., 1999). In this regard, the sliding defect of the Msh6-G1142D and related reduced assembly of Msh6-G1142D-Mlh1-Pms1 complexes can be partially overcome at very high ATP concentrations (data not shown).

In this study we have performed a detailed biochemical characterization of three strong dominant mutant Msh2-Msh6 complexes and one weak dominant mutant Msh2-Msh6 complex. This analysis has defined two different biochemical defects that underlie dominant mutations in *MSH6*. In addition, these mutations have allowed further dissection of the early biochemical steps in mismatch recognition and MMR. This basic strategy may be applicable to the analysis of other biochemical steps in MMR.

3.5 EXPERIMENTAL PROCEDURES

Proteins

Wild-type and Msh6 mutant Msh2-Msh6 complexes and wild-type Mlh1-Pms1 complex were purified as previously described (Hess et al., 2002; Mendillo et al., 2005). The LacI protein was provided by Kathleen Matthews (Rice University).

Nucleotide binding and ATP hydrolysis assays

Nucleotide binding assays were performed in 20 μl volumes containing 4 pmoles of wild-type or mutant Msh2-Msh6, 25 mM Hepes Buffer pH 7.5, 100 mM NaCl, 1 mM dithiolthreitol, 100 μg/ml BSA, 1 mM EDTA, 1-100 μM [α-^{32}P]ATP (0.6-30 Ci/mmol, Amersham Biosciences), 15% glycerol and 1 μM of the indicated previously described dsDNA substrates (Hess et al., 2002). Proteins were mixed with DNA substrates for 5 min at room temperature and then ATP was added for 12 min. In some experiments the 12 min incubation with ATP preceded the 5 min incubation with DNA. The reactions were then transferred to ice, diluted with 3 ml of ice-cold stop-buffer consisting of 25 mM Hepes buffer pH 7.5, 100 mM NaCl and 1 mM EDTA, and immediately filtered over 25 μm nitrocellulose filters (Millipore HAWPO2500). The filters were washed 2 times with 5 ml of stop-buffer and the bound radioactivity determined by liquid scintillation counting. In experiments containing [^{35}S]ATPγS (2.5-12.5 Ci/mmol, Perkin Elmer) instead of [α-^{32}P]ATP, the EDTA in all buffers was replaced with 10 mM $MgCl_2$.

ATPase activity was measured as previously described in 20 μl reactions consisting of 25 mM HEPES buffer pH 7.8, 10 mM $MgCl_2$, 0.1 mM EDTA, 100 mM NaCl, 1 mM DTT, 10% glycerol, 0.001% IGEPAL 40, 75 μg/ml acetylated BSA (Promega), 10-250 μM [γ-^{32}P]ATP and 200 nM of the indicated previously described dsDNA substrates (Hess et al., 2002). The reactions were started by adding wild-type or mutant Msh2-Msh6 to 60 nM, incubated at 30ºC and processed as previously described (Hess et al., 2002). All values were determined by subtracting the value obtained for a no-protein control.

UV crosslinking experiments

Reactions were performed in 20 μl volumes containing 4 pmoles wild-type or mutant Msh2-Msh6, 50 mM Tris pH 8.0, 110 mM NaCl, 2 mM dithiolthreitol, 200 μg/ml BSA, 0.5 mM EDTA and 5% glycerol. Proteins were mixed with 100 μM [γ-^{32}P]ATP (25 Ci/mmol, Amersham Biosciences) incubated on ice for 10 minutes, followed by 20 minutes of crosslinking using a Stratalinker (Stratagene). Reaction mixtures were then fractionated by SDS-PAGE and radiolabeled bands were detected and quantified using a PhosphorImager (Molecular Dynamics). Crosslinking to BSA (present in all samples) was not detected.

Total Internal Reflectance Measurements

A 236 basepair DNA substrate that was biotinylated at one end, contained either a central GT mispair or GC basepair and had the *lac* O_1 operator sequence

incorporated at the other end was made as described previously (Mendillo et al., 2005). In the case of the GT substrate the G is located at nucleotide 103 of the top strand and the T is located in the complementary position of the bottom strand where the C would be located in the GC control substrate. An additional substrate containing a +A insertion was constructed by the same method. In this case, the biotinylated top strand was made by PCR amplification using plasmid RDK4720 as template DNA and the bottom strand was made by PCR amplification using the plasmid RDK4719 as template. The top strand contains the +A insertion at nucleotide 104; in addition, nucleotide 103 of the top strand has been changed to a C and a G is present as its complement in the bottom strand.

Experiments analyzing either Msh2-Msh6 binding or the Msh2-Msh6-Mlh1-Pms1 ternary complex formation on the GT mispair, +A insertion, or the GC basepair substrates were performed using an IAsys Auto Plus instrument using a running buffer consisting of 25 mM Tris, (pH 8.0), 110 mM NaCl, 4 mM $MgCl_2$ 0.5 mM dithiothreitol, 2% Glycerol, 0.05% IGEPAL CA-630 (NP-40), 25 μM ADP and 250 μM ATP as previously described (Mendillo et al., 2005). For Msh2-Msh6 binding to unblocked DNA substrates, the equilibration buffer was removed and replaced with 50 μL of the same buffer, but containing 50 nM wild-type or mutant Msh2-Msh6. Incubation was carried out for approximately 3.5 min or until equilibrium was reached. For experiments on end-blocked DNA substrates, 30 nM LacI was included in the running buffer, both during the equilibration and Msh2-Msh6 binding phases. The baseline of the association curves of MMR proteins depicted was taken after LacI

was bound to the DNA substrates, so the binding curves reflect association of MMR proteins only. The dissociation of Msh2-Msh6 off of the end of the DNA substrate was monitored by adding 5 μL of running buffer containing 10 mM IPTG to the 50 μL of protein-containing buffer in the cuvette. This allowed dissociation of LacI bound ($t_{1/2}$ ~1.6 sec) at the ends of the DNA substrate without significantly altering the concentrations of protein in solution. All experiments were performed at 25°C.

Analysis of Mlh1-Pms1 binding to the Msh2-Msh6-DNA complex was performed as follows. The cuvette containing the indicated bound DNA substrate was first equilibrated in running buffer lacking ATP and containing 30 nM LacI. This buffer was then replaced with 50 μL of running buffer lacking ATP and containing 20 nM of wild-type or mutant Msh2-Msh6, 30 nM LacI and 40 nM Mlh1-Pms1, as indicated. Incubation was carried out for approximately 3.5 min or until equilibrium was reached; Mlh1-Pms1 does not interact with Msh2-Msh6 and DNA in the presence of ADP alone (Mendillo et al., 2005). Next, ternary complex formation was initiated by adding 5 μL of running buffer containing 2.75 mM ATP, which resulted in a final concentration of 250 μM ATP. Binding was then monitored for approximately 8 min. All experiments were performed at 25° C.

3.6 ACKNOWLEDGEMENTS

The authors would like to thank Chris Putnam and Scarlet Shell for helpful discussions and comments on the manuscript, and Kathleen Matthews for generously providing the LacI protein used in these studies. This work was supported by NIH Grants GM50006 and CA92584 to RDK and an American Cancer Society postdoctoral fellowship to DJM.

Chapter 3, in full, is a reprint of the material as it appears in Hess, M. T., Mendillo, M. L., Mazur, D. J. & Kolodner, R. D. "Biochemical basis for dominant mutations in the Saccharomyces cerevisiae Msh6 gene." *Proc Natl Acad Sci U S A* 2006 Jan 17; 103(3): 558-563. The dissertation author and Martin T. Hess contributed equally as primary authors of this paper.

3.7 REFERENCES

Acharya, S., Foster, P. L., Brooks, P., and Fishel, R. (2003). The coordinated functions of the E. coli MutS and MutL proteins in mismatch repair. Mol Cell *12*, 233-246.

Acharya, S., Wilson, T., Gradia, S., Kane, M. F., Guerrette, S., Marsischky, G. T., Kolodner, R., and Fishel, R. (1996). hMSH2 forms specific mispair-binding complexes with hMSH3 and hMSH6. Proc Natl Acad Sci U S A *93*, 13629-13634.

Alani, E. (1996). The Saccharomyces cerevisiae Msh2 and Msh6 proteins form a complex that specifically binds to duplex oligonucleotides containing mismatched DNA base pairs. Mol Cell Biol *16*, 5604-5615.

Antony, E., and Hingorani, M. M. (2003). Mismatch recognition-coupled stabilization of Msh2-Msh6 in an ATP-bound state at the initiation of DNA repair. Biochemistry *42*, 7682-7693.

Blackwell, L. J., Martik, D., Bjornson, K. P., Bjornson, E. S., and Modrich, P. (1998). Nucleotide-promoted release of hMutSalpha from heteroduplex DNA is consistent with an ATP-dependent translocation mechanism. J Biol Chem *273*, 32055-32062.

Das Gupta, R., and Kolodner, R. D. (2000). Novel dominant mutations in Saccharomyces cerevisiae MSH6. Nat Genet *24*, 53-56.

Drummond, J. T., Li, G. M., Longley, M. J., and Modrich, P. (1995). Isolation of an hMSH2-p160 heterodimer that restores DNA mismatch repair to tumor cells. Science *268*, 1909-1912.

Flores-Rozas, H., and Kolodner, R. D. (1998). The Saccharomyces cerevisiae MLH3 gene functions in MSH3-dependent suppression of frameshift mutations. Proc Natl Acad Sci U S A *95*, 12404-12409.

Genschel, J., Littman, S. J., Drummond, J. T., and Modrich, P. (1998). Isolation of MutSbeta from human cells and comparison of the mismatch repair specificities of MutSbeta and MutSalpha. J Biol Chem *273*, 19895-19901.

Gradia, S., Acharya, S., and Fishel, R. (1997). The human mismatch recognition complex hMSH2-hMSH6 functions as a novel molecular switch. Cell *91*, 995-1005.

Gradia, S., Subramanian, D., Wilson, T., Acharya, S., Makhov, A., Griffith, J., and Fishel, R. (1999). hMSH2-hMSH6 forms a hydrolysis-independent sliding clamp on mismatched DNA. Mol Cell *3*, 255-261.

Harfe, B. D., and Jinks-Robertson, S. (2000). DNA mismatch repair and genetic instability. Annu Rev Genet *34*, 359-399.

Hess, M. T., Gupta, R. D., and Kolodner, R. D. (2002). Dominant Saccharomyces cerevisiae msh6 mutations cause increased mispair binding and decreased dissociation from mispairs by Msh2-Msh6 in the presence of ATP. J Biol Chem *277*, 25545-25553.

Hopfner, K. P., Karcher, A., Shin, D. S., Craig, L., Arthur, L. M., Carney, J. P., and Tainer, J. A. (2000). Structural biology of Rad50 ATPase: ATP-driven conformational control in DNA double-strand break repair and the ABC-ATPase superfamily. Cell *101*, 789-800.

Jones, P. M., and George, A. M. (1999). Subunit interactions in ABC transporters: towards a functional architecture. FEMS Microbiol Lett *179*, 187-202.

Junop, M. S., Obmolova, G., Rausch, K., Hsieh, P., and Yang, W. (2001). Composite active site of an ABC ATPase: MutS uses ATP to verify mismatch recognition and authorize DNA repair. Mol Cell *7*, 1-12.

Kolodner, R. (1996). Biochemistry and genetics of eukaryotic mismatch repair. Genes Dev *10*, 1433-1442.

Kolodner, R. D., and Marsischky, G. T. (1999). Eukaryotic DNA mismatch repair. Curr Opin Genet Dev *9*, 89-96.

Lamers, M. H., Perrakis, A., Enzlin, J. H., Winterwerp, H. H., de Wind, N., and Sixma, T. K. (2000). The crystal structure of DNA mismatch repair protein MutS binding to a G x T mismatch. Nature *407*, 711-717.

Lynch, H. T., and de la Chapelle, A. (1999). Genetic susceptibility to non-polyposis colorectal cancer. J Med Genet *36*, 801-818.

Lynch, H. T., and de la Chapelle, A. (2003). Hereditary colorectal cancer. N Engl J Med *348*, 919-932.

Marsischky, G. T., Filosi, N., Kane, M. F., and Kolodner, R. (1996). Redundancy of Saccharomyces cerevisiae MSH3 and MSH6 in MSH2-dependent mismatch repair. Genes Dev *10*, 407-420.

Marsischky, G. T., and Kolodner, R. D. (1999). Biochemical characterization of the interaction between the Saccharomyces cerevisiae MSH2-MSH6 complex and mispaired bases in DNA. J Biol Chem *274*, 26668-26682.

Mendillo, M. L., Mazur, D. J., and Kolodner, R. D. (2005). Analysis of the interaction between the Saccharomyces cerevisiae MSH2-MSH6 and MLH1-PMS1 complexes

with DNA using a reversible DNA end-blocking system. J Biol Chem *280*, 22245-22257.

Modrich, P. (1991). Mechanisms and biological effects of mismatch repair. Annu Rev Genet *25*, 229-253.

Modrich, P., and Lahue, R. (1996). Mismatch repair in replication fidelity, genetic recombination, and cancer biology. Annu Rev Biochem *65*, 101-133.

Nikaido, K., and Ames, G. F. (1999). One intact ATP-binding subunit is sufficient to support ATP hydrolysis and translocation in an ABC transporter, the histidine permease. J Biol Chem *274*, 26727-26735.

Obmolova, G., Ban, C., Hsieh, P., and Yang, W. (2000). Crystal structures of mismatch repair protein MutS and its complex with a substrate DNA. Nature *407*, 703-710.

Palombo, F., Gallinari, P., Iaccarino, I., Lettieri, T., Hughes, M., D'Arrigo, A., Truong, O., Hsuan, J. J., and Jiricny, J. (1995). GTBP, a 160-kilodalton protein essential for mismatch-binding activity in human cells. Science *268*, 1912-1914.

Palombo, F., Iaccarino, I., Nakajima, E., Ikejima, M., Shimada, T., and Jiricny, J. (1996). hMutSbeta, a heterodimer of hMSH2 and hMSH3, binds to insertion/deletion loops in DNA. Curr Biol *6*, 1181-1184.

Peltomaki, P. (2003). Role of DNA mismatch repair defects in the pathogenesis of human cancer. J Clin Oncol *21*, 1174-1179.

Prolla, T. A., Pang, Q., Alani, E., Kolodner, R. D., and Liskay, R. M. (1994). MLH1, PMS1, and MSH2 interactions during the initiation of DNA mismatch repair in yeast. Science *265*, 1091-1093.

Reenan, R. A., and Kolodner, R. D. (1992). Isolation and characterization of two Saccharomyces cerevisiae genes encoding homologs of the bacterial HexA and MutS mismatch repair proteins. Genetics *132*, 963-973.

Selmane, T., Schofield, M. J., Nayak, S., Du, C., and Hsieh, P. (2003). Formation of a DNA mismatch repair complex mediated by ATP. J Mol Biol *334*, 949-965.

Sia, E. A., Kokoska, R. J., Dominska, M., Greenwell, P., and Petes, T. D. (1997). Microsatellite instability in yeast: dependence on repeat unit size and DNA mismatch repair genes. Mol Cell Biol *17*, 2851-2858.

Sixma, T. K. (2001). DNA mismatch repair: MutS structures bound to mismatches. Curr Opin Struct Biol *11*, 47-52.

Wang, T. F., Kleckner, N., and Hunter, N. (1999). Functional specificity of MutL homologs in yeast: evidence for three Mlh1-based heterocomplexes with distinct roles during meiosis in recombination and mismatch correction. Proc Natl Acad Sci U S A *96*, 13914-13919.

Wheeler, J. M., Bodmer, W. F., and Mortensen, N. J. (2000). DNA mismatch repair genes and colorectal cancer. Gut *47*, 148-153

CHAPTER 4

Inhibition of Msh6 ATPase activity by mispaired DNA induces a Msh2(ATP)-Msh6(ATP) state that is capable of hydrolysis independent movement along DNA

4.1 ABSTRACT

The Msh2-Msh6 heterodimer plays a key role in the repair of mispaired bases in DNA. Critical to its role in mismatch repair is the ATPase activity that resides within each subunit. Here we show both subunits can simultaneously bind ATP and identify the Msh6 subunit as containing the high affinity ATP binding site and Msh2 as containing a high affinity ADP binding site. Stable binding of ATP to Msh6 causes decreased affinity of Msh2 for ADP and binding to mispaired DNA stabilized the binding of ATP to Msh6. Our results support a model in which mispair binding encourages a dual occupancy state with ATP bound to Msh6 and Msh2 and that this state supports hydrolysis-independent sliding along DNA.

4.2 INTRODUCTION

The mutation rate in most cells is actively reduced to extremely low levels (~$1x10^{-9}$/cell division) as high mutation rates can lead to cell death or cancer development (Drake, 1991). A network of DNA repair pathways reduce the number of errors incorporated into the genome or increase removal of errors or error causing lesions. The Mismatch Repair (MMR) pathway is a critical component of this network and is required to keep the mutation rate low (Harfe and Jinks-Robertson, 2000; Kolodner, 1996; Modrich, 1991). The importance of the MMR pathway is demonstrated by its' conservation from bacteria to humans and by the fact that defects in MMR can underlie the development of cancer (Lynch and de la Chapelle, 2003; Peltomaki, 2003; Wheeler et al., 2000). One role for MMR is the repair of bases incorrectly incorporated by DNA replication, with the first step in this pathway, mispair identification, being the best characterized step. In bacterial MMR, mispair recognition is performed by the MutS protein. The MutS protein contains an ATP binding domain, forms a homodimer and has a higher affinity for mispaired DNA compared to fully paired DNA (Joshi et al., 2000; Schofield et al., 2001; Su and Modrich, 1986). Subsequent to mispair recognition, in a process that requires ATP, MutS interacts with the MutL protein to form a ternary complex that appears to be involved in downstream MMR events (Acharya et al., 2003; Grilley et al., 1989; Schofield et al., 2001). The MMR system is more complicated in eukaryotes where three MutS Homologue (MSH) proteins, all of which have ATP binding domains,

form two heterodimeric complexes, Msh2-Msh6 and Msh2-Msh3, which recognize base-base mispairs and insertion/deletions or only insertion/deletions, respectively (Acharya et al., 1996; Drummond et al., 1995; Kolodner, 1996; Marsischky et al., 1996; Palombo et al., 1996). Following mispair recognition, and in a reaction requiring ATP, the MSH proteins interact with MutL related heterodimers to form a ternary complex which is thought to coordinate downstream events (Acharya et al., 2003; Grilley et al., 1989; Habraken et al., 1998; Mendillo et al., 2005). Eukaryotic MMR reconstitution experiments indicate that these downstream events require additional proteins (Zhang et al., 2005).

While it has been shown that the ATP binding domains of the MSH proteins are required for MMR (Haber and Walker, 1991), the role that ATP binding and hydrolysis plays in the function of these proteins is not well understood. This is illustrated by the fact that three substantially disparate models have been put forth to describe the events, including ATP binding and hydrolysis, that occur during mispair recognition to initiate downstream events in MMR. In the first model, termed the molecular switch model, MutS (or the Msh heterodimer) binds to mispaired DNA in an ADP bound state. Upon mispair binding there is presumably a conformational change that allows exchange of ADP for ATP causing a second conformational change that allows MutS (or the Msh heterodimer) to form a sliding clamp. In this model it is the binding of ATP, but not hydrolysis, which signals downstream processes, such as movement of MutS or the Msh heterodimers and formation of ternary complex with MutL or the eukaryotic MutL related heterodimers, to occur

(Gradia et al., 1997; Gradia et al., 1999). A second model, the ATP-dependent translocation model, also predicts ATP-dependent movement of MutS or Msh heterodimers and formation of ternary complexes with MutL or the MutL related heterodimers. However, this model uses ATP hydrolysis to actively move the repair complex unidirectionally along DNA (Allen et al., 1997; Blackwell et al., 1998). A final model, termed the static transactivation model, utilizes a kinetic proofreading mechanism and does not invoke movement of MutS once the mispair is located. In this model MutS must be bound to ATP and the mispair simultaneously to recruit MutL; ATP binding in this model verifies mispair recognition (Junop et al., 2001).

While all the models utilize ATP in some manner, the role of ATP binding/hydrolysis has not been well established. The Msh6 and Msh2 subunits each contain an ATP binding site, and both ATP binding sites are critical for MMR (Alani et al., 1997; Das Gupta and Kolodner, 2000). While the *S. cerevisiae* and human Msh2-Msh6 heterodimers appear to have a relatively weak ATPase, DNA has been shown to stimulate steady state levels of ATPase activity with mispaired DNA stimulating to an even greater extent (Gradia et al., 1997; Hess et al., 2002). In addition, a burst phase during ATP hydrolysis, involving rapid ADP formation followed by a much slower steady state rate, has been observed for MutS as well as *S. cerevisiae* Msh2-Msh6 (Antony and Hingorani, 2003; Bjornson et al., 2000). Interestingly, mispaired DNA inhibits this initial burst phase while fully basepaired DNA does not cause this inhibitory effect. Additionally, a recent study has indicated that a mutation effecting the ATP binding site of Msh6 eliminated the burst phase

(Antony et al., 2005). While these studies provide valuable information regarding ATP binding and hydrolysis, the function of nucleotide binding and hydrolysis by each site has not been determined. Here we use a crosslinking approach to measure nucleotide binding to each subunit and visualize the specific nucleotide bound states that exist. Our results support a model of ATP binding/hydrolysis by Msh2-Msh6 that provides a novel mechanism for increasing the specificity of mispair binding by Msh2-Msh6. Furthermore, we have determined the specific ATP binding and hydrolysis requirements that allow for movement of Msh2-Msh6 along DNA.

4.3 RESULTS

The Msh6 subunit of *S. cerevisiae* Msh2-Msh6 contains the high affinity ATP binding site while the Msh2 subunit contains the lower affinity ATP binding site

Nucleotide binding and hydrolysis by Msh2-Msh6 (*S. cerevisiae* and human, as well as bacterial MutS) is critical for mismatch repair and has been the focus of several recent studies (Antony and Hingorani, 2003; Bjornson et al., 2000; Gradia et al., 1999). Studies of the *S. cerevisiae* complex not only demonstrate that the Msh2 and Msh6 subunits both contain a functional ATP binding site but also show asymmetric binding of ATP with one high affinity site being filled prior to the second low affinity site. To definitively identify the high affinity and low affinity ATP binding sites for the Msh2-Msh6 protein, crosslinking experiments were performed with [γ-^{32}P]ATP and purified Msh2-Msh6. These experiments allow for K_d determinations for both sites by direct visualization of ATP binding to specific subunits. Msh2-Msh6 was incubated with 0.1-200 μM [γ-^{32}P]ATP in buffer lacking Mg^{2+} (to eliminate ATP hydrolysis) and crosslinked. Initial experiments showed that crosslinking ATP to Msh2 and Msh6 does not affect their migration on SDS-PAGE gels (data not shown). Our analysis shows that the Msh6 subunit crosslinks to ATP at very low ATP levels, with an apparent K_d of 0.3 μM, while the Msh2 subunit binds ATP with a much lower affinity, apparent K_d of 37 μM (Figure 4-1A & D, Table 4-1). These values are consistent with published results using the non-hydrolyzable

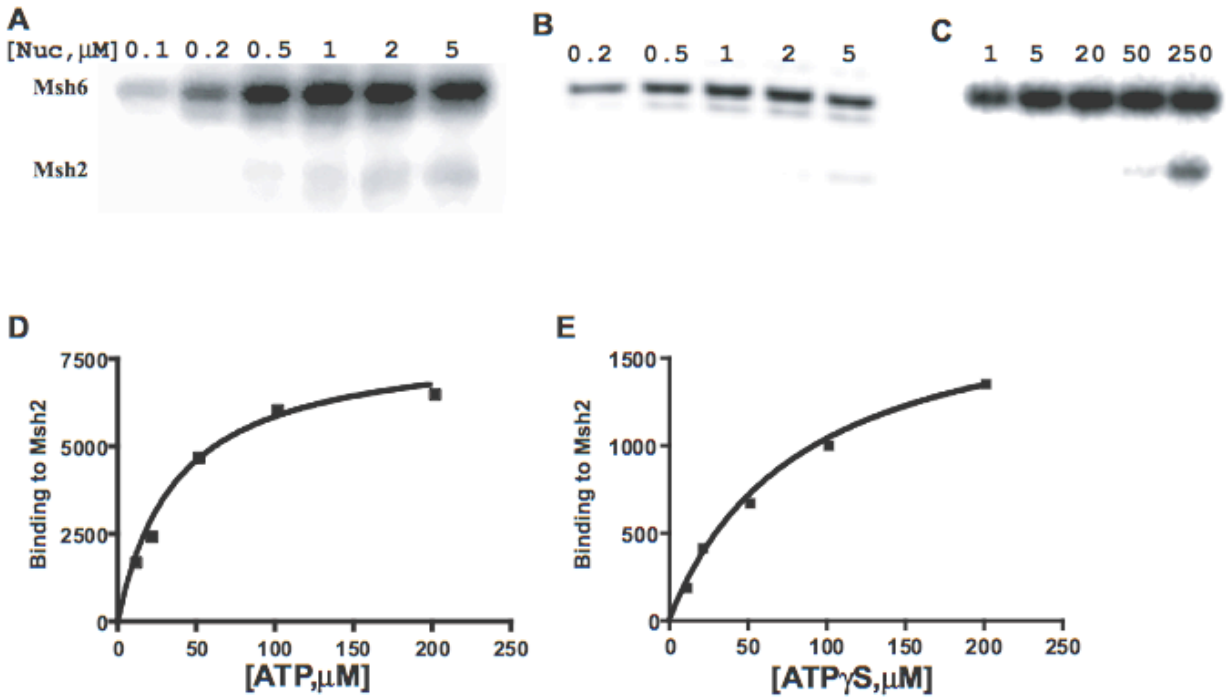

Figure 4-1. The Msh2 and Msh6 subunits both bind ATP but with different affinities. Standard crosslinking reactions (20 μl) contained 0.4 pmoles (A-C) or 4 pmoles (D,E) of wild-type Msh2-Msh6 and labeled ATP (A,D), ATPγS (B,E) or AMP-PNP (C), at the indicated concentrations. Dissociation constants (K_d) are presented in Table 4-1.

Table 4-1. Nucleotide binding affinities for Msh2 and Msh6.

Subunit	Ligand	Kd (μM)
Msh2	ATP(-Mg^{2+})	37.3 ± 6.0
Msh2	ATPγS	84.6 ± 12.9
Msh2	AMP-PNP	nd
Msh2	ADP	1.4 ± 0.7
Msh2	ADP + (5 μM ATPγS)	23.9 ± 5.0
Msh2(K694M)	ATP(-Mg^{2+})	nd
Msh6	ATP(-Mg^{2+})	0.25 ± 0.09
Msh6	ATP(-Mg^{2+}) + GC	0.50 ± 0.17
Msh6	ATP(-Mg^{2+}) + GT	0.74 ± 0.33
Msh6	ATPγS	0.15 ± 0.09
Msh6	ATPγS + (5 μM ADP)	0.33 ± 0.10
Msh6	AMP-PNP	0.57 ± 0.10
Msh6	ADP	nd
Msh6(K988M)	ATP(-Mg^{2+})	11.5 ± 2.6

All reactions contain Mg^{2+} (5 μM) unless specified and "nd" means not determined due to low apparent binding even at high nucleotide concentrations. All experiments were performed a minimum of twice.

nucleotide analogue ATPγS which report a K_d for the high affinity site to be 3.7 μM and a K_d of 17 μM for the low affinity site (Antony and Hingorani, 2003). While there would seem to be a disparity between our high affinity K_d of 0.3 μM and the previously reported 3.7 μM note that another study found the human Msh2-Msh6 high affinity site had a K_d of 0.8 μM (Martik et al., 2004). Another apparent inconsistency between the two previously published reports relates to the possibility of having ATP bound in both high and low affinity sites simultaneously. While one study demonstrated that two ATPγS molecules can be bound to one *S. cerevisiae* Msh2-Msh6 heterodimer the other study was able to detect only one nucleotide per human heterodimer. Since we see dual occupancy starting at ~20 μM ATP (Figure 4-1), our results indicate that at high nucleotide concentrations both sites can be filled with ATP. Possible explanations for the inability to detect simultaneously filled sites in some studies will be discussed below.

Although the above experiments indicate the Msh6 subunit contains the high affinity ATP binding site, it could be argued that the lack of Mg^{2+} alters nucleotide binding. Therefore, crosslinking experiments were performed with the non-hydrolyzable nucleotide analogues [^{35}S]ATPγS and [α-^{32}P]AMP-PNP in the presence of Mg^{2+}. Results of crosslinking studies with ATPγS are in agreement with the ATP without Mg^{2+} results, with the apparent K_d of Msh6 and Msh2 for ATPγS being 0.15 μM and 84.6 μM respectively (Figure 4-1B & E, Table 4-1). Results of the analysis of AMP-PNP binding also agree with the analysis of ATP–Mg^{2+} binding and indicate that Msh6 contains the high affinity nucleotide binding site, with an apparent K_d of

0.57 μM for AMP-PNP (Figure 4-1C, Table 4-1), consistent with a K_d of 1.6 μM for binding of AMP-PNP by human Msh2-Msh6 (binding to individual subunits was not evaluated, (Martik et al., 2004). Interestingly, the Msh2 nucleotide-binding site only had a limited ability to bind AMP-PNP, with crosslinking to the Msh2 site only being detectable at the highest concentration of AMP-PNP (250 μM); as a consequence, we could not determine the K_d of binding to Msh2. The analysis of AMP-PNP binding highlights the usefulness of UV-crosslinking for studies of nucleotide binding; our apparent K_d for binding to Msh6 matches well with the results of the study that used filter binding to analyze AMP-PMP binding to human Msh2-Msh6 (Martik et al., 2004) and in addition we were able to identify a serious defect in AMP-PNP binding to the Msh2 subunit.

Amino acid substitutions in the ATP binding sites of Msh2 or Msh6 affect crosslinking to the mutated subunit only

One complicating factor in the biochemical analysis of Msh2-Msh6 is that the ATP binding pockets of both Msh2 and Msh6 are partially comprised of residues from the other subunit, Msh6 and Msh2, respectively, that function in phosphate coordination (Junop et al., 2001; Lamers et al., 2000; Obmolova et al., 2000). This potentially creates a problem with the interpretation of crosslinking data. For example, although we see crosslinking to Msh6 at much lower ATP concentrations compared to crosslinking to Msh2, it is possible that the high affinity ATP binding site lies within Msh2 but crosslinking takes place to Msh6 amino acids that are in close

proximity. Therefore, control experiments were conducted to confirm the validity of the previous K_d analysis. We prepared Msh2-Msh6 heterodimers with amino acid substitutions within the Walker A motifs of either Msh6 [Msh2-Msh6(K988M)] or Msh2 [Msh2(K694M)-Msh6] (Junop et al., 2001). These mutations specifically disrupt the ATP binding pocket within the mutated subunit and were used in crosslinking studies identical to those described above in the absence of magnesium. The Msh2(K694M)-Msh6 mutant protein is predicted to have significantly decreased affinity for binding of ATP the Msh2 subunit, but would not be expected to be altered for binding of ATP to the Msh6 subunit. As can be seen in (Figure 4-2A & B), crosslinking to the Msh2(K694M) subunit was reduced to undetectable levels while crosslinking to the Msh6 subunit was not affected. Identical experiments were performed with the Msh6(K988M) mutant. As shown in Figure 4-2C & D, crosslinking to the Msh6(K988M) subunit was significantly reduced, with a K_d of 11.5 μM compared to a K_d of 0.25 μM for wild-type, while the K_d of binding to Msh2 was not affected. These results demonstrate that crosslinking is useful for characterizing the nucleotide binding properties of Msh2-Msh6, and confirms that ATP crosslinking to a specific subunit is a result of ATP binding to that specific subunit. These data identify the Msh6 subunit as containing the high affinity ATP binding pocket and the Msh2 subunit as containing the lower affinity site.

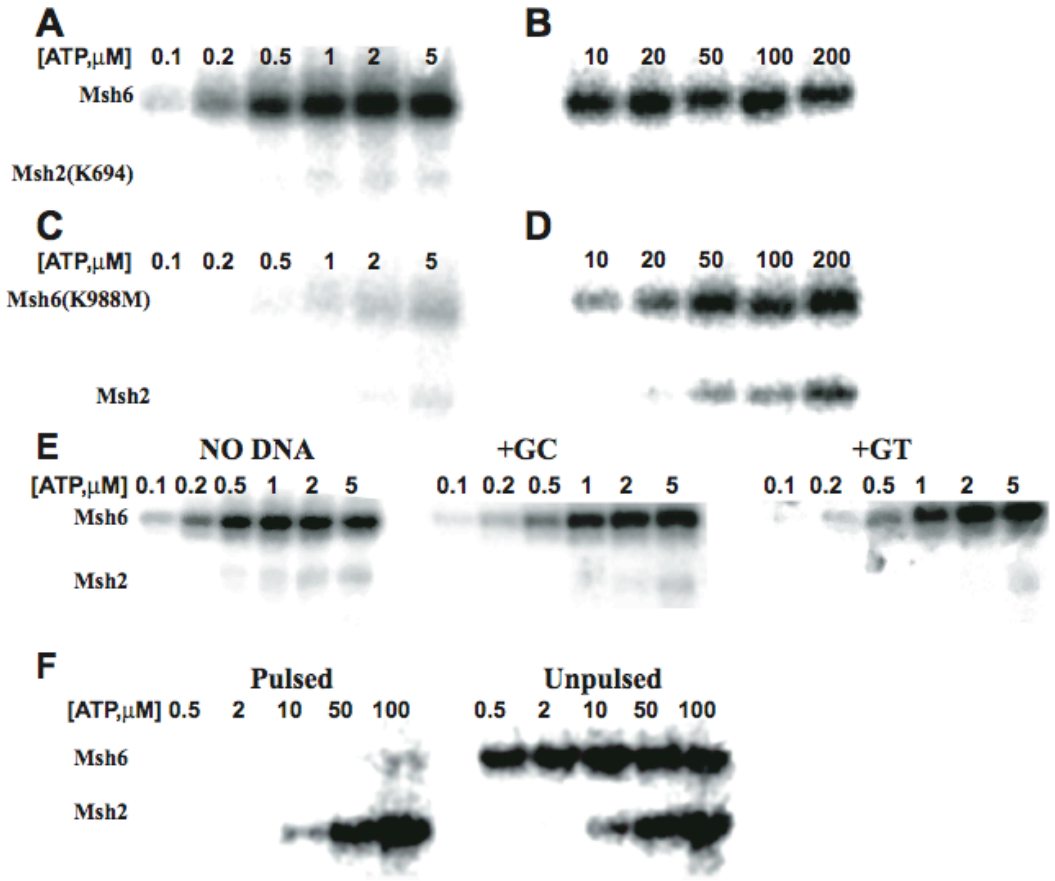

Figure 4-2. Analysis of the effect of ATP binding mutants and DNA on ATP binding by Msh2 and Msh6. Standard crosslinking reactions contained the ATP binding mutants Msh2(K694M)-Msh6 (**A,B**), Msh2-Msh6(K988M) (**C,D**) or wild-type Msh2-Msh6 containing no DNA, paired DNA or mispair containing DNA **(E)** . The apparent Kd of nucleotide binding determined for wild-type and mutant Msh2 and Msh6 are displayed in Table 4-1. Pulse chase experiments (**F**) contained Msh2-Msh6 and [γ-^{32}P]ATP, at indicated concentrations.

Nucleotide binding affinity is slightly decreased when Msh2-Msh6 is pre-bound to paired or mispaired DNA

Since a major role of Msh2-Msh6 is to detect mispairs, we next determined the affect of DNA binding on the ATP binding characteristics of Msh2 and Msh6 in the absence of magnesium. Crosslinking experiments were performed essentially as described above except double stranded DNA, with or without a central GT mispair, was added to reactions prior to the addition of nucleotide. Both DNAs, mispaired and paired, caused a slight decrease in the affinity of the Msh6 subunit for ATP, increasing the K_d to 0.74 μM and 0.50 μM for GT and GC, respectively (Figure 4-2E). Binding of ATP to the Msh2 site was not affected when Msh2-Msh6 was pre-bound to mispaired or paired DNA (data not shown). Taken together with previous crosslinking data (Figure 4-1) these results argue that, regardless of the DNA bound state, when both nucleotide binding sites are empty ATP will bind to the Msh6 subunit with much higher affinity than to the Msh2 site. Moreover, if hydrolysis by the Msh6 subunit is inhibited, in this case by using nonhydrolyzable nucleotide analogues, the Msh2 subunit is competent to bind ATP while the Msh6 subunit is still occupied. The importance of this observation is discussed below.

The ATP binding site of Msh6 is static, while the Msh2 ATP binding site appears to be more dynamic

A potential argument against simultaneous occupancy of both of the Msh2 and Msh6 ATP binding sites by ATP is that even though the K_d of ATP binding to the

Msh6 site is 100 times lower than that of the Msh2 site, the ATP seen bound to the Msh2 site might only be bound to Msh2-Msh6 heterodimers that do not have an ATP bound to the Msh6 site. Perhaps the Msh6 bound ATP might dissociate and only then does ATP fill the Msh2 site; this seems unlikely based on the fact that crosslinking of ATP to the Msh6 subunit saturates at very low concentrations of ATP and does not decline as ATP binding to Msh2 increases. Nevertheless, we have investigated the dynamic state of the nucleotide bound to the two subunits using crosslinking experiments. In these experiments, unlabeled ATP was added to Msh2-Msh6 either before or together with [γ-^{32}P]ATP in the absence of magnesium. If the nature of the Msh6-ATP or Msh2-ATP interaction is dynamic, then the bound, unlabeled ATP should be freely exchangeable with the labeled ATP added later. However, as can be seen in Figure 4-2F, when Msh2-Msh6 was pulsed with unlabeled ATP and then chased with [γ-^{32}P]ATP, there was a considerable reduction in the amount of labeled ATP crosslinked to the Msh6 subunit as compared with crosslinking experiments performed without the unlabeled ATP pulse. Interestingly, the Msh2 subunit did not show the same effect as pre-incubation with unlabeled ATP did not appear to decrease the amount of labeled ATP crosslinked to Msh2. Pulse chase experiments performed with AMP-PNP + Mg^{2+} yielded similar results in regard to ATP binding to the Msh6 site (data not shown) indicating the static nature of ATP binding to Msh6 is not simply a lack of Mg^{2+} effect. These results argue that the ATP bound to the Msh6 site is relatively static, suggesting that hydrolysis is required prior to nucleotide exchange,

while the ATP bound to the Msh2 subunit is not as tightly bound and is able to more readily exchange with free ATP pools, at least while the Msh6 subunit is occupied.

The Msh2 site binds ADP with high affinity, while the Msh6 site binds ADP poorly

Under non-hydrolytic conditions, the Msh6 subunit binds ATP with much higher affinity than does the Msh2 subunit. However, while previous crosslinking experiments provide important information regarding the ATP binding affinities of Msh2 and Msh6, they do not allow detection of hydrolysis-dependent nucleotide bound species and may not reflect the steady state nucleotide bound species of Msh2-Msh6. To gain insight into additional nucleotide states that may exist, we performed crosslinking studies with Msh2-Msh6 in the presence of magnesium. Our initial experiments indicated a striking difference in the states detected under hydrolytic conditions compared to when the analysis was done in the absence of magnesium. As seen in Figure 4-3A, low concentrations (0.5-20 μM) of [α-^{32}P]ATP –Mg^{2+} resulted in crosslinking predominantly to the Msh6 subunit (at 20 μM 86% of crosslinked label is on Msh6 subunit), whereas the same experiment performed in the presence of Mg^{2+} resulted in the majority of nucleotide being bound to the Msh2 subunit (Figure 4-3B, at 20 μM 92% of crosslinked label in on Msh2 subunit). This dramatic change in nucleotide occupancy under hydrolytic conditions not only indicates that the Msh6-ATP state is short-lived, likely due to rapid hydrolysis, but that the Msh6-ADP interaction is also unstable (since [α-^{32}P]ATP was used and will report the presence of

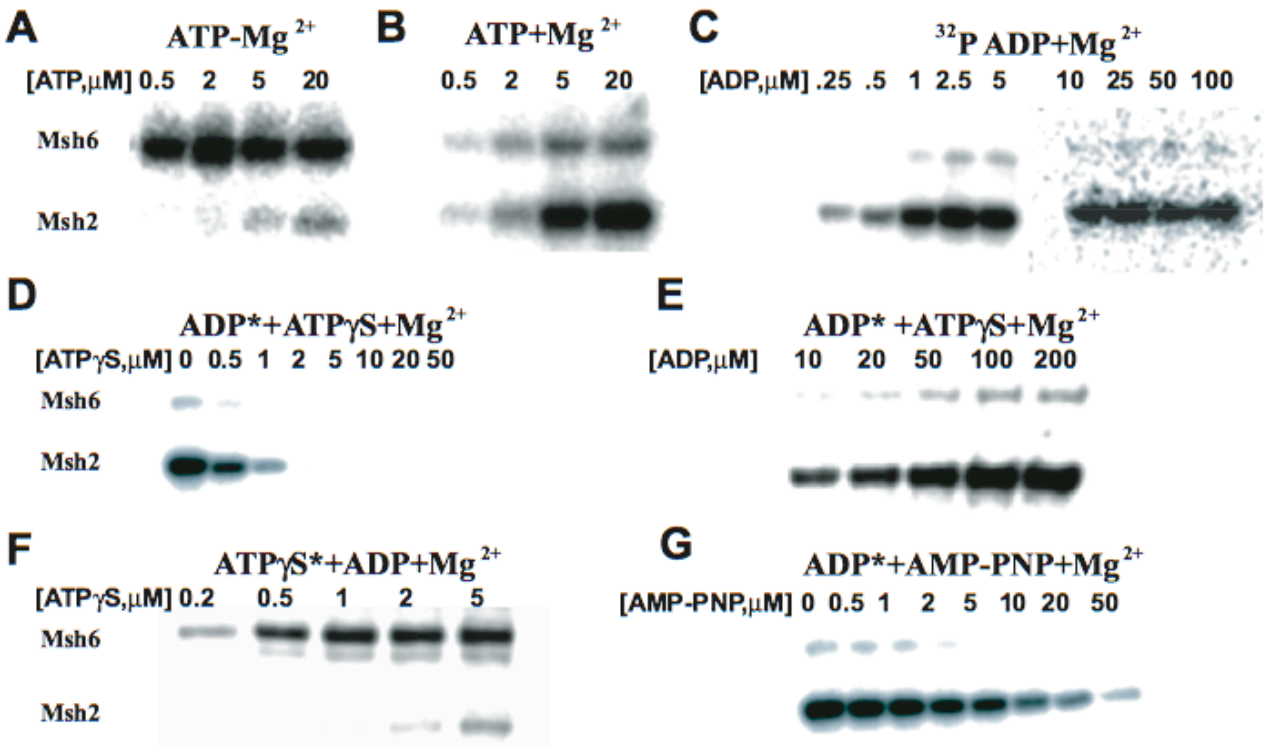

Figure 4-3. Nucleotide binding characteristics of Msh2-Msh6. Standard crosslinking reactions containing different concentrations of [α-^{32}P]ATP with Mg^{2+} as indicated (**A,B**), [α-^{32}P]ADP **(C)**, 5 μM [α-^{32}P]ADP and unlabeled ATPγS (**D**), different concentrations of [α-^{32}P]ADP in the presence of 5 μM ATPγS **(E)**, preincubation of 5 μM ADP followed by the addition of [^{35}S]ATPγS, at concentrations indicated **(F)**, and 5 μM [α-^{32}P]ADP with unlabeled AMP-PNP, at concentrations indicated (**G**). The * indicates nucleotide containing the label [^{32}P]ATP or [^{35}S]ATPγS. The Apparent K_d measurements determined for all reactions are displayed in Table 4-1.

ATP or ADP). Crosslinking performed using [γ-^{32}P]ATP (data not shown, and Figure 4-4A) did not label either Msh6 or Msh2, suggesting the nucleotide bound to Msh2 is ADP. The results of this analysis can be interpreted in a number of ways. For instance, nucleotide crosslinking to Msh2 under these conditions may indicate that hydrolysis of ATP by Msh6 allows Msh2 to bind and then hydrolyze ATP at much lower ATP concentrations than in reactions lacking magnesium. Another possibility is that Msh2 only binds ADP pools generated by the ATPase activity of Msh6 in reactions containing magnesium. In order to test the later hypothesis we examined the ability of the Msh6 and Msh2 sites to bind ADP. This analysis showed the Msh2 subunit binds ADP with a K_d of 1.4 μM (Figure 4-3C, Table 4-1), while ADP binding to Msh6 was not detected at the concentrations of ADP tested, demonstrating that ADP binding by Msh2-Msh6 is opposite of what was seen in the ATP–Mg^{2+} and AMP-PNP+Mg^{2+} binding experiments. This is consistent with studies showing that each Msh2-Msh6 heterodimer has one high affinity ATP binding site (Antony and Hingorani, 2003), shown here to be Msh6, and one high affinity ADP binding site (Martik et al., 2004), shown here to be Msh2. This result also indicates that the switching of nucleotide occupancy from the Msh6 site to the Msh2 site under hydrolytic conditions is due to rapid hydrolysis of ATP by Msh6, release of ADP by Msh6 followed by stable binding of this ADP by Msh2, although sequential hydrolysis is still a possibility.

Binding of nucleotide to Msh6 affects ADP binding by Msh2

We next tested the ability of ADP and ATPγS to compete with each other for binding. Msh2-Msh6 was incubated with [α-^{32}P]ADP (5 μM) + Mg^{2+} followed by the addition of increasing amounts of ATPγS. The results show a significant reduction in ADP binding by the Msh2 site when 0.5 μM ATPγS, which only significantly binds to the Msh6 site at this concentration, was added to binding reactions. Moreover, addition of 2 μM ATPγS completely eliminated ADP binding by the Msh2 site (Figure 4-3D). These results were unexpected since the K_d of ATPγS for the Msh2 site, is ~85 μM. Interestingly the K_d of ATPγS for the high affinity site, shown here to be the Msh6 site, is 0.15 μM. These results suggest that the reduced binding of ADP seen in the presence of ATPγS is not due to direct competition between ATPγS and ADP for binding to the Msh2 site. More likely, binding of ATPγS to the Msh6 site causes a reduction in the binding affinity for ADP by the Msh2 site. To more carefully quantify the effect of the ATPγS-Msh6 interaction on Msh2 binding of ADP, we determined the apparent K_d for binding ADP by Msh2 in the presence of 5 μM ATPγS. Our results demonstrate that the Msh6-ATPγS interaction significantly decreased the affinity of Msh2 for ADP, resulting in a K_d of 24 μM, as compared to a K_d of 1.4 μM in the absence of ATPγS (Figure 4-3E). We also investigated the effect of Msh2-bound ADP on nucleotide binding by Msh6. The results indicate a slight decrease in apparent affinity of Msh6 for ATPγS when Msh2 is prebound to ADP (K_d=0.3 μM, Figure 4-3F). These results argue for communication between the two subunits, with nucleotide binding by one subunit affecting nucleotide binding by the

other subunit. To confirm this hypothesis, we tested the ability of AMP-PNP to displace ADP from the Msh2 subunit. Since we have determined AMP-PNP does not significantly bind to the Msh2 site until concentrations of ~250 μM, any decrease in ADP binding to the Msh2 site should not be due to direct competition with AMP-PNP. As predicted, AMP-PNP caused a significant decrease in ADP binding to the Msh2 subunit (Figure 4-3G). Although AMP-PNP was not as potent as ATPγS in decreasing the binding of ADP, we did see a 50% reduction in ADP binding in the presence of 2 μM AMP-PNP, consistent with the 1 μM K_d we determined for Msh6 binding of AMP-PNP. In addition, we saw greater than a 90% reduction in ADP binding with the addition of 50 μM AMP-PNP, a concentration well below the 250 μM we have shown to be required for significant AMP-PNP binding by the Msh2 subunit. These data agree with previous studies which demonstrate differential specificities for ADP and ATP within the hMsh2-Msh6 complex (Martik et al., 2004); however, our studies have also identified the ADP and ATP preference for each subunit. Interestingly, our results are not in agreement with conclusions of those studies regarding simultaneous occupancy of ATPγS and ADP. In our studies we see loss of ADP from Msh2 when ATPγS or AMP-PNP are bound by Msh6, while another study of human Msh2-Msh6 suggests ATPγS and ADP can be bound simultaneously. This apparent disparity will be discussed later.

Mispaired DNA inhibits hydrolysis by the Msh6 subunit

As stated earlier, a burst phase of ATP hydrolysis by Msh2-Msh6 has been observed, and this burst phase is inhibited in the presence of mispaired DNA (Antony and Hingorani, 2003). To gain insight into the nature of the burst phase, we performed crosslinking studies under hydrolytic conditions in the presence of mispaired and fully paired DNA substrates. Experiments were performed with α or γ^{32}P -labeled ATP in the presence or absence of magnesium, to control hydrolysis. Control experiments lacking Mg^{2+} demonstrated the characteristic preferential labeling of the Msh6 subunit (Figure 4-4A). Addition of Mg^{2+} to the [α-^{32}P]ATP reaction caused the switch to preferential labeling of Msh2, likely due to binding of ADP generated by ATP hydrolysis, while [γ-^{32}P]ATP failed to label either subunit most likely because of rapid hydrolysis of [γ-^{32}P]ATP bound to Msh6. Addition of basepaired DNA to these reactions caused a change in the amount of protein labeled but no significant change in the labeling pattern under any condition tested; however, addition of mispaired DNA revealed, for the first time, labeling of the Msh6 subunit by [γ-^{32}P]ATP under hydrolytic conditions. This mispair specific increase in the stability of Msh6-bound ATP is most consistent with mispaired DNA causing an inhibition of ATP hydrolysis by Msh6. These results indicate the burst of ATP hydrolysis occurs at the Msh6 site and is inhibited when Msh2-Msh6 is bound to mispaired DNA. It should be noted that the observed inhibition may be underestimated due to the possibility of some of the Msh2-Msh6 protein not being

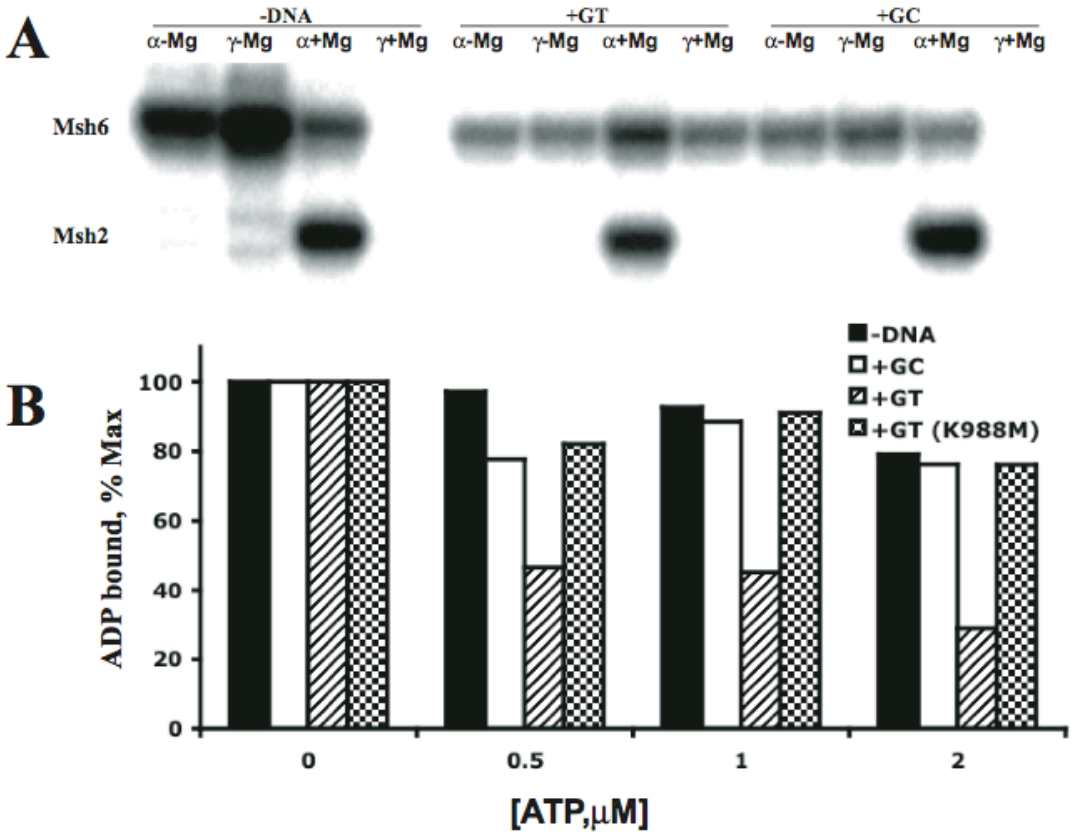

Figure 4-4. Mispaired DNA inhibits ATP hydrolysis by Msh6 which causes reduced binding of ADP by Msh2. (A) Standard crosslinking reactions containing Msh2-Msh6 (4 pmoles) and ATP (10 μM) were prepared. The presence of α or γ labeled ATP, Mg^{2+} and mispaired or paired DNA is indicated. **(B)** Crosslinking reactions with Msh2-Msh6 (4 pmoles) and [α-^{32}P]ADP (5 μM) were prepared. The presence of ATP (0, 0.5, 1.0, 2.0 μM) and mispaired or fully paired DNA (20 pmoles) is indicated. ADP binding was set at 100% for the level seen in the absence of ATP.

bound to mispaired DNA, as ATP binding also causes dissociation of Msh2-Msh6 from mispaired DNA.

Mispaired DNA increases ATP induced dissociation of ADP from Msh2

In the experiments described above, we observed that ATPγS causes a significant reduction in ADP binding to the Msh2 subunit; however, ATP did not have the same effect. A possible explanation is that ATP is rapidly hydrolyzed by the Msh6 subunit allowing ADP to remain bound to Msh2, conversely ATPγS is not hydrolyzed efficiently and it is only under these conditions, when nucleotide is more stably bound by Msh6, that dissociation of ADP bound by Msh2 is increased. To test this hypothesis, we examined the ability of mispaired DNA, which inhibits ATP hydrolysis by Msh6, to facilitate release of ADP by Msh2 by increasing the longevity of the Msh6-ATP interaction. As shown in Figure 4-4B, mispaired DNA caused a marked reduction in Msh2 bound ADP at ATP levels shown not to cause dissociation of ADP in the absence of mispaired DNA. Fully paired DNA was also able to increase dissociation of ADP by ATP, but not to the extent seen with mispaired DNA. It should be noted that the level of dissociation was not as great as that seen with ATPγS. However, since mispaired DNA is not able to inhibit ATP hydrolysis to the levels required to mimic occupancy of the Msh6 site with ATPγS we did not anticipate seeing similar levels of ADP dissociation. These results are consistent with the idea that mispaired DNA stabilizes ATP binding to the Msh6 site which causes a reduction

in the binding affinity for ADP by the Msh2 site. To further test this hypothesis we performed the same experiment with the Msh2-Msh6(K988M) mutant. Since the Msh2-Msh6(K988M) mutant protein recognizes mispaired bases in DNA (data not shown) and also binds ATP in the Msh6 site with lower affinity than wild type we did not anticipate a reduction in Msh2 bound ADP when low levels (2 μM) of ATP were added in the presence of mispaired DNA. As shown in Figure 4-4B, in the presence of mispaired DNA, ATP caused only a slight reduction in ADP bound to Msh2 using the Msh6(K988M) mutant.

Sliding of Msh2-Msh6 occurs when both nucleotide binding sites are occupied by ATP

When Msh2-Msh6 is bound to a mispaired base, it is converted to a form that slides along DNA upon binding ATP (Gradia et al., 1999; Mendillo et al., 2005). However, the specific nucleotide bound state required for sliding has not been determined. To investigate this, we have performed experiments that analyze the mispair-induced sliding state of Msh2-Msh6 with nucleotide bound to one, or both of the subunits. For these studies we used an IAsys Biosensor to follow the association and dissociation of Msh2-Msh6 on DNA containing a central mispair, under hydrolytic and non-hydrolytic conditions. In addition, we used a reversible DNA end-blocking system that allows one end of the DNA to be blocked or remain free (Mendillo et al., 2005). For these studies the Msh2-Msh6 protein was bound to mispair containing DNA in the absence of nucleotide and dissociation of Msh2-Msh6

was monitored in the presence of ATP or ATPγS. Dissociation of Msh2-Msh6 was determined at multiple concentrations of nucleotide (Figure 4-5A & B). Since we were interested in the nucleotide requirements for sliding, we subtracted the dissociation obtained from blocked DNA (which should not contain a sliding component) from that obtained with unblocked DNA. Analysis of the results yielded an apparent K_d for sliding of 17.9 μM for ATP and 81.5 μM for ATPγS (Figure 4-5C & D). These values show a striking correlation between the apparent K_d for binding of nucleotide to the Msh2 subunit of 37.3 μM and 84.6 μM for ATP and ATPγS, respectively. This result is consistent with the view that sliding of Msh2-Msh6 only occurs at nucleotide concentrations where ATP is bound in both the Msh2 and Msh6 sites and confirms previous results that sliding does not require ATP hydrolysis (Mendillo et al., 2005). In addition, we have recently characterized several different Msh2-Msh6(mutant) complexes that have defects in ATP binding by the Msh2 subunit (Hess et al., 2006) in experiments similar to those presented in Figure 4-5. Consistent with our view that sliding of Msh2-Msh6 only occurs in the dual ATP bound state, we were unable to detect sliding for mutants that have Msh2 ATP binding defects.

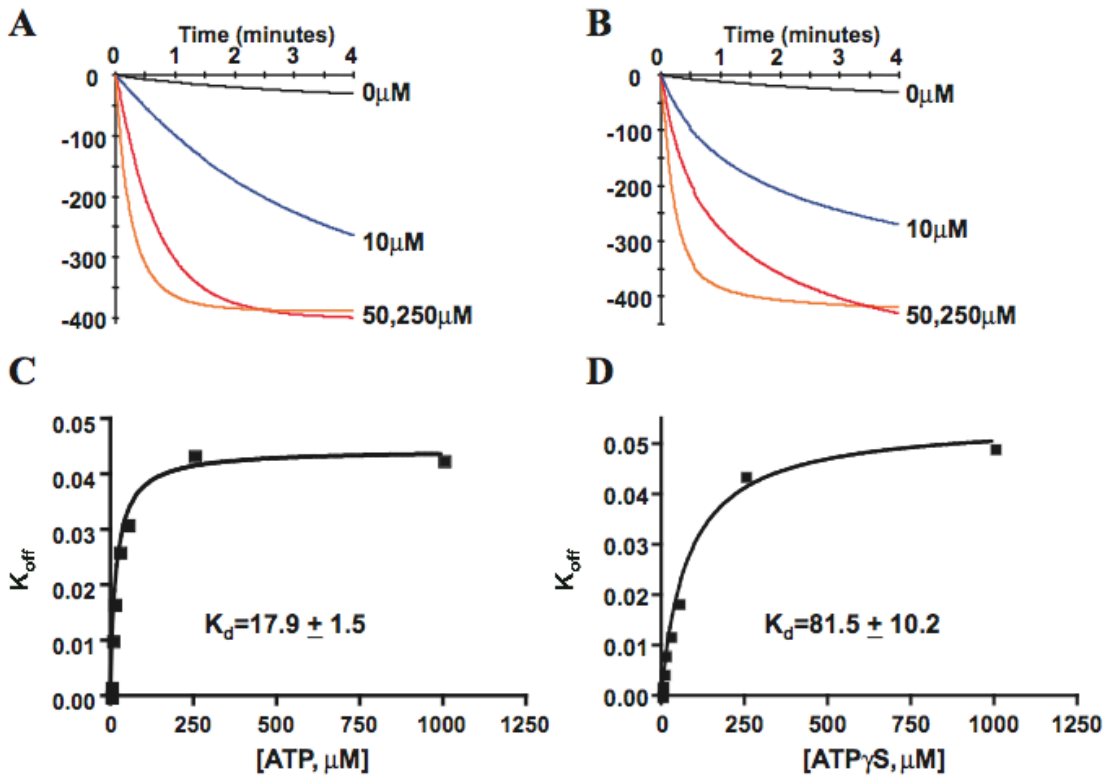

Figure 4-5. Sliding of Msh2-Msh6 requires nucleotide binding to both subunits but does not require hydrolysis. End-dependent dissociation of the Msh2-Msh6 complex from an unblocked, mispaired DNA substrate was determined by Biosensor analysis. Dissociation data generated with a LacI blocked substrate was subtracted from data generated with an unblocked substrate. Dissociation of Msh2-Msh6 from a DNA substrate after addition of ATP (**A**) or ATPγS (**B**) at the concentrations indicated. A plot of K_{off} vs. ATP (**C**) or ATPγS (**D**) concentration was performed yielding an apparent K_d for sliding of 17.9 + 1.4 μM and 81.5 ± 10.2 μM, respectively

4.4 DISCUSSION

In the present studies we have used crosslinking methods to visualize the nucleotide binding properties of the *S. cerevisiae* Msh2-Msh6 heterodimer. Our results demonstrate that Msh6 contains a high affinity ATP binding site (K_d =0.3 μM), Msh2 binds ATP with lower affinity (K_d =37 μM) and that when hydrolysis is inhibited ATP binding to Msh2 and Msh6 can occur simultaneously. In addition, we have shown that binding affinity for ADP is the reverse of that found for ATP, with Msh2 containing the high affinity ADP binding site (K_d = 1.3 μM) and Msh6 not detectably binding ADP under the conditions tested. Moreover, our studies demonstrate the static versus dynamic nature of Msh6 and Msh2, respectively, with Msh6 appearing to require hydrolysis to allow rapid exchange with ATP pools and Msh2 more readily exchanging ATP or ADP (pulse chase with ADP data not shown). Our results also demonstrate that binding to a mispair inhibits hydrolysis of ATP by the Msh6 subunit. While previous studies have shown a burst phase of ATP hydrolysis for Msh2-Msh6, which is inhibited by mispaired DNA and by a mutation in *MSH6* (Antony et al., 2005), our analysis is the first to directly identify Msh6 as the site to which the mispair exerts an ATPase inhibitory effect. Even more interesting is the observation that ADP binding by Msh2 is dramatically reduced when ATP binding at Msh6 is stabilized by either mispaired DNA or by binding of the non-hydrolyzable nucleotide analogue ATPγS in the Msh6 site. This implies communication between the two nucleotide binding sites such that binding of nucleotide at one site affects nucleotide binding at the other site. Finally, the ATP and ATPγS crosslinking studies,

combined with real-time Msh2-Msh6 dissociation data, for the first time demonstrate that mispair bound Msh2-Msh6 is converted to the form that moves along DNA when Msh6 and Msh2 simultaneously bind ATP. These results continue to support the view that there is no hydrolysis requirement for sliding as ATPγS yielded results similar to ATP.

Our results may explain the discrepancy between two reports regarding the potential nucleotide occupancy states of the Msh2-Msh6 protein. While one filter binding study was able to detect two moles of ATPγS per mole heterodimer, another study detected a single mole of ATPγS per mole Msh2-Msh6 (Antony and Hingorani, 2003; Martik et al., 2004). A possible explanation for this difference is the dynamic nature of the Msh2-nucleotide interaction. Since binding of ATPγS to the Msh6 site is very stable, recovery of the ATPγS bound to this site is not readily affected by washing conditions that may strip away bound nucleotide and result in no apparent binding. However, since the Msh2-nucleotide interaction is more dynamic, likely due to a lower affinity for ATP, it would be more difficult to quantitatively recover ATPγS bound to this site in filter binding assays. Additionally, one study focused on the *S. cerevisiae* proteins while the other analyzed human Msh2-Msh6 raising the possibility that the human Msh2-ATP interaction is more dynamic than that of the *S. cerevisiae* Msh2-ATP interaction. Interestingly, other studies have shown apparent simultaneous binding of ADP and ATPγS to both MutS and human Msh2-Msh6 (Bjornson and Modrich, 2003; Martik et al., 2004). While these data appear to be inconsistent with our results, it is possible that both results are correct. Our data demonstrate that ADP

binds to Msh2 with reduced affinity in the presence of ATPγS; however, our results actually do not preclude dual occupancy, only that this dual occupancy would be predicted to be short-lived as it is unstable and would most easily be observed at high ADP concentrations. Thus, depending on incubation times and nucleotide and protein concentrations used, it may be possible to obtain high levels of the Msh2(ADP)-Msh6(ATP) dual occupancy state.

The observations presented here allow for the development of a refined model of nucleotide binding to Msh2-Msh6 that provides insights into the nucleotide bound states that are competent for mispair binding and conversion to the sliding form of Msh2-Msh6 (Figure 4-6). In the absence of mispaired DNA, the Msh2(ADP)-Msh6(empty) state is the most stable while ATP bound states appear to be less stable. The Msh2(ADP)-Msh6(empty) state can be achieved in two ways: by incubation with ADP in which case ADP directly binds both subunits but is only stably bound in the Msh2 site; or in the presence of ATP under conditions of ATP hydrolysis where ATP binds both sites and subsequent hydrolysis leaves ADP in the Msh6 site that dissociates and ADP in the Msh2 site that is stably bound. Interestingly, when Msh2-Msh6 is bound to a mispaired base in the presence of ATP or ATPγS (Msh2-Msh6 must be bound to the mispair before the addition of ATPγS due to lack of hydrolysis whereas hydrolysis can occur in the case of ATP allowing mispair binding) the Msh2-ADP interaction becomes less stable while the stability of the Msh6-ATP interaction, due to ATP binding that occurs after binding to the mispair, appears to increase. Binding of Msh2-Msh6 to mispaired DNA does not affect subsequent ATP binding

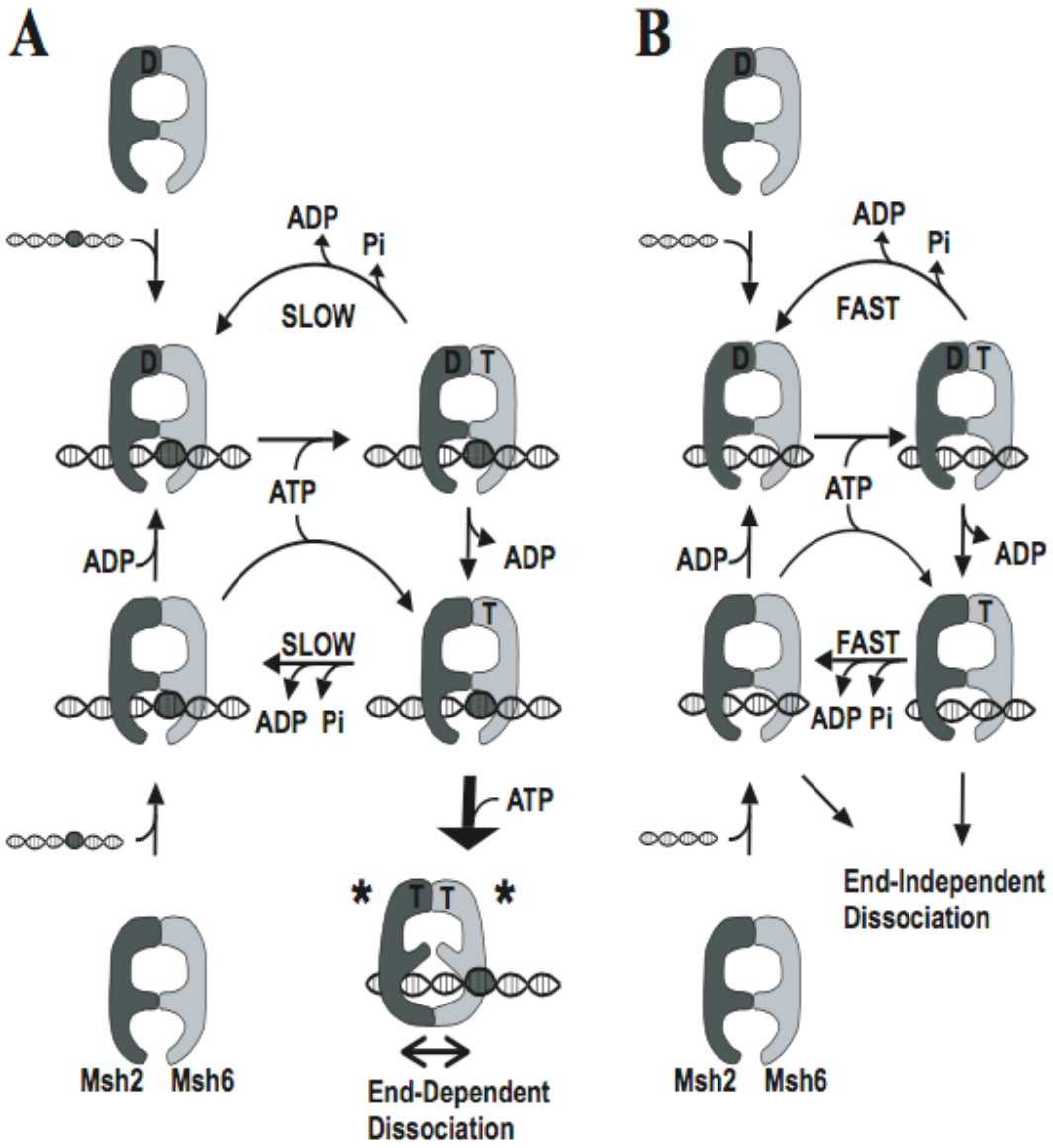

Figure 4-6. Model of ATP binding and hydrolysis which increases mispair specific binding of Msh2-Msh6. A. Mispaired DNA causes a shift to the doubly occupied state that is required for downstream MMR events. Msh2-Msh6, in the empty or Msh2(ADP) states, binds with high affinity to mispaired DNA which then stabilizes ATP bound by Msh6. This stably bound ATP allows release of ADP by Msh2, which then binds ATP to form the dual ATP occupied state "*" that allows End-Dependent Dissociation (sliding) and possibly other downstream MMR events. **B**. The absence of mispaired DNA shifts Msh2-Msh6 to an empty or Msh2(ADP) state. The nucleotide binding model for non-DNA bound Msh2-Msh6 is identical to the paired DNA model. Unbound Msh2-Msh6 is shifted to the empty or Msh2(ADP) states which are shown binding DNA and entering the cycles in A and B. Although end-dependent dissociation (sliding) has not been detected on paired DNA it could occur at a low level. This greatly reduced level of sliding in the absence of mispaired DNA is partially caused by rapid hydrolysis of ATP bound by Msh6, which in turn causes a decrease in the dual ATP occupancy state required for sliding. End-independent dissociation from paired DNA likely occurs for all Msh2-Msh6 states [for a discussion, see (Mendillo et al., 2005)], also resulting in a decrease in the dual ATP occupancy state on paired DNA. Bound ATP and ADP are indicated by "T" and "D", respectively.

but does inhibit ATP hydrolysis at the Msh6 site, thereby increasing the stability of the Msh6(ATP) state and shifting the equilibrium from Msh2(ADP)-Msh6(Empty) to Msh2(ADP)-Msh6(ATP). However Msh2 does not stably bind ADP when Msh6 is occupied with ATP shifting the equilibrium to Msh2(Empty)-Msh6(ATP). The empty Msh2 site is now able to bind ATP creating a doubly occupied Msh2(ATP)-Msh6(ATP) state, which is the state that our ATP titration experiments indicate is competent for sliding. Because Msh2-Msh6 prebound to a mispair can be converted to the sliding form by ATP and ATPγS, ATP hydrolysis does not appear to be required for conversion to the sliding form. In addition, because AMP-PNP binds normally to the Msh6 site but does not bind to the Msh2 site, studies that investigate AMP-PNP binding and AMP-PNP induced dissociation of Msh2-Msh6 from DNA should be carefully interpreted. It should be further noted that while the preformed Msh2(ATP)-Msh6(ATP) complex cannot bind to mispaired bases without ATP hydrolysis, studies of mispair binding by Msh2-Msh6 mutant complexes that cannot bind ATP in the Msh2 site, analysis of mispair binding by Msh2-Msh6 in the presence of different concentrations of ATP and analysis of mispair binding by Msh2-Msh6 in the presence of different concentrations of AMP-PNP (Gradia et al., 1997) indicate that the Msh2(empty)-Msh6(ATP) state can bind directly to mispairs.

The results presented here suggest modifications to previously proposed models for the early steps of MMR. In regard to the molecular switch model (Gradia et al., 1997), our results suggest that recognition of mismatched nucleotides by Msh2-Msh6 does not directly provoke ADP-ATP exchange at the same nucleotide binding

site. Rather, when ATP binds to Msh6, hydrolysis is inhibited, and this leads to a prolonged Msh6-ATP interaction, which causes a reduction in the affinity of Msh2 for ADP; this mechanism would account for the previously observed mismatch provoked ADP-ATP exchange albeit by a quite different mechanism. This reduced affinity for ADP allows for ATP binding by Msh2 and the dual occupancy state that is required for downstream MMR events such as sliding and/or possibly complex formation with Mlh1-Pms1. Our results demonstrating movement of Msh2-Msh6 in the presence of ATPγS support the sliding clamp model of movement (Gradia et al., 1999) and argue against the translocation model due to its requirements for hydrolysis (Allen et al., 1997; Blackwell et al., 1998). Any differences in the steady state level of mispair binding in the presence of ATP and ATPγS (Blackwell et al., 1998) appear to be attributable to inhibition of initial DNA binding events by ATPγS and not subsequent steps involving movement along DNA (Mendillo et al., 2005). In addition, our results provide evidence for a type of kinetic proofreading, although not the type previously proposed for the bacterial MutS (Junop et al., 2001), which argues that downstream MMR events only occur when MutS is bound to mispaired DNA and ATP, and that ATP binding authorizes repair. Our results support a second mechanism for generating mispair specific binding, where only on mispaired DNA is hydrolysis by Msh6 inhibited which allows for the dual occupancy state that is required for downstream MMR events. This would provide two separate mechanisms for mispair specificity, the first being preferential binding of Msh2-Msh6 to mispaired DNA and

the second being mispair specific inhibition of hydrolysis by Msh6 that allows for the dual occupied state required for downstream MMR events.

4.5 EXPERIMENTAL PROCEDURES

DNA substrates

Biotinylated oligonucleotides were synthesized by Midland Certified Reagent Company Inc., (Midland, Texas). All other oligonucleotides were synthesized by MWG, (www.mwgbiotech.com). The 236 nucleotide DNA, containing a central GT mispair, was prepared using a previously described PCR-base protocol (Mendillo et al., 2005).

Proteins

The Msh2-Msh6 complex was expressed in bacteria and purified essentially as described (Antony and Hingorani, 2003), with the addition of a PBE94 column after the SP-sepharose; Msh2-Msh6 purified from *S. cerevisiae* behaved similarly in all experiments (Hess et al., 2002). LacI protein was kindly provided by Dr. Kathleen Matthews (Rice University).

Nucleotides

All unlabeled nucleotides and nucleotide analogs were from Sigma, [α-^{32}P]ATP, [γ-^{32}P]ATP and [^{35}S]ATPγS were from Amersham/GE Healthcare, and [α-^{32}P]AMP-PNP was from ICN/MP Biomedicals. ADP contamination of selected batches of nucleotides including all batches of unlabeled ATPγS and AMP-PMP was verified by HPLC to be less than 1% and all experiments were performed with at least

two independent batches of nucleotide. To prepare labeled ADP, 42 pmol of [α-^{32}P]ATP (Amersham) was incubated with 0.4 unit of hexokinase (Sigma) and 3 mM glucose in 40 mM HEPES buffer pH 7.0, 50 mM KOAc, 5 mM $Mg(OAc)_2$ and 5 mM dithiothreitol at 25°C for 45 min. The solution was diluted 20-fold with 0.02 M NH_40Ac and applied to a GenPak Fax HPLC column (Waters). The [α-^{32}P]ADP was eluted with a 0.02-0.5 M NH_4OAc gradient and was further purified by passage through a SEP-PAK C18 cartridge (Waters-Millipore) equilibrated with H_20. The NH_40Ac was removed by sublimation.

Crosslinking Experiments

All incubations, including crosslinking step, were performed on ice. Reactions (20 μl) containing Msh2-Msh6 (0.4 pmoles for 0.1-5 μM nucleotide titrations and 4 pmoles for 10-200 μM nucleotide titrations) were performed in binding buffer containing 50 mM Tris buffer pH 8.0, 110 mM NaCl, 2 mM dithiolthreitol, 100 μg/ml BSA, 0.5 mM EDTA and 5% glycerol. Where specified, mispaired and paired DNA (Hess et al., 2002), was added 10 minutes prior to addition of nucleotide. Proteins were mixed with [α or γ-^{32}P]ATP (25 Ci/mmol for 10-200 μM titrations, 500 Ci/mmol for 0.1-5 μM titrations) and incubated on ice for 10 minutes. Binding reactions using ATPγS (25 Ci/mmol for 10-200 μM titrations, 500 Ci/mmol for 0.2-5 μM titrations) or AMP-PNP (20 Ci/mmol) were performed in the presence of Mg^{2+} (5 mM). Samples were then subjected to 20 minutes of crosslinking (Stratalinker) followed immediately with fractionation by SDS-PAGE using 4-15% gradient gels. Gels were stained with

Commassie blue and washed extensively with 7% acetic acid and 5% methanol. Radiolabeled bands were quantified using a PhosphorImager (Molecular Dynamics). Nonlinear regression and standard errors were determined using GraphPad Prism. Positioning of the Msh2 and Msh6 proteins was confirmed by markers at positions corresponding to stained Msh2 and Msh6 bands. No labeling was detected without crosslinking indicating that labeling could not be due to a contaminating protein kinase and crosslinking to BSA (present in all crosslinking experiments) was not detected. Experiments with AMP-PNP were performed at least twice and all other experiments were performed at least four times.

Pulse-chase crosslinking experiments

Pulsed reactions (5 μl) containing 1 pmole Msh2-Msh6 in Binding Buffer containing 50 mM Tris buffer pH 8.0, 2 mM DTT, 0.5 mM EDTA, 100 μg/ml BSA and the specified concentrations of unlabeled ATP were incubated on ice for 10 minutes followed by a chase of 15 μl Binding Buffer containing the specified concentrations of [γ-^{32}P]ATP (50 Ci/mmol). Samples were incubated for 10 minutes after addition of labeled ATP. Unpulsed reactions were identical to pulsed reactions except unlabeled ATP and [γ-^{32}P]ATP (50 Ci/mmol) were mixed and added to protein simultaneously. Crosslinking and quantification were performed as described above. Experiments with AMP-PMP were performed at least twice and all other experiments were performed at least four times.

Sliding of Msh2-Msh6 measured by total internal Reflectance

Interaction of the Msh2-Msh6 complex with DNA, with and without a LacI end block, was measured by total internal reflectance using the IAsys Auto Plus system (Thermo Affinity Sensors), essentially as described previously (Mendillo et al., 2005). An apparent K_d of nucleotide binding required for sliding was generated by fitting the off rates data to the hyperbolic (one site binding) equation:

$$Y = (Bmax) * e^{X/(K_d+X)} \qquad \text{(Eq. 4-1)}$$

where Bmax is maximal binding and Y is off rate and K_d is the concentration of nucleotide required for half-maximal off rate.

4.6 ACKNOWLEDGEMENTS

We thank Chris Putnam and Brian Orelli for insightful discussions, Manju Hingorani for providing the *E. coli* Msh2-Msh6 expression vector and Kathleen Matthews for providing the LacI protein. This work was supported by NIH Grant GM50006 to RDK and a postdoctoral fellowship from the American Cancer Society to DJM.

Chapter 4, in full, is a reprint of the material as it appears in Mazur, D. J., Mendillo, M. L., & Kolodner, R. D. "Inhibition of Msh6 ATPase activity by mispaired DNA induces a Msh2(ATP)-Msh6(ATP) state capable of hydrolysis-independent movement along DNA." *Molecular Cell* 2006 22: 39-49. The dissertation author was a secondary author on this paper.

4.7 SUPPLEMENTARY MATERIALS

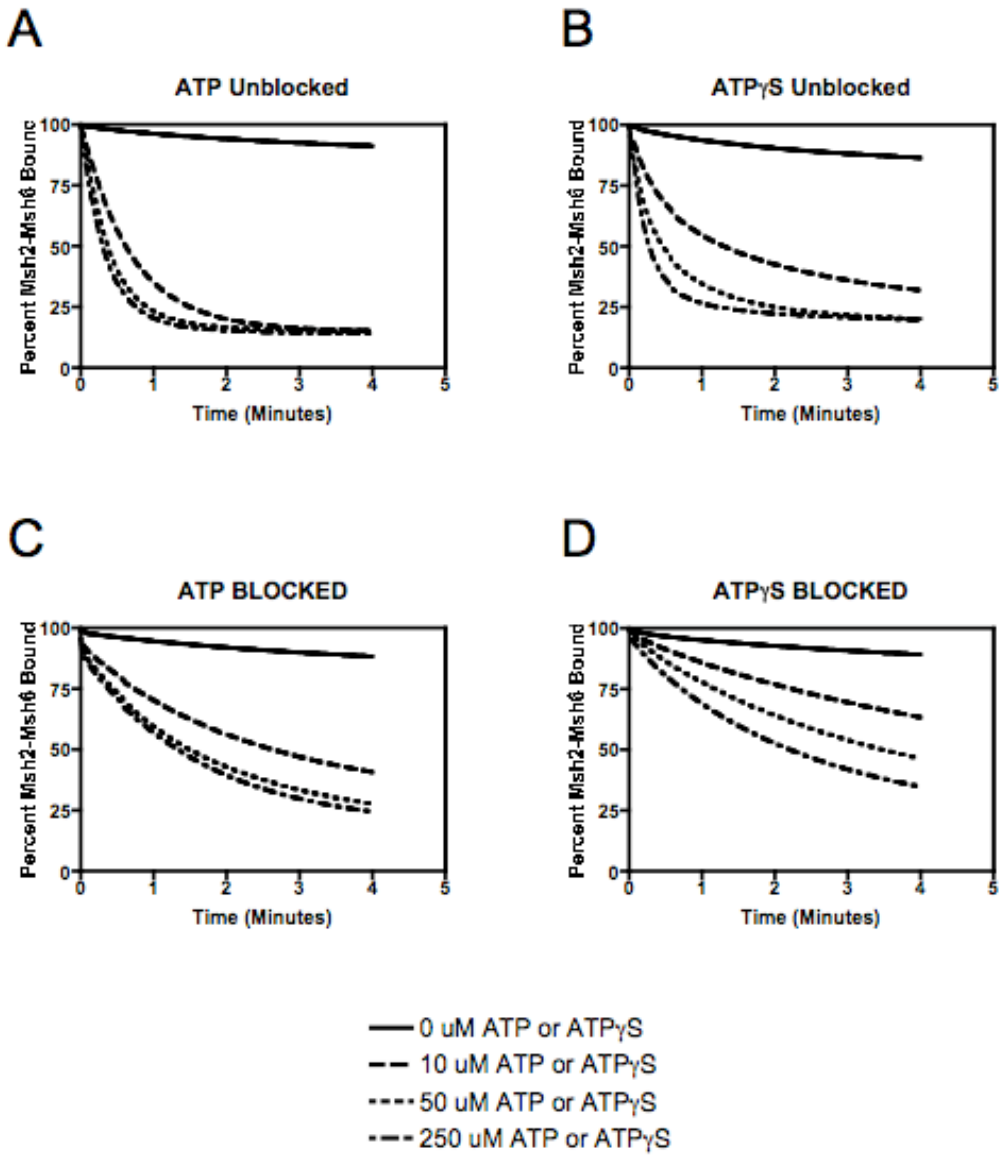

Supplemental Figure 4-S1. Biosensor analysis of various concentrations of ATP (A and C) or ATPγS (B and D) induced dissociation of the Msh2-Msh6 complex off of a DNA substrate containing a GT mispair with a free end (A and B) or end-blocked with LacI (C and D) under standard conditions as described under "Experimental Procedures."

4.8 REFERENCES

Acharya, S., Foster, P. L., Brooks, P., and Fishel, R. (2003). The coordinated functions of the E. coli MutS and MutL proteins in mismatch repair. Mol Cell *12*, 233-246.

Acharya, S., Wilson, T., Gradia, S., Kane, M. F., Guerrette, S., Marsischky, G. T., Kolodner, R., and Fishel, R. (1996). hMSH2 forms specific mispair-binding complexes with hMSH3 and hMSH6. Proc Natl Acad Sci U S A *93*, 13629-13634.

Alani, E., Sokolsky, T., Studamire, B., Miret, J. J., and Lahue, R. S. (1997). Genetic and biochemical analysis of Msh2p-Msh6p: role of ATP hydrolysis and Msh2p-Msh6p subunit interactions in mismatch base pair recognition. Mol Cell Biol *17*, 2436-2447.

Allen, D. J., Makhov, A., Grilley, M., Taylor, J., Thresher, R., Modrich, P., and Griffith, J. D. (1997). MutS mediates heteroduplex loop formation by a translocation mechanism. Embo J *16*, 4467-4476.

Antony, E., and Hingorani, M. M. (2003). Mismatch recognition-coupled stabilization of Msh2-Msh6 in an ATP-bound state at the initiation of DNA repair. Biochemistry *42*, 7682-7693.

Antony, E., Khubchandani, S., Chen, S., and Hingorani, M. M. (2005). Contribution of Msh2 and Msh6 subunits to the asymmetric ATPase and DNA mismatch binding activities of Saccharomyces cerevisiae Msh2-Msh6 mismatch repair protein. DNA Repair (Amst).

Bjornson, K. P., Allen, D. J., and Modrich, P. (2000). Modulation of MutS ATP hydrolysis by DNA cofactors. Biochemistry *39*, 3176-3183.

Bjornson, K. P., and Modrich, P. (2003). Differential and simultaneous adenosine di- and triphosphate binding by MutS. J Biol Chem *278*, 18557-18562.

Blackwell, L. J., Martik, D., Bjornson, K. P., Bjornson, E. S., and Modrich, P. (1998). Nucleotide-promoted release of hMutSalpha from heteroduplex DNA is consistent with an ATP-dependent translocation mechanism. J Biol Chem *273*, 32055-32062.

Das Gupta, R., and Kolodner, R. D. (2000). Novel dominant mutations in Saccharomyces cerevisiae MSH6. Nat Genet *24*, 53-56.

Drake, J. W. (1991). A constant rate of spontaneous mutation in DNA-based microbes. Proc Natl Acad Sci U S A *88*, 7160-7164.

Drummond, J. T., Li, G. M., Longley, M. J., and Modrich, P. (1995). Isolation of an hMSH2-p160 heterodimer that restores DNA mismatch repair to tumor cells. Science *268*, 1909-1912.

Gradia, S., Acharya, S., and Fishel, R. (1997). The human mismatch recognition complex hMSH2-hMSH6 functions as a novel molecular switch. Cell *91*, 995-1005.

Gradia, S., Subramanian, D., Wilson, T., Acharya, S., Makhov, A., Griffith, J., and Fishel, R. (1999). hMSH2-hMSH6 forms a hydrolysis-independent sliding clamp on mismatched DNA. Mol Cell *3*, 255-261.

Grilley, M., Welsh, K. M., Su, S. S., and Modrich, P. (1989). Isolation and characterization of the Escherichia coli mutL gene product. J Biol Chem *264*, 1000-1004.

Haber, L. T., and Walker, G. C. (1991). Altering the conserved nucleotide binding motif in the Salmonella typhimurium MutS mismatch repair protein affects both its ATPase and mismatch binding activities. Embo J *10*, 2707-2715.

Habraken, Y., Sung, P., Prakash, L., and Prakash, S. (1998). ATP-dependent assembly of a ternary complex consisting of a DNA mismatch and the yeast MSH2-MSH6 and MLH1-PMS1 protein complexes. J Biol Chem *273*, 9837-9841.

Harfe, B. D., and Jinks-Robertson, S. (2000). DNA mismatch repair and genetic instability. Annu Rev Genet *34*, 359-399.

Hess, M. T., Gupta, R. D., and Kolodner, R. D. (2002). Dominant Saccharomyces cerevisiae msh6 mutations cause increased mispair binding and decreased dissociation from mispairs by Msh2-Msh6 in the presence of ATP. J Biol Chem *277*, 25545-25553.

Hess, M. T., Mendillo, M. L., Mazur, D. J., and Kolodner, R. D. (2006). Biochemical basis for dominant mutations in the Saccharomyces cerevisiae MSH6 gene. Proc Natl Acad Sci U S A *103*, 558-563.

Joshi, A., Sen, S., and Rao, B. J. (2000). ATP-hydrolysis-dependent conformational switch modulates the stability of MutS-mismatch complexes. Nucleic Acids Res *28*, 853-861.

Junop, M. S., Obmolova, G., Rausch, K., Hsieh, P., and Yang, W. (2001). Composite active site of an ABC ATPase: MutS uses ATP to verify mismatch recognition and authorize DNA repair. Mol Cell *7*, 1-12.

Kolodner, R. (1996). Biochemistry and genetics of eukaryotic mismatch repair. Genes Dev *10*, 1433-1442.

Lamers, M. H., Perrakis, A., Enzlin, J. H., Winterwerp, H. H., de Wind, N., and Sixma, T. K. (2000). The crystal structure of DNA mismatch repair protein MutS binding to a G x T mismatch. Nature *407*, 711-717.

Lynch, H. T., and de la Chapelle, A. (2003). Hereditary colorectal cancer. N Engl J Med *348*, 919-932.

Marsischky, G. T., Filosi, N., Kane, M. F., and Kolodner, R. (1996). Redundancy of Saccharomyces cerevisiae MSH3 and MSH6 in MSH2-dependent mismatch repair. Genes Dev *10*, 407-420.

Martik, D., Baitinger, C., and Modrich, P. (2004). Differential specificities and simultaneous occupancy of human MutSalpha nucleotide binding sites. J Biol Chem *279*, 28402-28410.

Mendillo, M. L., Mazur, D. J., and Kolodner, R. D. (2005). Analysis of the interaction between the Saccharomyces cerevisiae MSH2-MSH6 and MLH1-PMS1 complexes with DNA using a reversible DNA end-blocking system. J Biol Chem *280*, 22245-22257.

Modrich, P. (1991). Mechanisms and biological effects of mismatch repair. Annu Rev Genet *25*, 229-253.

Obmolova, G., Ban, C., Hsieh, P., and Yang, W. (2000). Crystal structures of mismatch repair protein MutS and its complex with a substrate DNA. Nature *407*, 703-710.

Palombo, F., Iaccarino, I., Nakajima, E., Ikejima, M., Shimada, T., and Jiricny, J. (1996). hMutSbeta, a heterodimer of hMSH2 and hMSH3, binds to insertion/deletion loops in DNA. Curr Biol *6*, 1181-1184.

Peltomaki, P. (2003). Role of DNA mismatch repair defects in the pathogenesis of human cancer. J Clin Oncol *21*, 1174-1179.

Schofield, M. J., Nayak, S., Scott, T. H., Du, C., and Hsieh, P. (2001). Interaction of Escherichia coli MutS and MutL at a DNA mismatch. J Biol Chem *276*, 28291-28299.

Su, S. S., and Modrich, P. (1986). Escherichia coli mutS-encoded protein binds to mismatched DNA base pairs. Proc Natl Acad Sci U S A *83*, 5057-5061.

Wheeler, J. M., Bodmer, W. F., and Mortensen, N. J. (2000). DNA mismatch repair genes and colorectal cancer. Gut *47*, 148-153.

Zhang, Y., Yuan, F., Presnell, S. R., Tian, K., Gao, Y., Tomkinson, A. E., Gu, L., and Li, G. M. (2005). Reconstitution of 5'-directed human mismatch repair in a purified system. Cell *122*, 693-705.

CHAPTER 5

Escherichia coli MutS tetramerization domain structure reveals that stable dimers but not tetramers are essential for DNA mismatch repair *in vivo*

5.1 ABSTRACT

The *E. coli* mispair binding protein MutS forms dimers and tetramers *in vitro*, although the functional form *in vivo* is under debate. Here we demonstrate that the MutS tetramer is extended in solution using small angle X-ray scattering (SAXS) and the crystal structure of the C-terminal 34 amino acids of MutS containing the tetramer-forming domain fused to maltose binding protein (MBP). Wild-type C-terminal MBP fusions formed tetramers and could bind MutS and MutS-MutL-DNA complexes. In contrast, Asp835Arg and Arg840Glu mutations predicted to disrupt tetrameric interactions only allowed dimerization of MBP. A chromosomal MutS truncation mutation eliminating the dimerization/tetramerization domain eliminated mismatch repair, whereas the tetramer-disrupting MutS Asp835Arg and Arg840Glu mutations only modestly affected MutS function. These results demonstrate that dimerization but not tetramerization of the MutS C-terminus is essential for mismatch repair.

5.2 INTRODUCTION

Errors during DNA replication can result in base-base mispairs and small insertion or deletion mispairs, that when left unrepaired, give rise to mutations during subsequent rounds of replication. The mismatch repair (MMR) pathway normally corrects these errors (Iyer et al., 2006), and the importance of this pathway is demonstrated by its conservation from bacteria to humans and its role in preventing the development of human cancers (Lynch and de la Chapelle, 2003; Peltomaki, 2003).

In bacteria, mispairs are first recognized by the MutS protein, which is both a mispair-specific DNA binding protein and an ATPase (Haber and Walker, 1991; Su and Modrich, 1986). The MutS-mispair complex then recruits another conserved ATPase, the MutL homodimer (Ban and Yang, 1998; Grilley et al., 1989). In *Escherichia coli* methyl-directed MMR, MutS and MutL activate the MutH endonuclease, which cleaves hemimethylated GATC sequences in DNA duplexes on the newly synthesized strand lacking methyl groups (Au et al., 1992). The nick then targets helicases, nucleases, and DNA polymerases to initiate strand-specific excision and resynthesis to repair the mismatch (Lahue et al., 1989). While this repair reaction has been reconstituted *in vitro* (Lahue et al., 1989), the molecular mechanism that coordinates the initial events of MMR (mispair recognition) with downstream events (nicking, excision and replacement of the error-containing strand) is not well understood. Accordingly, several models have been proposed that attempt to explain

the orchestration of these events (Acharya et al., 2003; Allen et al., 1997; Junop et al., 2001; Selmane et al., 2003).

At high concentrations, MutS proteins from *E. coli, Thermus aquaticus*, and *Thermus thermophilus* undergo a dimer to tetramer transition (Biswas et al., 1999; Bjornson et al., 2003; Stanislawska-Sachadyn et al., 2003; Takamatsu et al., 1996). The C-terminal region mediates tetramerization and includes the last 53 amino acids in *E. coli* MutS (Figure 5-1) (Lamers et al., 2000). C-terminal truncations were used to obtain dimeric crystal structures of MutS and MutS bound to DNA and hence little is know about the structure of the C-terminal 53 amino acids of MutS (Lamers et al., 2000; Obmolova et al., 2000). Despite its crystallographic utility, the *E. coli* deletion protein, MutSΔ800, has severe biochemical defects in key functions including mispair recognition and MutH stimulation (Bjornson et al., 2003). Further, functional complementation of *E. coli mutS* deletion strains by the *mutSΔ800* protein for mutation avoidance requires overexpression from plasmids (Calmann et al., 2005b). Integration of the *mutSΔ800* mutation into the genome demonstrates that this allele results in a substantial MMR defect (Calmann et al., 2005a). In contrast, the antirecombination defects in *mutSΔ* null strains are not complemented by MutSΔ800 protein, even with overexpression (Calmann et al., 2005b).

The *in vitro* and *in vivo* defects caused by the C-terminal deletion and the fact that the *E. coli* tetramer disassociation constant is close to the *in vivo* MutS concentration has led to the suggestion that tetramerization is important for MMR (Bjornson et al., 2003; Calmann et al., 2005a). However, the MutSΔ800 protein has

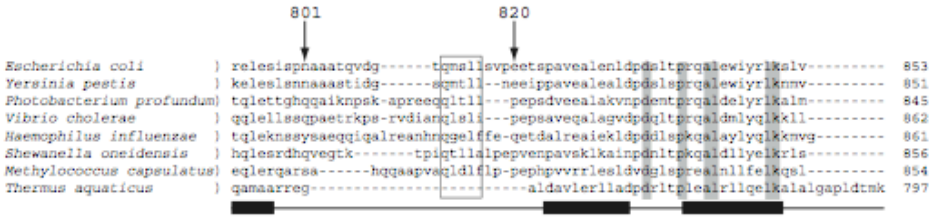

Figure 5-1. Sequence alignment of the C-terminal residues of MutS from a variety of bacteria. Absolutely conserved residues in this alignment are in shaded grey boxes. Residues lining up with the β sliding clamp binding sequence in *E. coli* MutS (Lopez de Saro et al., 2006) are outlined in a black box. Black bars underneath the alignment indicate the positions of α-helices from consensus secondary structure predictions (McGuffin et al., 2000). Arrows at 801 and 820 indicate the positions of these residues in the *E. coli* sequence.

dimerization defects in addition to tetramerization defects (Lamers et al., 2004; Manelyte et al., 2006). Thus the ability of MutSΔ800 to complement *mutS* strains only when overexpressed might be due to stabilization of the dimer (Calmann et al., 2005a; Calmann et al., 2005b). Further, the reported association constant for tetramerization ranges over two orders of magnitude, from $2.1x10^{-7}$ M^{-1} to $2.2x10^{-6}$ M^{-1} for *E. coli* (Bjornson et al., 2003; Lamers et al., 2004) and up to $1.3x10^{-5}$ M^{-1} for *T. aquaticus* (Biswas et al., 1999). This result is at odds with the idea that MutS concentrations are kept close to the concentration at which tetramers form. Despite this, recent experimental data indicate that a point mutation, Asp835Arg, which causes defects in tetramerization of a peptide corresponding to the C-terminus of MutS, is genetically identical to *mutSΔ800* in an overexpression assay, which has suggested a role for tetramerization *in vivo* (Manelyte et al., 2006).

In the present study, we have determined that the MutS tetramer is extended by small angle X-ray scattering (SAXS), and our model explained why MutS does not assemble into complexes larger than tetramers. To gain insight into MutS tetramerization, we fused the C-terminal 53 and 34 residues of *E. coli* MutS onto maltose binding protein (MBP) and showed that the fusions cause monomeric MBP to tetramerize. The crystal structure of the tetramerization domain revealed an extensively associated dimer interface, which made weak interactions to form tetramers. The MBP fusions bound MutS and MutS-MutL-DNA complexes, and binding required tetramerization motifs on both MBP and MutS. Deletions of the tetramerization motif predicted to affect both dimerization and tetramerization caused

substantial MMR defects when the deletion mutations were integrated into the chromosome. In contrast, MutS tetramer-disrupting point mutations were mostly functional when present at the chromosomal *mutS* locus. Together, our data resolve the controversies surrounding MutS tetramerization by demonstrating that the dimer-stabilizing role of the MutS C-terminus is essential for MMR, but that the tetramer-forming role is not.

5.3 RESULTS

Full length MutS is tetrameric, whereas MutSΔ800 is substantially monomeric

To establish that preparations of wild-type MutS were tetrameric, both MutS and the MutSΔ800 proteins were analyzed by size-exclusion chromatography (Figure 5-2A). Similar to previous observations, the Stokes' radius (R_s) of the wild-type tetrameric MutS, 83.3 Å, was larger than would be predicted for a globular MutS tetramer, which has an expected R_s of 59.0 Å and a MW of 358 kDa (Bjornson et al., 2000). By contrast, the MutSΔ800 truncation (monomeric molecular weight of 89.5 kDa) eluted with an R_s of 42.5 Å, similar to a 113 kDa globular protein, which was much smaller than the R_s of 49 Å and MW of 179 kDa expected for a globular MutS dimer. Dimerization defects in the MutSΔ800 have been previously observed (Lamers et al., 2004; Manelyte et al., 2006). The wild-type protein also discriminated between fully base paired DNAs and those containing single mispairs and formed MutS-MutL-DNA-ATP complexes as demonstrated in total internal reflectance and surface plasmon resonance experiments, whereas MutSΔ800 had substantial defects even in binding to mispair-containing DNA (data not shown), consistent with previous data (Bjornson et al., 2003).

SAXS data collected on wild-type MutS and MutSΔ800 agreed with the size-exclusion chromatography data (Figure 5-2B). The radius of gyration (R_g), which is an X-ray analog of R_s, was 38.3 Å for MutSΔ800 and 80.8 Å for MutS. Unlike R_s and R_g, the scattering intensity at zero angle, I(0), is independent of shape and can be used

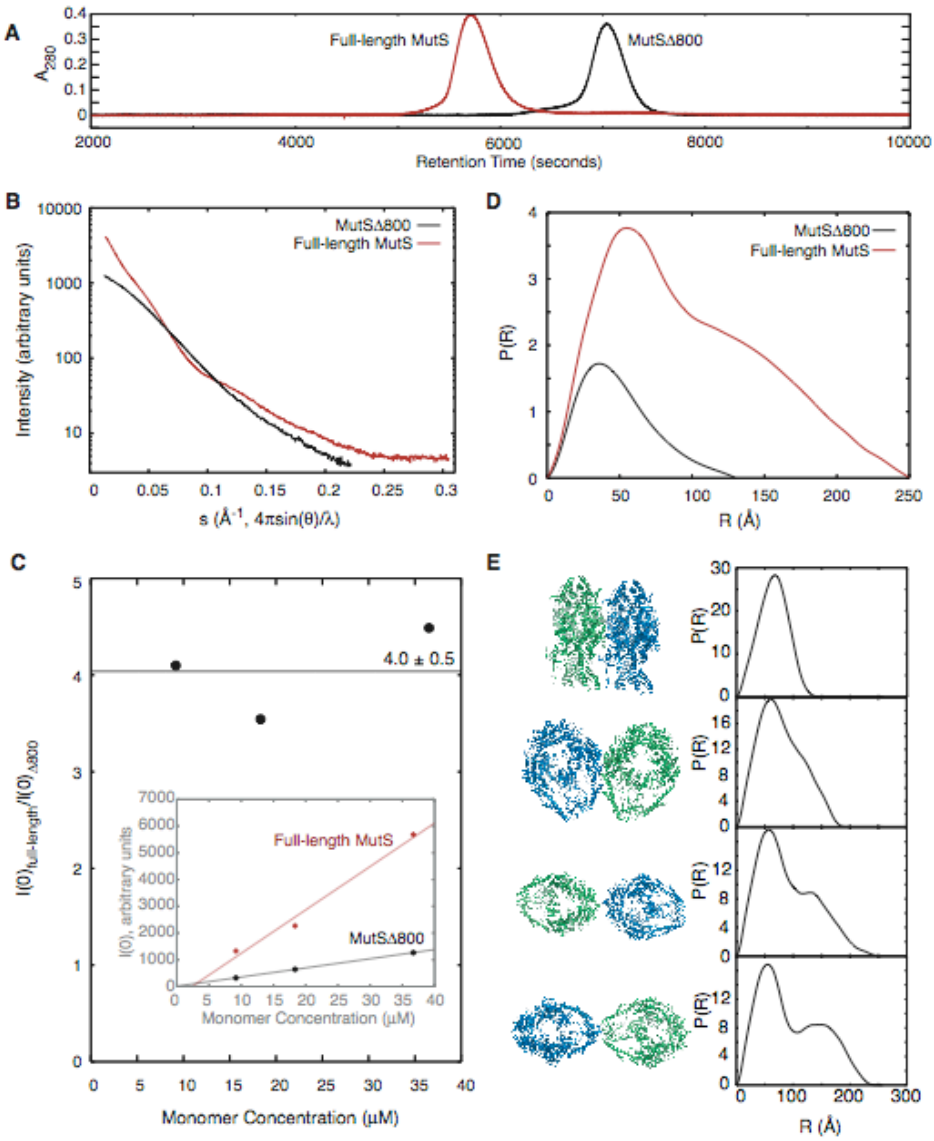

Figure 5-2. The MutS tetramer is extended in solution. A. Elution profile of full-length MutS and MutSΔ800 on size-exclusion chromatography. The Stokes' radius (R_s) of full-length MutS is 83.3 Å, whereas MutSΔ800, with a monomeric molecular weight of 89.5 kDa, has an R_s of 42.5 Å, and is equivalent to a globular molecular weight of 113 kDa. B. Scattering curves for full-length MutS and MutSΔ800 measured at 36.7 μM monomer concentrations. C. The ratio of I(0) of the full-length to I(0) of MutSΔ800 is 4.0 ± 0.5, indicating that the truncation is predominantly monomeric, consistent with gel filtration results. D. P(R) functions calculated for full-length and MutSΔ800 reveal that full-length MutS is extended. E. P(R) functions were calculated from different theoretical tetramers generated from the dimeric MutS crystal structure (blue and green, PDB id 1e3m (Lamers et al., 2000)) and reveal that only extended tetramers are consistent with the experimental data.

to determine stoichiometry of oligomers. I(0) depends linearly upon protein concentration (Figure 5-2C, inset) and depends on the square of the molecular weight of the scattered particle (Doniach, 2001). In protein solutions with equal molar concentrations of monomers, multimerization increases the molecular weight and decreases the concentration of scattering particles by the same integral factor. Thus the ratio of I(0) of the multimer to the I(0) of the monomer gives the stoichiometry of the complex. The ratio between wild-type MutS, which is known to form tetramers, and MutSΔ800 was 4.0 ± 0.5 (Figure 5-2C), indicating a tetrameric assembly for wild-type MutS and a monomeric assembly for MutSΔ800 under our conditions.

The MutS tetramer is extended

To understand the structure of the MutS tetramer in solution, we calculated the Fourier transforms of the SAXS curves to generate the pair-distribution function, P(R) (Figure 5-2D). The P(R) is a histogram of distances between electrons in the scattering particle and can be directly compared to P(R) functions calculated from atomic models (Figure 5-2E). Potential MutS tetramers constructed with face-to-face or side-to-side contacts of the MutS rings were not consistent with the experimental P(R) function with a D_{max} of ~250 Å. Instead, only elongated tetramers with contacts either at the ATPase domains (head-to-head tetramers) or the DNA clamping domains (tail-to-tail tetramers) were consistent with the experimental P(R) function. These elongated structures were consistent with the fact that wild-type MutS tetramers had a larger R_s than would be predicted by the molecular weight of the tetramer (Bjornson et

al., 2000) (Figure 5-2A). Among the potential extended MutS tetramers, the C-termini required for tetramerization were brought together only in the head-to-head tetramer and suggested this arrangement over the tail-to-tail or head-to-tail tetramers. This head-to-head tetramer is consistent with the observation that oligomers larger than tetramers were not observed in analytical ultracentrifugation experiments (Bjornson et al., 2003; Lamers et al., 2004). In contrast to potential multimers formed by head-to-tail, face-to-face or side-to-side arrangements of MutS rings, a head-to-head tetramer sterically occludes the C-terminal domain mediating the tetramerization and would block the formation of higher order oligomers.

Addition of the MutS C-terminus causes MBP to tetramerize

The C-terminal 53 amino acid domain could tetramerize MutS by two distinct mechanisms. In the first, the domain might only form a dimer and cause MutS to tetramerize by pairing with a symmetry-related partner from another MutS dimer through an alternative dimer interaction. In the second, the domain itself might tetramerize, thereby bringing together two MutS dimers. To distinguish these possibilities, we fused the last 53 amino acids of *E. coli* MutS (residues 801-853, Figure 5-1) to the MBP C-terminus to generate MBP801. The purified MBP801 protein eluted earlier in size-exclusion chromatography (R_s of 52.6 Å) than monomeric MBP (R_s of 15.7 Å; Figure 5-3A). The elution time matches the expected elution time for a MBP tetramer; however, elongated molecules have a larger R_s than would be predicted by molecular weight alone so this does not constitute strong proof

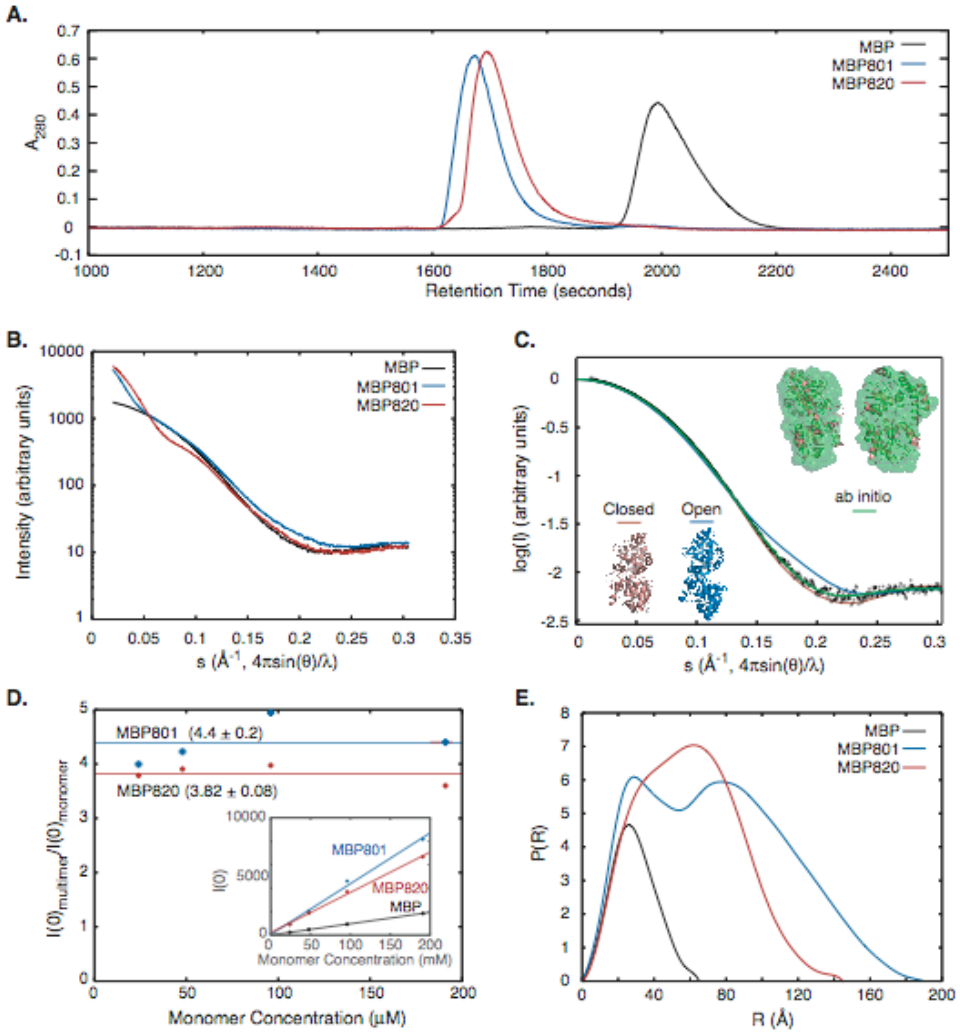

Figure 5-3. The final 34 amino acids of *E. coli* MutS mediate tetramerization of MBP. A. Size-exclusion chromatography of MBP (black), MBP801 (blue), and MBP820 (red) reveals that the C-terminal MutS fusions mediate multimerization of MBP801 and MBP820. B. X-ray scattering of equal monomer concentrations of MBP (black), MPB801 (blue), and MBP820 (red). C. X-ray scattering of monomeric MBP (black points) was compared to calculated scattering of the open (blue line, PDB id 1peb (Telmer and Shilton, 2003)) and closed (red line, PDB id 1fqc (Duan et al., 2001)) crystal structures of MBP using CRYSOL (Svergun et al., 1995). The experimental scattering (R_g 22.4 Å) fit the closed MBP structure (χ 3.1, R_g 21.97 Å) better than the open structure (χ 10.6, R_g 23.0 Å). Similarly, *ab initio* reconstruction of the MBP shape generated by GASBOR (Svergun et al., 2001) fits the experimental scattering (green line) and the closed crystal structure well (average chi = 1.2 ± 0.1, n=10). D. The ratio of I(0)multimer/I(0)monomer reveals that the complexes formed by MBP801 (blue) and MBP820 (red) are tetrameric. The average ratio is 4.4 ± 0.2 for MBP801 and 3.82 ± 0.08 for MBP820. The I(0) for each protein is linear with respect to concentration (inset). E. Pair distribution function calculated for MBP (black), MBP801 (blue), and MBP820 (red).

of tetramer formation.

The 53 amino acids in the C-terminal motif can be divided into a non-conserved N-terminal region not predicted to form secondary structure and a C-terminal region predicted to form two amphipathic helices (Figure 5-1). A second MBP fusion, MBP820, was generated, which contained the region of the C-terminal motif predicted to form secondary structure (residues 820-853). The expressed protein chromatographed almost identically to MBP801 with an R_s of 46.8 Å (Figure 5-3A), which indicated that the last 34 residues are sufficient to increase the R_s of the MBP fusion.

SAXS data were collected for MBP801, MBP820, and MBP to understand conformation and stoichiometry of the MBP constructs (Figure 5-3B). The R_g was 58.1, 45.7, and 22.1 Å for MBP801, MBP820, and monomeric MBP, respectively. This was consistent with both the R_s and oligomerization observed by size-exclusion chromatography. MBP exists in an "open" unbound state and a "closed" maltose-bound state (Shilton et al., 1996). Comparison of calculated scattering from crystal structures of known MBP conformations indicated that the MBP monomer was closed (Figure 5-3C), similar to previous SAXS results (Shilton et al., 1996). Additionally, *ab initio* structure generation from the SAXS data using GASBOR (Svergun et al., 2001) fits the known crystal structure of the closed form of MBP.

Stoichiometric measurement by I(0) ratios at equivalent monomer concentrations indicated that MBP801 and MBP820 were tetramers (Figure 5-3D), consistent with analytical ultracentrifugation analysis of the isolated MutS peptide

comprising residues 801 to 853 (Manelyte et al., 2006). These data show that the C-terminal motif directly mediates tetramerization, which is consistent with the head-to-head extended MutS tetramer solution assembly predicted by the SAXS analysis. Unlike monomeric MBP, the P(R) function of MBP801 and MBP820 had two peaks, suggesting that the average distances between the centers of the MBP domains in the MBP801 and MBP820 tetramers were 78 Å and 62 Å, respectively (Figure 5-3E). The larger distances observed with MBP801 were consistent with longer linker distances.

MBP801 can interact with MutS and MutS-MutL-DNA complexes

The MBP801 fusion retained the ability of wild-type MBP to bind with high affinity to starch matrices and could be eluted from such matrices with maltose (Figure 5-4A). Thus, we sought to determine if the MBP fusions could specifically bind MutS. MBP801 was bound to a starch matrix and MutS or MutSΔ800 was added. After washing, the bound proteins were eluted with 10 mM maltose and analyzed by SDS-PAGE. Full length MutS copurified with MBP801 in the maltose elution, but was not eluted from the starch column by maltose in the absence of MBP801. Similarly, MutSΔ800 did not co-purify with MBP801 nor did full length MutS co-purify with wild-type MBP. Thus, the formation of heterotetramers between MutS and MBP801 were dependent upon the presence of the tetramerization motif.

Since MutS could be immobilized on a starch matrix through interaction with MBP801, we addressed the question of whether or not this interaction would be

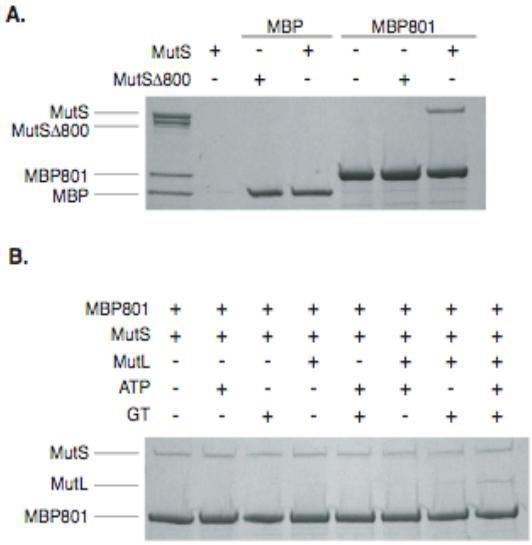

Figure 5-4. MBP801 can bind MutS and MutS-MutL-DNA complexes. A. MBP or MBP801 were immobilized onto amylose resin to which MutS or MutSΔ800 were added. After washing, MBP and bound proteins were eluted with 10 mM maltose and run on a SDS-PAGE gel that was stained with Coomassie Brilliant Blue. B. To amylose resin bound by MBP801 and MutS, combinations of MutL, ATP, and DNA containing a central GT mispair were added. After washing, bound proteins were eluted with maltose. MutS and MBP801 were specifically bound to the resin, whereas MutL retention required mispair-containing DNA and was stimulated by ATP.

disrupted by the formation of a ternary complex containing MutS, MutL, and mispaired DNA (Figure 5-4B). MutS, MutL, ATP, and mispaired DNA were added to a starch matrix containing prebound MBP801. In the presence of maltose, MutS and MutL co-eluted with MBP801, indicating that ternary complexes can form a complex with MBP801. The binding of MutL to MBP801 required MutS, mispaired DNA, and was stimulated by ATP (Figure 5-4B), consistent with known requirements for the formation of ternary complexes *in vitro* (Acharya et al., 2003; Baitinger et al., 2003; Grilley et al., 1989; Selmane et al., 2003). Thus, the ternary complex can form with MutS-MBP801 heterotetramer, and does not appear to require MutS homotetramerization.

Crystal structure of MBP820 reveals the fold of the tetramerization domain

MBP820 crystallized in the monoclinic spacegroup C2 with two molecules in the asymmetric unit, whereas MBP801 did not crystallize even at protein concentrations greater than 100 mg/mL. The 2.0 Å structure of MBP820 was solved by molecular replacement (Table 5-1), using the closed conformation of MBP as a model (PDB id 1fqc (Duan et al., 2001)). Electron density clearly showed MBP820-bound maltose, which was likely scavenged during the purification protocol (data not shown).

The crystal structure revealed that the tetramerization domain was generated from a helix-loop-helix structure that is reminiscent of a HEAT repeat (Andrade et al., 2001). Dimerization forms a two-layer structure that packs helices orthogonally. The

Table 5-1. Crystallographic Statistics.

Data Collection	
Space Group	C2
Cell dimensions	
a,b,c (Å)	174.3, 88.4, 61.4
α, β, γ (°)	90, 106.8, 90
Mosaicity (°)	0.58
Resolution (Å)	20.0 – 2.0 (2.07 – 2.0)*
R_{sym} (%)	5.8 (54.8)
I/σ	18.9 (3.2)
Completeness (%)	97.9 (95.6)
Redundancy	4.0 (3.4)
Refinement	
Resolution limits (Å)	20.0 – 2.0
R_{work}/R_{free} (%)	20.1 / 27.7
No. Atoms	
Protein	6,327
Ligands/Ions	51
Solvent	511
Rms deviations	
Bond lengths (Å)	0.023
Bond angles (°)	1.914

*Numbers after the slash indicate values for the high resolution shell.

dimer was symmetric, despite the fact that it was generated by non-crystallographic symmetry (Figure 5-5A). The dimer interface buried 912 $Å^2$ per monomer, which is a substantially larger than would be predicted based on the 3.9 kDa size of the domain (Jones and Thornton, 1995). Moreover, the interface was extensively hydrophobic and was comprised of side chains from residues in both amphipathic helices and the connecting loop. This loop had a defined geometry that is likely controlled by Pro834, Pro839, and Leu837, whose side chain was buried in the central hydrophobic core in a manner similar to the conserved hydrophobe in DNA-binding helix-hairpin-helix motifs (Thayer et al., 1995) (Figure 5-5B). Surprisingly, the conserved Lys850 appeared to stabilize the final turn of the first helix in the other monomer of the dimer by neutralizing the helix dipole rather than interacting with negatively charged side chains. Similarly, the conserved Asp835 formed hydrogen bonds with the Tyr847 side chain in the dimer, and only made salt bridging interactions in the tetramer as described below.

The tetramer interface was generated by a crystallographic two-fold relating two dimers (Figure 5-5C). Unlike the dimerization interface, this surface was relatively small, burying only 233 $Å^2$ per monomer. This surface sequestered few hydrophobes and rather remarkably was asymmetric with respect to the individual monomers in the dimer. One half of the interface was formed by the packing of two loops (Asp833 to Arg840) from one monomer of the dimer and the other half involved packing of the second helix (Arg840 to Arg848) in the other monomer. Thus the individual monomers of the tetramer can be distinguished by being loop-loop packed

Figure 5-5. Crystal structure of the MBP820 fusion.
A. The MutS C-terminal domain is comprised of two amphipathic helices with a long structured loop. The Lys850 side chain stablizes the C-terminus of the first helix and the loop is held rigid by prolines and hydrophobic side chains that pack into the central hydrophobic core. The non-crystallographic dimer (blue and salmon monomers) is held together by an extensive hydrophobic surface. The inset shows the MBP820 dimer structures rotated relative to the previous view by 90 degrees with the MutS C-terminal domain boxed. B. Difference electron density for the ordered loop (Pro834 to Pro839) connecting the two alpha helices is contoured at 3σ (yellow) and 5σ (green). C. The tetramer is formed from a two layer structure where loop-loop packed monomers (blue and green) are packed with helix-helix packed monomers (salmon and orange). Charge-charge interactions of Arg840 with Asp833 and Asp835 in the loop-loop packed monomers and with Glu844 in the helix-helix packed monomers stabilize the tetramer. D. Theoretical SAXS curves calculated from the dimeric (blue) and tetrameric (red) calculated with CRYSOL (Svergun et al., 1995) are superimposed onto the experimental MBP820 solution scattering curve (black crosses). E. Size-exclusion chromatography of MBP, MBP801, MBP801-D835R, and MBP801-R840E reveals that the mutations predicted to disrupt tetramerization but not dimerization generate MBP oligomers intermediate between the monomeric MBP and tetrameric MBP801. F. A model for the MutS tetramer was constructed by connecting the N-termini of the tetramerization domains to the C-termini of four *E. coli* MutS molecules (PDB id 1e3m (Lamers et al., 2000)) linked by 19 amino acid peptides of arbitrary conformation.

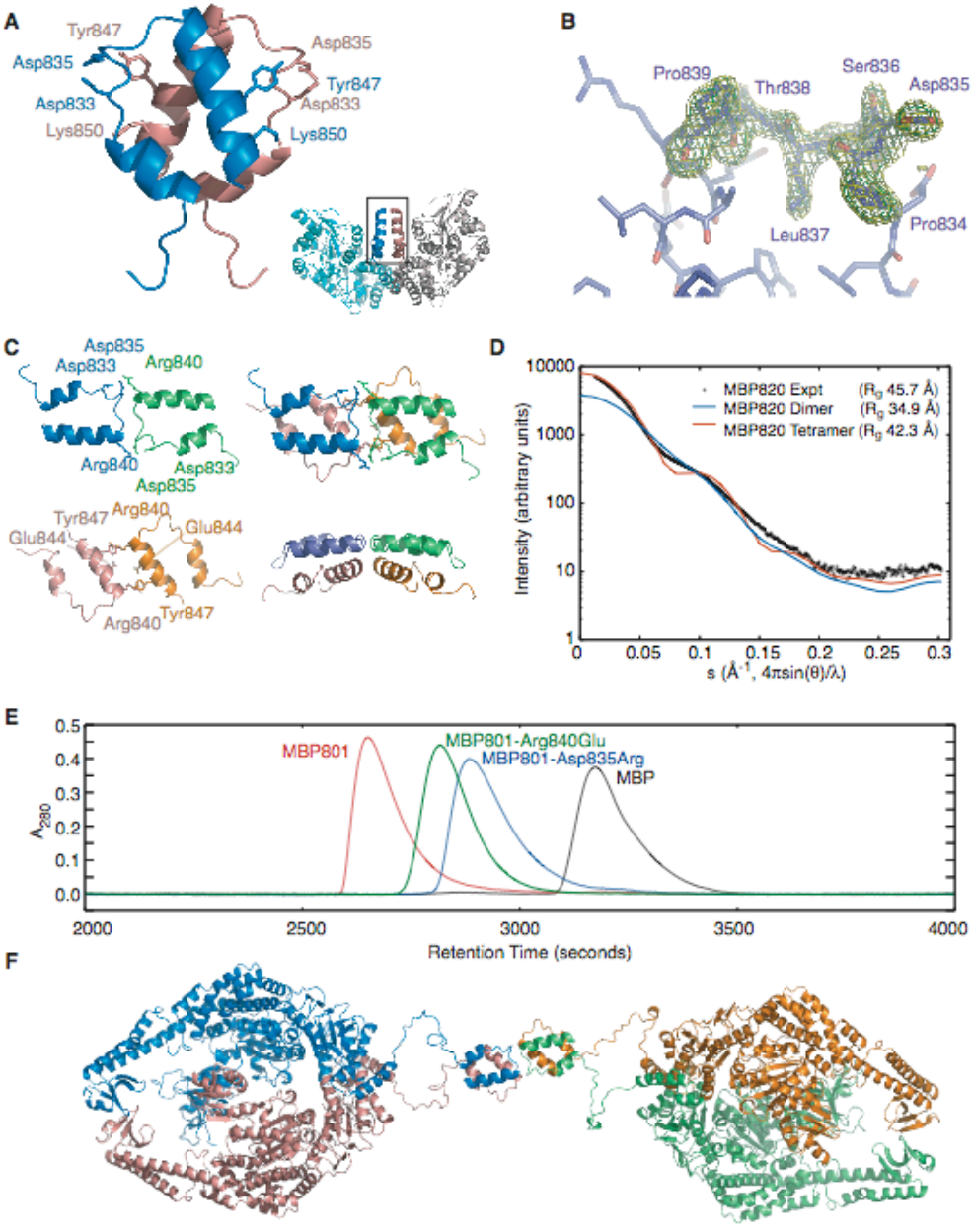
A
Tyr847
Asp835
Asp835
Tyr847
Asp833
Asp833
Lys850
Lys850
B
Pro839
Thr838
Ser836
Asp835
Leu837
Pro834
C
Asp835
Asp833
Arg840
Arg840
Asp833
Asp835
Tyr847
Arg840
Glu844
Glu844
Arg840
Tyr847
D
MBP820 Expt (Rg 45.7 Å)
MBP820 Dimer (Rg 34.9 Å)
MBP820 Tetramer (Rg 42.3 Å)
Intensity (arbitrary units)
s (Å-1, 4πsin(θ)/λ)
E
MBP801
MBP801-Arg840Glu
MBP801-Asp835Arg
MBP
A280
Retention Time (seconds)
F

monomers or helix-helix packed monomers. The tetramer buried two side chains of Leu843 from the helix-helix packed monomers and two side chains of Pro839 from the loop-loop packed monomers; however, the two other copies of each of these residues remain solvent exposed in the tetramer. Electrostatic interactions also appeared to play an important role at the interface. Two of the four Arg840's from loop-loop packed monomers made favorable salt bridge interactions with the Asp833 and Asp835 from the other loop, whereas the other two Arg840's from helix-helix packed monomers stacked against Tyr847 and made a salt bridge with Glu844 from the other helix.

Despite the small size of the observed tetramer interface, several lines of evidence suggest that the observed interface causes tetramerization in solution. First, the high dissociation constant measured for MutS tetramerization (Bjornson et al., 2003; Lamers et al., 2004), which is around or above the estimated concentration of MutS in the *E. coli* cell (Feng et al., 1996), suggested a small buried surface area. Second, the MBP820 tetramer in the crystal structure was consistent with solution SAXS data, with a calculated R_g for the tetramer of 42.3 Å as compared to an experimental R_g 45.7 Å, (Figure 5-5D). For comparison, the calculated R_g of the MBP820 dimer was only 34.9 Å. Differences in measured and calculated scattering profiles of the tetramer suggested that crystal-packing forces compacted MBP820 relative to the average solution conformation. Third, disruption of the electrostatic interactions in the observed tetramer interface, such as by the Asp835Arg mutation, previously shown to prevent tetramerization of the C-terminal peptide and MutS

(Manelyte et al., 2006), as well as by the Arg840Glu mutation, disrupted tetramerization without substantially affecting dimerization of the MBP801 fusion (Figure 5-5E). Thus, the crystallographically generated tetramerization interface is likely the interface that mediates formation of *E. coli* MutS tetramers (Figure 5-5F).

We noticed that the Asp835Arg version of MBP801, but not the Arg840Glu version, had an elution profile that was strongly concentration-dependent (data not shown). The elution positions were between those for the MBP monomers and MBP dimers, indicating that the Asp835Arg mutant had some dimerization defects. Consistent with this, Asp835 makes interactions in the dimer, whereas Arg840 does not. In the context of the full-length MutS protein, however, the Asp835Arg mutation did not appear to affect dimerization (Manelyte et al., 2006).

Dimerization, but not tetramerization, of MutS is critical for MMR *in vivo*

The structural characterization of the tetramerization C-terminal domains suggests that dimerization should be a stronger interaction than tetramerization. Truncation alleles, however, would be predicted to affect the role of the C-terminal domain in both processes. Thus, to understand the importance of the different functions of the C-terminal domain for MMR *in vivo*, we introduced mutant alleles of *mutS* onto the chromosome and tested the mutant strains for increased rates of mutations that give rise to rifampicin resistance, indicative of an MMR defect (Calmann et al., 2005a).

Mutation rates of strains bearing the chromosomal *mutSΔ800* allele were

approximately 2-fold lower than *mutSΔ11* null alleles (Table 5-2), similar to previously published results (Calmann et al., 2005a). Similarly, C-terminal deletions that eliminated successive secondary structural elements, *mutSΔ819* and *mutSΔ834*, were MMR defective and had mutation rates that were statistically indistinguishable from the *mutSΔ800* allele ($p = 0.3401$ and $p = 0.1249$, respectively; 2-tailed Mann-Whitney test was used for all pair-wise comparisons). In contrast, a *mutS* mutant where the ß sliding clamp interaction motif was deleted (*mutSΔ812-816*), in the region directly upstream of the predicted secondary structural elements, did not effect MMR *in vivo* (Lopez de Saro et al., 2006). These results indicated that the secondary structural elements within the C-terminal domain are important for MutS function, but do not indicate the relative significance of dimerization and tetramerization *in vivo*.

To specifically address the role of tetramerization, the point mutants *mutS-Asp835Arg* and *mutS-Arg840Glu* were introduced onto the chromosome. Both of these C-terminal motif mutations cause tetramerization defects without substantially affecting dimerization (Manelyte et al., 2006) (Figure 5-5E). When integrated onto the chromosome, these mutations caused only small MMR defects. These mutation rates were significantly different from the effects of the *mutSΔ800* allele ($p \leq 0.0001$ for both comparisons). This contradicts a previous study in which the *mutS-Asp835Arg* mutation was found to be indistinguishable from the *mutSΔ800* allele (Manelyte et al., 2006). However, that study tested plasmid encoded alleles resulting in increased expression, and it is known that overexpression of *mutSΔ800*, which encodes a MutS truncation with concentration-dependent dimerization defects,

Table 5-2. Mutation rates.

Strain	Relevant Genotype	Mutation rate (Rif^R)*
RDK4786	Wild type	1.0 [0.7-1.4] x 10^{-8} (1)
RDK4782	*mutSΔ11*	4.5 [3.3-7.5] x 10^{-7} (44)
RDK4783	*mutSΔ800*	1.9 [1.3-2.7] x 10^{-7} (19)
RDK4784	*mutSΔ819*	2.2 [1.4-5.6] x 10^{-7} (22)
RDK4785	*mutSΔ834*	3.0 [1.9-4.2] x 10^{-7} (29)
RDK4787	*mutS-Asp835Arg*	4.5 [3.5-7.2] x 10^{-8} (4)
RDK4788	*mutS-Arg840Glu*	5.2 [2.7-5.7] x 10^{-8} (5)

* The numbers in brackets represent low and high values, respectively, for the 95% confidence interval for each rate. The number in parentheses indicates rate relative to wild-type rate.

dramatically improves the ability of this allele to complement a *mutS* null strain (Calmann et al., 2005a). Our analysis of chromosomally integrated alleles together with specific mutations that disrupt tetramerization but not dimerization reveals that MutS tetramerization is not essential for MMR function *in vivo*. Consistent with this, overexpression of the MBP801 fusion to compete for MutS tetramerization *in vivo* had no effect on the mutation rate (data not shown).

5.4 DISCUSSION

In the present study, we have shown that the MutS tetramer is generated through an asymmetric tetramerization domain that generates strong dimeric, but weak tetrameric interactions. This domain mediated tetramerization of MBP fusions as well as MBP fusion interactions with MutS and MutS-MutL-DNA complexes. Further, we have shown that the MutS tetramer is extended in solution and when combined with the crystallography of the tetramerization motif reveals why oligomers larger than tetramers are not observed. Moreover, the MutS tetramer derived from SAXS data is remarkably similar to the structures observed by electron microscopy at the bases of DNA loops (Allen et al., 1997), assuming that these structures correspond to two MutS dimers, with each bound to different parts of the DNA molecule, as has been suggested by others (Bjornson et al., 2003; Iyer et al., 2006; Marti et al., 2002). Finally, our genetic data revealed that the tetramerization motif is required for MMR *in vivo*, presumably through stabilizing MutS dimers, but that formation of MutS tetramers by this domain is not significantly required for MMR.

After the asymmetric recognition of mispairs by MutS (Lamers et al., 2000; Obmolova et al., 2000) and formation of a MutS-MutL-DNA ternary complex (Acharya et al., 2003; Baitinger et al., 2003; Grilley et al., 1989; Selmane et al., 2003), the downstream events in MMR are poorly understood. In the methyl-directed mismatch repair system in *E. coli*, MutS and MutL somehow activate the MutH endonuclease, whereas events in other bacterial and eukaryotic systems are more

obscure. At least three competing models for MutS and/or MutS-MutL signaling have been proposed (Acharya et al., 2003; Allen et al., 1997; Selmane et al., 2003): bidirectional ATP-hydrolysis dependent MutS translocation, ATP-hydrolysis independent MutS sliding and signal transduction, and ATP-dependent authorization of MutS mispair recognition that does not involve dissociation of MutS from the mispair. Tetramer formation by MutS has been suggested to support the translocation model (Bjornson et al., 2003) or in models where one dimer remains bound to the mispair and the other dimer is involved in the strand discrimination signal (Marti et al., 2002; Sixma, 2001).

Our data indicating that the dimerization/tetramerization domain, but not tetramerization *per se*, is required for MMR suggest that aspects of these models may need revision. For example, MutS may drive reactions *in vitro*, such as formation of large tetramer-restrained DNA loops during ATP-dependent translocation(Allen et al., 1997), which may not be required for most MMR events *in vivo*. Our conclusions are at odds with the interpretation of others for the relevance of tetramerization to MMR (Bjornson et al., 2003; Manelyte et al., 2006); however, our conclusions are fully consistent with their data given that the MutSΔ800 protein has dimerization as well as tetramerization defects (Lamers et al., 2004; Manelyte et al., 2006) and that *mutSΔ800* can complement MMR defects in *mutSΔ* null strains, but only when overexpressed (Calmann et al., 2005b).

In addition, previous studies have shown that while the MutSΔ800 protein has a lower affinity for mispaired DNA, it retains specificity for mispaired DNA versus

homoduplex DNA and is only weakly functional in *in vitro* MMR reactions (Bjornson et al., 2003). In light of our data and other previously published data, this may not be surprising. A significant amount of MutSΔ800 protein might be expected to be monomeric (monomer to dimer K_d = 13 μM (Lamers et al., 2004)) due to lack of stabilization by the dimerization domain, especially at the sub-micromolar concentrations of protein that were used in these assays. This is consistent with *in vivo* results from MMR complementation assays, where normal levels of expression of the *mutSΔ800* allele from the chromosome results in a null phenotype, while higher level expression from a plasmid largely complements MMR defects of *mutSΔ* null strains (Calmann et al., 2005a; Calmann et al., 2005b; Obmolova et al., 2000). The concentrations of MutSΔ800 used for crystallization and present in the crystal lattice, however, are sufficient to drive dimerization as observed in the crystal structures (Lamers et al., 2000; Obmolova et al., 2000). Nevertheless, in contrast to the *mutSΔ800* allele, point mutations that disrupt the tetrameric interface, but not the dimeric interface, result in stable dimeric proteins that mostly complement *mutSΔ* null strains when present on the chromosome, while they behave identically in complementation assays when both alleles are expressed at higher levels from plasmids.

We have observed that while the portion of the C-terminal domain responsible for stabilizing the dimer is conserved in MutS proteins from the majority of bacteria, the charged amino acids contributing to the salt bridges that are essential for tetramerization of the *E. coli* MutS protein are conserved only in a subset of the

proteobacteria. Consistent with this, MutS from *T. thermophilus*, which lacks predicted salt-bridge forming residues (Figure 5-1), tetramerizes with a dissociation constant that is two orders of magnitude higher than the *E. coli* protein (Biswas et al., 1999; Bjornson et al., 2003). Moreover, we are unaware of any reports describing the tetramerization of eukaryotic Msh2-Msh6 and Msh2-Msh3 MutS homologue complexes, which lack this C-terminal domain that mediates both dimerization and tetramerization, consistent with tetramerization being dispensable for conserved MMR functions. We do note, however, that MutS function in MMR and homeologous recombination events appear to be differentially affected by the *mutSΔ800* allele (Calmann et al., 2005a), which is substantially different from engineered mutations in other regions of the MutHLS proteins, where no difference in the two processes were noted (Junop et al., 2003).

5.5 EXPERIMENTAL PROCEDURES

Plasmid and strain construction, and general genetics methods

A His_6-MutSΔ800 expression vector was created by replacing the *RsrII-BamHI* fragment from pTX412 (Feng and Winkler, 1995) (pET15b- His_6-MutS; gift of Malcolm Winkler) with the *RsrII-BamHI* fragment from MutSΔ800 B5 (gift of Paul Modrich) yielding His_6-MutSΔ800 in the pET15b expression vector (pRDK1240).

His_6-MBP was amplified by PCR from plasmid pMYB5 DNA (New England Biolabs) using a forward primer containing a *NcoI* restriction site followed by a His_6-tag and a reverse primer containing a *NdeI* restriction site and was ligated into pET15b (Novagen), yielding pRDK1232 (pET15b-His_6MBP). The *E. coli* MutS C-terminal DNA sequence encoding amino acids 801-853 and 820-853 were amplified by PCR with forward primers containing a *NdeI* restriction site and reverse primers containing a *BamHI* restriction site and ligated into pRDK1232. This created pRDK1233 and pRDK1234, which fused MutS801-853 and MutS820-853, respectively, to the C-terminus of His_6MBP. The MBP801-Asp835Arg (pRDK1235) and MBP801-Arg840Glu (pRDK1236) expression vectors were made as described above, except the mutant mutS was amplified off of the appropriate mutant mutS allele.

The strains for *in vivo* analysis were constructed by PCR-mediated recombination into an *E. coli* strain conditionally expressing the bacteriophage lambda Red system (Calmann et al., 2005a; Poteete et al., 2004). Briefly, the *bla* gene (encoding ampicillin resistance) was amplified using a forward oligonucleotide

incorporating 50 bases of homology to MutS for integration at the desired location in the *E. coli* MutS locus followed by a stop codon and a reverse oligonucleotide containing an additional 50 bases of homology immediately downstream of the native MutS codon. PCR products were transformed into strain TP798 (Poteete et al., 2004) and resulted in ampicillin-resistant strains with a stop codon followed by the *bla* gene after residues 11 (RDK4782), 800 (RDK4783), 819 (RDK4784), 834 (RDK4785), and 853 (end of wild type sequence) (RDK4786) of the chromosomal *mutS* locus. The *mutS* Asp835Arg (RDK4787) and Arg840Glu (RDK4788) point mutations were made by amplifying the *bla* gene from RDK4786 (MutS wild type-*bla*) genomic DNA using a forward oligo incorporating the desired point mutation and the same reverse oligonucleotide as above and transforming the cassette back into TP798. All chromosomal integrants were verified by PCR and sequencing.

Mutation rate assay

Mutation rates for rifampicin resistance were determined by fluctuation analysis using at least 15 independent cultures for each strain (Lea, 1948; Luria, 1943; Miller, 1992). Cultures were grown overnight and dilutions were plated on LB + 100 μg/mL ampicillin ± 100 μg/mL rifampicin and allowed to grow overnight at 37˚ C. Two-tailed Mann-Whitney test was performed to calculate P-values using Graphpad Prism version 4.0b for Macintosh (Graphpad Software, www.graphpad.com).

Protein expression and purification

His_6-MutS and His_6-MutL were expressed and purified essentially as described previously(Feng and Winkler, 1995), with the addition of a MonoQ column. His_6-MutSD800 was expressed in BL21(DE3)Tn10::mutS (gift of Paul Modrich). The his-tagged MBP proteins were expressed in BL21(DE3)Tn10::mutS and purified with a nickel column followed by binding to amylose resin and were eluted with 10 mM maltose. Proteins aliquots were frozen in liquid nitrogen and stored at -80° C.

Gel filtration chromatography

From 0.25 to 5 mg of the MBP-MutS fusions were loaded onto a Superdex 75 column (Amersham Biosciences) and run in buffer containing 20 mM Tris (pH 7.5), 150 mM NaCl and 0.5 mM EDTA. Both MutS and MutSΔ800 were loaded onto a Superose 6 column (Amersham Biosciences) at a monomeric concentration of 50 μM and run in buffer containing 20 mM Tris (pH 8.0), 300 mM NaCl, 0.5 mM EDTA and 4 mM dithiothreitol. Stokes radii were calculated with a linear regression of retention time versus radius using known standards.

Amylose pull-down assays

Binding reactions containing 600 pmol of MBP or MBP801 and 600 pmol of MutS or MutSΔ800 were incubated in 50 μL of buffer containing 20 mM Tris (pH 7.5), 4 mM $MgCl_2$ and 100 mM NaCl on ice for 15 min followed by addition of 100

μL Amylose resin (New England Biolabs; resuspended in above buffer) for an additional 15 min. After extensive washes, bound proteins were eluted with 100 μL buffer containing 20 mM maltose, separated by SDS-PAGE, and stained with Coomassie Brilliant Blue. Experiments analyzing formation of ternary complex with MutL were performed as follows. MBP801 and MutS were incubated and bound to Amylose resin, as described above. Samples were then washed with buffer ± 250 μM ATP, as indicated. Next, 300 pmol of MutL and/or 150 pmol of mispair containing DNA (71 bp) in buffer ± 250 μM ATP were added and incubated for 15 additional minutes on ice, as indicated. Samples were washed with buffer ± 250 μM ATP and eluted and processed above.

SAXS data collection and processing

SAXS data were collected at beamline 12.3.1 at the Advanced Light Source at Lawrence Berkeley National Laboratories. A wavelength of 1.115869 Å was used with a sample to detector distance of 1.48 meters. The resolution scale was calibrated using a silver behenate calibration standard that has diffraction maxima at 0.107633 and 0.215266 $Å^{-1}$. Buffer and samples were collected alternately with short exposures bracketing a longer exposure. The short exposures were compared to ensure that no radiation damage occurred, and data from all exposures were merged using PRIMUS. For each sample, data were collected at several different protein concentrations and the scattering was fit by the indirect Fourier transform method (Moore, 1980) as implemented in GNOM (Semenyuk and Svergun, 1991). Theoretical scattering from

atomic models were compared to experimental data using the program CRYSOL (Svergun et al., 1995).

Crystallization and structure determination

MBP820 was crystallized by the hanging drop method against a reservoir of 15% PEG 4K, 100 mM sodium citrate pH 5.6, and 100 mM lithium acetate. X-ray diffraction data were collected at beamline 11-1 at the Stanford Synchrotron Radiation Laboratory at a wavelength of 0.9795 Å. Data were integrated and merged with DENZO and SCALEPACK (Otwinowski, 1993). The structure was solved by molecular replacement using AMoRe in the CCP4 package (CCP4, 1994). Manual model building was performed via XtalView (McRee, 1999) and initially refined with CNS 1.1 (Brunger et al., 1998), followed by TLS refinement in Refmac 5 (Winn et al., 2001; Winn et al., 2003) using 11 optimal TLS groups as defined by TLSMD (Painter and Merritt, 2006). The refined structure was deposited in the Protein Database as entry 2ok2.

5.6 ACKNOWLEDGEMENTS

We thank Paul Modrich, Malcolm Winkler and Anthony Poteete for their generous gifts of plasmids and bacterial strains, Jeff Perry and SSRL beamline staff for assistance in crystallographic data collection, and Greg Hura for assistance in SAXS data collection. We also thank Scarlet Shell for helpful discussions and comments on this manuscript. This work was supported by NIH grants GM50006 and CA92584. C.D.P. was supported as a Robert Black fellow of the Damon Runyon Cancer Research Foundation.

Chapter 5, in full, is a reprint of the material as it appears in Mendillo, M. L., Putnam, C. D. and Kolodner R. D. "*Escherichia coli* MutS tetramerization domain structure reveals that stable dimers but not tetramers are essential for mismatch repair *in vivo*," *Journal of Biological Chemistry* (2007) Jun 1; 282(22): 16354-54. The dissertation author and Christopher D. Putnam contributed equally as primary authors of this paper.

5.7 REFERENCES

Acharya, S., Foster, P. L., Brooks, P., and Fishel, R. (2003). The coordinated functions of the E. coli MutS and MutL proteins in mismatch repair. Mol Cell *12*, 233-246.

Allen, D. J., Makhov, A., Grilley, M., Taylor, J., Thresher, R., Modrich, P., and Griffith, J. D. (1997). MutS mediates heteroduplex loop formation by a translocation mechanism. Embo J *16*, 4467-4476.

Andrade, M. A., Petosa, C., O'Donoghue, S. I., Muller, C. W., and Bork, P. (2001). Comparison of ARM and HEAT protein repeats. J Mol Biol *309*, 1-18.

Au, K. G., Welsh, K., and Modrich, P. (1992). Initiation of methyl-directed mismatch repair. J Biol Chem *267*, 12142-12148.

Baitinger, C., Burdett, V., and Modrich, P. (2003). Hydrolytically deficient MutS E694A is defective in the MutL-dependent activation of MutH and in the mismatch-dependent assembly of the MutS.MutL.heteroduplex complex. J Biol Chem *278*, 49505-49511.

Ban, C., and Yang, W. (1998). Crystal structure and ATPase activity of MutL: implications for DNA repair and mutagenesis. Cell *95*, 541-552.

Biswas, I., Ban, C., Fleming, K. G., Qin, J., Lary, J. W., Yphantis, D. A., Yang, W., and Hsieh, P. (1999). Oligomerization of a MutS mismatch repair protein from Thermus aquaticus. J Biol Chem *274*, 23673-23678.

Bjornson, K. P., Allen, D. J., and Modrich, P. (2000). Modulation of MutS ATP hydrolysis by DNA cofactors. Biochemistry *39*, 3176-3183.

Bjornson, K. P., Blackwell, L. J., Sage, H., Baitinger, C., Allen, D., and Modrich, P. (2003). Assembly and molecular activities of the MutS tetramer. J Biol Chem *278*, 34667-34673.

Brunger, A. T., Adams, P. D., Clore, G. M., Delano, W. L., Gros, P., Grosse-Kunstleve, R. W., Jiang, J. S., Kuszewski, J., Nilges, M., Pannu, N. S.*, et al.* (1998). Crystallography & NMR System: A New Software Suite for Macromolecular Structure Determination. Acta Cryst D *54*, 905-921.

Calmann, M. A., Nowosielska, A., and Marinus, M. G. (2005a). The MutS C terminus is essential for mismatch repair activity in vivo. J Bacteriol *187*, 6577-6579.

Calmann, M. A., Nowosielska, A., and Marinus, M. G. (2005b). Separation of mutation avoidance and antirecombination functions in an Escherichia coli mutS

mutant. Nucleic Acids Res *33*, 1193-1200.

CCP4 (1994). The CCP4 Suite: programs for protein crystallography. Acta Cryst D *50*, 760-763.

Doniach, S. (2001). Changes in biomolecular conformation seen by small angle X-ray scattering. Chem Rev *101*, 1763-1778.

Duan, X., Hall, J. A., Nikaido, H., and Quiocho, F. A. (2001). Crystal structures of the maltodextrin/maltose-binding protein complexed with reduced oligosaccharides: flexibility of tertiary structure and ligand binding. J Mol Biol *306*, 1115-1126.

Feng, G., Tsui, H. C., and Winkler, M. E. (1996). Depletion of the cellular amounts of the MutS and MutH methyl-directed mismatch repair proteins in stationary-phase Escherichia coli K-12 cells. J Bacteriol *178*, 2388-2396.

Feng, G., and Winkler, M. E. (1995). Single-step purifications of His6-MutH, His6-MutL and His6-MutS repair proteins of escherichia coli K-12. Biotechniques *19*, 956-965.

Grilley, M., Welsh, K. M., Su, S. S., and Modrich, P. (1989). Isolation and characterization of the Escherichia coli mutL gene product. J Biol Chem *264*, 1000-1004.

Haber, L. T., and Walker, G. C. (1991). Altering the conserved nucleotide binding motif in the Salmonella typhimurium MutS mismatch repair protein affects both its ATPase and mismatch binding activities. Embo J *10*, 2707-2715.

Iyer, R. R., Pluciennik, A., Burdett, V., and Modrich, P. L. (2006). DNA mismatch repair: functions and mechanisms. Chem Rev *106*, 302-323.

Jones, S., and Thornton, J. M. (1995). Protein-protein interactions: a review of protein dimer structures. Prog Biophys Molec Biol *63*, 31-65.

Junop, M. S., Obmolova, G., Rausch, K., Hsieh, P., and Yang, W. (2001). Composite active site of an ABC ATPase: MutS uses ATP to verify mismatch recognition and authorize DNA repair. Mol Cell *7*, 1-12.

Junop, M. S., Yang, W., Funchain, P., Clendenin, W., and Miller, J. H. (2003). In vitro and in vivo studies of MutS, MutL and MutH mutants: correlation of mismatch repair and DNA recombination. DNA Repair (Amst) *2*, 387-405.

Lahue, R. S., Au, K. G., and Modrich, P. (1989). DNA mismatch correction in a defined system. Science *245*, 160-164.

Lamers, M. H., Georgijevic, D., Lebbink, J. H., Winterwerp, H. H., Agianian, B., de

Wind, N., and Sixma, T. K. (2004). ATP increases the affinity between MutS ATPase domains. Implications for ATP hydrolysis and conformational changes. J Biol Chem *279*, 43879-43885.

Lamers, M. H., Perrakis, A., Enzlin, J. H., Winterwerp, H. H., de Wind, N., and Sixma, T. K. (2000). The crystal structure of DNA mismatch repair protein MutS binding to a G x T mismatch. Nature *407*, 711-717.

Lea, D. E., & Coulson, C.A. (1948). The distribution of the numbers of mutants in bacterial populations. Journal of Genetics *49*, 264-285.

Lopez de Saro, F. J., Marinus, M. G., Modrich, P., and O'Donnell, M. (2006). The beta sliding clamp binds to multiple sites within MutL and MutS. J Biol Chem *281*, 14340-14349.

Luria, S. F., & Delbruck, M. (1943). Mutations of bacteria from virus sensitivity to virus resistance. Genetics *28*, 491-511.

Lynch, H. T., and de la Chapelle, A. (2003). Hereditary colorectal cancer. N Engl J Med *348*, 919-932.

Manelyte, L., Urbanke, C., Giron-Monzon, L., and Friedhoff, P. (2006). Structural and functional analysis of the MutS C-terminal tetramerization domain. Nucleic Acids Res *34*, 5270-5279.

Marti, T. M., Kunz, C., and Fleck, O. (2002). DNA mismatch repair and mutation avoidance pathways. J Cell Physiol *191*, 28-41.

McGuffin, L. J., Bryson, K., and Jones, D. T. (2000). The PSIPRED protein structure prediction server. Bioinformatics *16*, 404-405.

McRee, D. E. (1999). XtalView/Xfit - a versatile program for manipulating atomic coordinates and electron density. J Struct Biol *125*, 156-165.

Miller, J. (1992). A short course in bacterial genetics: Cold Spring Harbor Laboratory Press).

Moore, P. B. (1980). Small-angle scattering: information content and error analysis. J Appl Cryst *13*, 168-175.

Obmolova, G., Ban, C., Hsieh, P., and Yang, W. (2000). Crystal structures of mismatch repair protein MutS and its complex with a substrate DNA. Nature *407*, 703-710.

Otwinowski, Z. (1993). Data collection and processing., In Proceedings of the CCP4 Study Weekend, L. Sawyer, N. Isaacs, and S. Bailey, eds. (Warrington: Science and

Engineering Research Council), pp. 56-62.

Painter, J., and Merritt, E. A. (2006). Optimal description of a protein structure in terms of multiple groups undergoing TLS motion. Acta Cryst *D62*, 439-450.

Peltomaki, P. (2003). Role of DNA mismatch repair defects in the pathogenesis of human cancer. J Clin Oncol *21*, 1174-1179.

Poteete, A. R., Fenton, A. C., and Nadkarni, A. (2004). Chromosomal duplications and cointegrates generated by the bacteriophage lamdba Red system in Escherichia coli K-12. BMC Mol Biol *5*, 22.

Selmane, T., Schofield, M. J., Nayak, S., Du, C., and Hsieh, P. (2003). Formation of a DNA mismatch repair complex mediated by ATP. J Mol Biol *334*, 949-965.

Semenyuk, A. V., and Svergun, D. I. (1991). GNOM - a program package for small-angle scattering data processing. J Appl Cryst *24*, 537-540.

Shilton, B. H., Flocco, M. M., Nilsson, M., and Mowbray, S. L. (1996). Conformational changes of three periplasmic receptors for bacterial chemotaxis and transport: the maltose-, glucose/galactose- and ribose-binding proteins. J Mol Biol *264*, 350-363.

Sixma, T. K. (2001). DNA mismatch repair: MutS structures bound to mismatches. Curr Opin Struct Biol *11*, 47-52.

Stanislawska-Sachadyn, A., Sachadyn, P., Jedrzejczak, R., and Kur, J. (2003). Construction and purification of his6-Thermus thermophilus MutS protein. Protein Expr Purif *28*, 69-77.

Su, S. S., and Modrich, P. (1986). Escherichia coli mutS-encoded protein binds to mismatched DNA base pairs. Proc Natl Acad Sci U S A *83*, 5057-5061.

Svergun, D. I., Barberato, C., and Koch, M. H. J. (1995). CRYSOL - a program to evaluate X-ray solution scattering of biological macromolecules from atomic coordinates. J Appl Cryst *28*, 768-773.

Svergun, D. I., Petoukhov, M. V., and Koch, M. H. (2001). Determination of domain structure of proteins from X-ray solution scattering. Biophys J *80*, 2946-2953.

Takamatsu, S., Kato, R., and Kuramitsu, S. (1996). Mismatch DNA recognition protein from an extremely thermophilic bacterium, Thermus thermophilus HB8. Nucleic Acids Res *24*, 640-647.

Telmer, P. G., and Shilton, B. H. (2003). Insights into the conformational equilibria of maltose-binding protein by analysis of high affinity mutants. J Biol Chem *278*, 34555-

34567.

Thayer, M. M., Ahem, H., Xing, D., Cunningham, R. P., and Tainer, J. A. (1995). Novel DNA binding motifs in the DNA repair enzyme endonuclease III crystal structure. EMBO J *14*, 4108-4120.

Winn, M. D., Isupov, M. N., and Murshudov, G. N. (2001). Use of TLS parameters to model anisotropic displacements in macromolecular refinement. Acta Cryst D *57*, 122-133.

Winn, M. D., Murshudov, G. N., and Papiz, M. Z. (2003). Macromolecular TLS refinement in REFMAC at moderate resolutions. Methods in Enzymology *374*, 300-321.

CHAPTER 6

Summary and future directions

6.1 SUMMARY

The studies described in this dissertation explore the molecular mechanism of the initiation of DNA mismatch repair using biochemical, structural and genetic methods. These studies clarify seemingly conflicting data regarding the effects of ATP hydrolysis on the interaction of MMR proteins and movement along DNA, as well as the effects of the oligomerization state of MutS. Importantly, these studies do not conflict with previously published data, but rather provide insight on the disparities of previous studies, allowing the re-interpretation of these data and thus resolving some of the conflicts within the field of MMR.

6.2 ANALYSIS OF MMR PROTEIN MOBILITY ALONG DNA

The *lac* repressor-*lac* operator interaction was used as a reversible DNA end-blocking system in conjunction with a surface biosensor, which detects total internal reflectance and allows monitoring of binding and dissociation in real time, as a system to study the ability of MMR proteins to move along DNA (Mendillo et al., 2005). The reversibility of the end-block, in conjunction with the ability to follow the experiment in real time and perform steady-state analysis offered significant advantages as compared to the previously described methods for studying the dynamics of MMR complexes on DNA. The Msh2-Msh6 complex, and the Mlh1-Pms1 complex from *Saccharomyces cerevisiae* were initially examined using this system. These studies revealed several notable features of the Msh2-Msh6 complex, the Msh2-Msh6-Mlh1-Pms1 ternary complex, and their interaction with DNA.

Multiple modes of binding and dissociation of Msh2-Msh6

First, Msh2-Msh6 has at least two different modes of dissociation off of DNA. The first mode of dissociation requires ATP binding, but not ATP hydrolysis, does not require a mispair or a free end of DNA and thus directly dissociates off of the DNA helix. The second mode of dissociation is rapid compared to the first, but similarly requires ATP binding, but not ATP hydrolysis. In contrast to the first mode, it requires a mispair and is dependent on the DNA having at least one free end. In the context of the cell, this implies that the Msh2-Msh6 complex can slide away from the mispair, along the DNA helix.

Second, Msh2-Msh6 demonstrated two different modes of DNA binding. Under conditions where ATP was present, but ATP hydrolysis was prevented, Msh2-Msh6 weakly bound to DNA and showed little, if any, specificity for the mispaired substrate. Further, while it was capable of the slow, direct mode of dissociation, it could not be converted to the form that slides along DNA. In contrast, when Msh2-Msh6 was bound in the absence of nucleotide, in the presence of ADP, or in the presence of ATP under hydrolyzing conditions (where ATP could first hydrolyze to ADP), Msh2-Msh6 bound to the DNA in a highly mispair specific manner, and could be converted to the form capable of sliding along the DNA helix. Thus, Msh2-Msh6 binds the mispair productively only in the ADP-bound or nucleotide free form. In the presence of ATP, Msh2-Msh6 must first hydrolyze the ATP to ADP, and then can productively bind the mispaired DNA.

Msh2-Msh6-Mlh1-Pms1-DNA ternary complex

Our studies, similar to several previous reports, showed that the Mlh1-Pms1 complex binds to Msh2-Msh6 in a reaction that requires ATP and a DNA substrate (Blackwell et al., 2001; Bowers et al., 2001; Bowers et al., 2000; Kijas et al., 2003; Plotz et al., 2002; Raschle et al., 2002). In the presence of ATP, but under nonhydrolyzing condition, Mlh1-Pms1 formed a stable complex with Msh2-Msh6 on the end of DNA; this complex demonstrated no specificity for the mispair. This mispair-independent interaction was observed in both immunoprecipitation experiments as well as surface biosensor experiments. Most studies previously reported were performed under similar reaction conditions and either showed no

mispair specificity or did not examine mispair specificity (Bowers et al., 2001; Bowers et al., 2000; Kijas et al., 2003; Plotz et al., 2002; Raschle et al., 2002).

Under conditions that supported ATP hydrolysis, the ternary complex formed on mispaired DNA that appeared to be dynamic; this observation required use of the surface biosensor, as its formation was not detected in the same immunoprecipitation experiments that were used to examine the complex under nonhydrolyzing conditions. This complex also formed on the basepair control substrate, but to a lesser degree; it was similarly dynamic.

Blocking the ends of the DNA substrate had several effects. First, there was a reduction in ternary complex formation on the basepair control that was more pronounced under conditions where ATP hydrolysis was prevented. Thus, a significant amount of ternary complex that was detected on the control substrate was forming on the ends of the DNA. Second, steady-state binding of the ternary complex to mispaired DNA increased when the DNA substrate was blocked, in a manner similar to Msh2-Msh6 in the absence of Mlh1-Pms1. The increase, however, was not as striking, but the analysis was confounded because the ternary complex demonstrated a modest affinity for the free DNA ends, even under conditions where ATP could be hydrolyzed. Lastly, the dissociation of the ternary complex off of the mispaired substrate was reduced in the presence of the end-block; once again the effect was not as striking as that seen by Msh2-Msh6 in the absence of Mlh1-Pms1, perhaps due to its affinity for DNA ends.

These data suggest that the ternary complex is still capable of sliding away from the mispair, and since the MLH complex is presumably responsible for

stimulating downstream MMR events, its mobility might be important for MMR mechanism. In addition, it is tempting to speculate that the affinity of the ternary complex for DNA ends might have functional significance *in vivo*. The ternary complex formed at the mispair might slide until it reaches a nick [nicks are required in eukaryotic MMR reconstitution reactions *in vitro* (Constantin et al., 2005; Zhang et al., 2005) and perhaps the cell takes advantage of preexisting nicks *in vivo* as well] where it can stimulate the activity of Exo1 or other, as yet unidentified nucleases.

ATP Binding versus ATP Hydrolysis

These studies resolve some apparently conflicting reports on the effects of ATP binding versus ATP hydrolysis on sliding clamp formation of the MSH complexes as well as the interaction between the MSH complexes with MLH complexes. Our studies are consistent with two previous reports that demonstrated that ATP can induce dissociation of Msh2-Msh6 off of mispaired DNA, which can be reduced by blocking the ends of the DNA substrate (Blackwell et al., 1998; Gradia et al., 1999). However, one study noted that there was a reduction in trapped complex under conditions where ATP hydrolysis was prevented; they conclude that hydrolysis is required for efficient trapping and therefore movement along DNA (Blackwell et al., 1998). While we disagree with the interpretation, our studies are consistent with this result. It is clear that blocking DNA ends reduce Msh2-Msh6 dissociation upon ATP addition independent of hydrolysis conditions, however there is still direct dissociation from the DNA, and only conditions where hydrolysis is permitted can Msh2-Msh6 rebind the mispaired substrate.

Our studies on ternary complex formation in the presence of ATPγS also explain the apparent discrepancy observed between two studies that examined ternary complex formation between MutL and the same ATP hydrolysis defective mutant MutS protein (Baitinger et al., 2003; Selmane et al., 2003). One study mixed the two proteins in the presence of ATP and a mispaired DNA substrate and failed to observe ternary complex formation (Baitinger et al., 2003); our results predict that no ternary complex would form because the mutant MutS protein would not be able to hydrolzye ATP to ADP and therefore would not productively bind the mispair. In contrast, the other study first bound the mutant MutS protein in the absence of nucleotide and then added MutL along with ATP and observed ternary complex formation (Selmane et al., 2003); our results predict that once MutS is bound to the mispair , addition of ATP, even in the absence of hydrolysis, would allow ternary complex formation to occur.

6.3 DOMINANT MUTANT MSH2-MSH6 COMPLEXES

A previous study described four dominant *msh6* mutations that interfere with the function of both Msh2-Msh6 and Msh2-Msh3-dependent MMR (Das Gupta and Kolodner, 2000). Initial biochemical studies showed that the dominant mutant Msh2-Msh6 complexes had altered ATPase activity, as well as the three strong dominant mutant complexes had reduced ATP-induced dissociation off of mispaired bases (Hess et al., 2002). In chapter 3, we described a detailed biochemical analysis of these mutant Msh2-Msh6 complexes that further examined the ATP-binding and ATP hydrolysis properties as well as examined the ability of these proteins to function in downstream MMR events, including the ability to form sliding clamp and interact with the Mlh1-Pms1 complex (Hess et al., 2006).

The results reveal two mechanisms for dominance. In the first, the mutant Msh2-Msh6 complex can bind the mispaired base, but is defective for the ATP-induced sliding clamp formation and assembly of ternary complexes with Mlh1-Pms1 and occludes the mispaired base from functional Msh complexes. In the second, the mutant complex can bind the mispaired base, is defective for ATP-induced sliding clamp formation, but retains the ability to interact with Mlh1-Pms1. In this case, either the mispair base is occluded or Mlh1-Pms1 is sequestered and not available to act in alternate MMR pathways.

Interestingly, under the conditions tested, the Msh6-G1142D mutant complex had significant defects in ATP binding, did not appear to exhibit sliding, but still had the ability to interact with Mlh1-Pms1. Regardless of the hypothesis suggested to

explain the behavior of this mutant complex, it seems to be a separation-of-function mutation that results in a complex that is defect in sliding, but retains the ability to interact with Mlh1-Pms1 and thus downstream MMR factors. This supports the view that the sliding clamp confirmation is essential for MMR activity. In addition, a recent study describes a series of experiments using *E. coli* proteins that demonstrates that MutH activation is greatly reduced by introducing either a blockade or a double-strand break to interrupt the shorter distance between the mispair and the hemimethlyated GATC sequence on a plasmid (Pluciennik and Modrich, 2007). Taken together, both the sliding clamp confirmation, and an available path along the DNA seem to be essential for the downstream activities of MMR.

6.4 NUCLEOTIDE BINDING AND MSH2-MSH6 SLIDING

Studies in chapters 2 and 3 revealed that the MSH and MLH complexes slide along DNA in a reaction dependent on ATP binding, but not hydrolysis and that sliding appears to be essential for MMR. In chapter 4 an assay is described that utilizes a crosslinking approach to measure nucleotide binding to each subunit of Msh-Msh6 and visualize the specific nucleotide bound states under several conditions (Mazur et al., 2006).

Crosslinking nucleotides to the Msh2-Msh6 complex revealed that Msh6 has the high affinity ATP binding site, while the site in Msh2 has a low affinity for ATP but high affinity for ADP. When bound to mispaired DNA, ATP hydrolysis by Msh6 is inhibited which results in a decreased affinity for ADP by Msh2. This allows for a state of dual ATP occupancy, which is the form that allows Msh2-Msh6 to slide along DNA. This implies that there is a communication between the two nucleotide binding sites such that nucleotide binding at one site affects nucleotide binding at the other. Furthermore, this provides an additional mechanism for the specificity for MMR. The mispair now plays two roles in iniating MMR. First, the mispair acts as a high affinity substrate for Msh2-Msh6; indeed Msh2-Msh6 displays a 10-20-fold specificity for mispaired DNA as compared to homoduplex DNA (Iyer et al., 2006). Second, only mispair-bound Msh2-Msh6 has ATP hydrolysis inhibited in Msh6; this allows for the appropriate nucleotide state for downstream MMR events (sliding) to occur. These data offer mechanistic insight on why we failed to observe sliding clamp formation by

Msh2-Msh6 on homoduplex DNA substrates in the studies described in chapter 2 and chapter 3.

6.5 A MODEL FOR FULL LENGTH MUTS IN MMR

In chapter 5 we used small angle x-ray scattering (SAXS) to demonstrate that the MutS tetramer is extended in solution (Mendillo et al., 2007). MutS tetramerization is mediated through its C-terminal 34 residues, which when fused onto the C-terminus of monomeric Maltose Binding Protein (MBP), also causes it to tetramerize. The MBP fusions retained the ability to interact with MutS and MutS-MutL-DNA complexes. A crystal structure of the tetramerization domain fused to MBP revealed an extensively associated dimer interface, with a much smaller tetramer interface. Mutations of residues involved in the weak tetramer interface resulted in MBP fusion proteins that were dimeric. A truncation eliminating the C-terminal 34 amino acids, as well as the point mutations limiting the MBP fusion protein to a dimer were introduced onto the *E. coli* MutS chromosome *in vivo.* While the truncation was nonfunctional, the tetramer-preventing point mutants were mostly functional. These results demonstrate that the MutS tetramer is not essential for mismatch repair, however the C-terminus of MutS is essential in stabilizing MutS as a dimer. These data explain why integration of MutSΔ800 onto the *E. coli* chromosome results in a substantial MMR defect, while the overexpression from a plasmid can complement for a mutS deletion for MMR function (Calmann et al., 2005a; Calmann et al., 2005b).

Tetramer formation has by others has been suggested to support the ATP hydrolysis-driven translocation model of MutS movement (Bjornson et al., 2003) as well as models where one dimer is bound at the mispair and the other is involved in the strand discrimination signal (Sixma, 2001). Our data from chapter 5 are at odds

with these interpretations but are consistent with the data from previous studies showing the *in vivo* and *in vitro* defects of MutSΔ800 that led to these suggestions (Bjornson et al., 2003; Calmann et al., 2005a). In addition, we are unaware of any reports of the eukaryotic MSH complexes tetramerizing, suggesting that tetramerization is not conserved and thus is dispensible for MMR.

6.6 FUTURE DIRECTIONS

The results described in this dissertation support a model of MMR initiation where a nucleotide-free (or ADP bound), dimeric MSH complex recognizes the mispair, binds ATP but is prevented from hydrolyzing ATP in its high affinity site, which enables the second site to be occupied by another ATP. The dual ATP-bound state drives a conformational change that facilitates sliding along the DNA helix where downstream signaling can occur. These studies lead to numerous questions, many of which are currently being addressed.

Nucleotide Occupancy, conformational changes and ternary complex

While Msh2-Msh6 must be bound by two ATP molecules (or at least one in Msh2, the lower affinity ATP binding site) in order to slide along DNA, it remains to be seen what state is competent for Mlh1-Pms1 interaction. I hypothesize that the ternary complex-competent nucleotide occupancy state of Msh2-Msh6 occurs when Msh6 (the high affinity ATP binding site), is occupied by ATP. There are several reasons why this might be so. First, Msh2-Msh6 forms ternary complex with Mlh1-Pms1 relatively efficiently on homoduplex DNA whereas there is no detectable sliding clamp formation. ATP hydrolysis in Msh6 is inhibited most efficiently in the presence of a mispair; without it, the dual ATP occupancy state is less likely to form. Thus, sliding, which requires ATP bound in both sites (or at least the low affinity ATP binding site), does not occur on homoduplex DNA. Second, it appears that the dominant mutant Msh6-G1142D complex readily forms ternary complex, yet is

refractory to sliding. One interpretation of this is that this mutation only prevents the second ATP-binding induced conformational change from occurring. It is possible, however, that this does not offer evidence for a distinct second ATP conformation and that both the ternary complex competent and sliding competent conformation are the same, but the mutation simply interferes with the part of the protein responsible for sliding. However, a study using *Taq* MutS and *S. cerevisiae* Msh2-Msh6 with the ATP analogue ADP-beryllium fluoride (ABF) indicate that the first scenario may be correct (Alani et al., 2003). In the presence of ABF, Msh2-Msh6 binds Mlh1-Pms1, but does not dissociate off of DNA. The simplest explanation is that there are two distinct ATP-bound conformations of the MSH complex and that it is trapped in the ternary complex competent conformation.

In this regard, additional Msh2-Msh6 mutant complexes have been isolated with an array of nucleotide binding defects. Ternary complex formation with Mlh1-Pms1 is also being examined under various nucleotide concentrations, similar to our studies examining sliding. Further, a collaboration with the laboratory of Dr. Virgil Woods is underway to examine the structural changes that nucleotide binding induces using Deuterium Exchange Mass Spectrometry (DXMS).

Ternary complex structure, mobility & DNA end-binding

While the studies presented in this dissertation suggest that the MSH-MLH ternary complex is mobile, its end-binding affinity hampered more detailed analysis using our surface biosensor system. A previously published method used fluorescence resonance energy transfer (FRET) to show that σ70 translocates with RNA

polymerase along DNA (Mukhopadhyay et al., 2003). A similar study could be designed that monitors the Msh2-Msh6-Mlh1-Pms1 complex dissociating off of the mispair and approaching the end of an end-blocked DNA substrate using FRET. In addition, remains to be seen if the high affinity ternary complex formation observed on DNA ends has any physiological relevance. For instance, while it is hard to imagine a scenario where Mlh1-Pms1 would encounter a double strand DNA break in MMR, the complex does have access to a nick. Indeed, the presence of a nick is required for *in vitro* MMR reconstitution reactions utilizing eukaryotic proteins (Constantin et al., 2005; Zhang et al., 2005).

An additional collaboration is underway utilizing SAXS to monitor the bending of DNA by following Gold-nanoclusters that are present on the ends of DNA substrates. Changes in gold-gold distances are indicative of changes in the bend angle of the DNA substrate. MutS imposes a bend at the mispair when bound to DNA containing a mispair (Lamers et al., 2000; Obmolova et al., 2000). We hypothesize that the bend will be lost in the sliding clamp conformation. It is difficult to imagine that a protein freely diffusing along DNA can simultaneously induce a conformational constraint on DNA. It will be interesting to see what affect MutL binding has on the bend angle. In addition, the system is set up to do time resolved studies using a photocaged-ATP. This should allow detailed kinetic analysis of the bend angle changes.

We also aim to get a better understanding of the MSH-MLH ternary complex utilizing a combined approach of SAXS (in order to get low resolution structural information) and DXMS (protein-protein interface information). We hope that a

better understanding of the ternary complex will yield mechanistic insight, much as the crystal structures of MutS did for mispair binding.

6.7 REFERENCES

Alani, E., Lee, J. Y., Schofield, M. J., Kijas, A. W., Hsieh, P., and Yang, W. (2003). Crystal structure and biochemical analysis of the MutS.ADP.beryllium fluoride complex suggests a conserved mechanism for ATP interactions in mismatch repair. J Biol Chem *278*, 16088-16094.

Baitinger, C., Burdett, V., and Modrich, P. (2003). Hydrolytically deficient MutS E694A is defective in the MutL-dependent activation of MutH and in the mismatch-dependent assembly of the MutS.MutL.heteroduplex complex. J Biol Chem *278*, 49505-49511.

Bjornson, K. P., Blackwell, L. J., Sage, H., Baitinger, C., Allen, D., and Modrich, P. (2003). Assembly and molecular activities of the MutS tetramer. J Biol Chem *278*, 34667-34673.

Blackwell, L. J., Martik, D., Bjornson, K. P., Bjornson, E. S., and Modrich, P. (1998). Nucleotide-promoted release of hMutSalpha from heteroduplex DNA is consistent with an ATP-dependent translocation mechanism. J Biol Chem *273*, 32055-32062.

Blackwell, L. J., Wang, S., and Modrich, P. (2001). DNA chain length dependence of formation and dynamics of hMutSalpha.hMutLalpha.heteroduplex complexes. J Biol Chem *276*, 33233-33240.

Bowers, J., Tran, P. T., Joshi, A., Liskay, R. M., and Alani, E. (2001). MSH-MLH complexes formed at a DNA mismatch are disrupted by the PCNA sliding clamp. J Mol Biol *306*, 957-968.

Bowers, J., Tran, P. T., Liskay, R. M., and Alani, E. (2000). Analysis of yeast MSH2-MSH6 suggests that the initiation of mismatch repair can be separated into discrete steps. J Mol Biol *302*, 327-338.

Calmann, M. A., Nowosielska, A., and Marinus, M. G. (2005a). The MutS C terminus is essential for mismatch repair activity in vivo. J Bacteriol *187*, 6577-6579.

Calmann, M. A., Nowosielska, A., and Marinus, M. G. (2005b). Separation of mutation avoidance and antirecombination functions in an Escherichia coli mutS mutant. Nucleic Acids Res *33*, 1193-1200.

Constantin, N., Dzantiev, L., Kadyrov, F. A., and Modrich, P. (2005). Human mismatch repair: reconstitution of a nick-directed bidirectional reaction. J Biol Chem *280*, 39752-39761.

Das Gupta, R., and Kolodner, R. D. (2000). Novel dominant mutations in Saccharomyces cerevisiae MSH6. Nat Genet *24*, 53-56.

Gradia, S., Subramanian, D., Wilson, T., Acharya, S., Makhov, A., Griffith, J., and Fishel, R. (1999). hMSH2-hMSH6 forms a hydrolysis-independent sliding clamp on mismatched DNA. Mol Cell *3*, 255-261.

Hess, M. T., Gupta, R. D., and Kolodner, R. D. (2002). Dominant Saccharomyces cerevisiae msh6 mutations cause increased mispair binding and decreased dissociation from mispairs by Msh2-Msh6 in the presence of ATP. J Biol Chem *277*, 25545-25553.

Hess, M. T., Mendillo, M. L., Mazur, D. J., and Kolodner, R. D. (2006). Biochemical basis for dominant mutations in the Saccharomyces cerevisiae MSH6 gene. Proc Natl Acad Sci U S A *103*, 558-563.

Iyer, R. R., Pluciennik, A., Burdett, V., and Modrich, P. L. (2006). DNA mismatch repair: functions and mechanisms. Chem Rev *106*, 302-323.

Kijas, A. W., Studamire, B., and Alani, E. (2003). Msh2 separation of function mutations confer defects in the initiation steps of mismatch repair. J Mol Biol *331*, 123-138.

Lamers, M. H., Perrakis, A., Enzlin, J. H., Winterwerp, H. H., de Wind, N., and Sixma, T. K. (2000). The crystal structure of DNA mismatch repair protein MutS binding to a G x T mismatch. Nature *407*, 711-717.

Mazur, D. J., Mendillo, M. L., and Kolodner, R. D. (2006). Inhibition of Msh6 ATPase activity by mispaired DNA induces a Msh2(ATP)-Msh6(ATP) state capable of hydrolysis-independent movement along DNA. Mol Cell *22*, 39-49.

Mendillo, M. L., Mazur, D. J., and Kolodner, R. D. (2005). Analysis of the interaction between the Saccharomyces cerevisiae MSH2-MSH6 and MLH1-PMS1 complexes with DNA using a reversible DNA end-blocking system. J Biol Chem *280*, 22245-22257.

Mendillo, M. L., Putnam, C. D., and Kolodner, R. D. (2007). Escherichia coli MutS tetramerization domain structure reveals that stable dimers but not tetramers are essential for DNA mismatch repair in vivo. J Biol Chem *282*, 16345-16354.

Mukhopadhyay, J., Mekler, V., Kortkhonjia, E., Kapanidis, A. N., Ebright, Y. W., and Ebright, R. H. (2003). Fluorescence resonance energy transfer (FRET) in analysis of transcription-complex structure and function. Methods Enzymol *371*, 144-159.

Obmolova, G., Ban, C., Hsieh, P., and Yang, W. (2000). Crystal structures of mismatch repair protein MutS and its complex with a substrate DNA. Nature *407*, 703-710.

Plotz, G., Raedle, J., Brieger, A., Trojan, J., and Zeuzem, S. (2002). hMutSalpha forms an ATP-dependent complex with hMutLalpha and hMutLbeta on DNA. Nucleic Acids Res *30*, 711-718.

Pluciennik, A., and Modrich, P. (2007). Protein roadblocks and helix discontinuities are barriers to the initiation of mismatch repair. Proc Natl Acad Sci U S A *104*, 12709-12713.

Raschle, M., Dufner, P., Marra, G., and Jiricny, J. (2002). Mutations within the hMLH1 and hPMS2 subunits of the human MutLalpha mismatch repair factor affect its ATPase activity, but not its ability to interact with hMutSalpha. J Biol Chem *277*, 21810-21820.

Selmane, T., Schofield, M. J., Nayak, S., Du, C., and Hsieh, P. (2003). Formation of a DNA mismatch repair complex mediated by ATP. J Mol Biol *334*, 949-965.

Sixma, T. K. (2001). DNA mismatch repair: MutS structures bound to mismatches. Curr Opin Struct Biol *11*, 47-52.

Zhang, Y., Yuan, F., Presnell, S. R., Tian, K., Gao, Y., Tomkinson, A. E., Gu, L., and Li, G. M. (2005). Reconstitution of 5'-directed human mismatch repair in a purified system. Cell *122*, 693-705.